

UNCLASSIFIED

AD NUMBER

AD822047

LIMITATION CHANGES

TO:

Approved for public release; distribution is unlimited.

FROM:

Distribution authorized to U.S. Gov't. agencies only; Test and Evaluation; SEP 1967. Other requests shall be referred to Naval Air Systems Command, Washington, DC 20360.

AUTHORITY

usnasc ltr, 14 Nov 1974

THIS PAGE IS UNCLASSIFIED

7

AD82204Z



**REPORT E907**  
**MODEL F-4J**  
**DIRECT LIFT CONTROL**

**FINAL REPORT**  
**1 SEPTEMBER 1967**

**W.B. WEBER, R.H. MATHEWS, and R.E. VAUGHN**  
**MCDONNELL COMPANY**  
**ST. LOUIS, MISSOURI**

**Each transmittal of this document outside the agencies of the U.S. Government must have prior approval of the Chief, Naval Air Systems Command, Washington D.C., 20360.**

**(Prepared under Contract NOw 66-0372f for the Naval Air Systems Command, Department of the Navy, by McDonnell Company, St. Louis, Missouri)**

**REPORT E907**

**COPY NO.** 

**MODEL F-4J**  
**DIRECT LIFT CONTROL**  
**(FINAL REPORT)**

**1 SEPTEMBER 1967**  
**(INITIAL SUBMITTAL OF MANUSCRIPT DECEMBER 1966)**

**W.B. WEBER, R.H. MATHEWS, and R.E. VAUGHN**  
**MCDONNELL COMPANY**  
**ST. LOUIS, MISSOURI**

**Each transmittal of this document outside the agencies of the  
U.S. Government must have prior approval of the Chief, Naval  
Air Systems Command, Washington D.C., 20360.**

**(Prepared under Contract NOw 66-0372f for the Naval Air Systems Command,  
Department of the Navy, by McDonnell Company, St. Louis, Missouri)**

FOREWORD

This report was prepared by the McDonnell Company, St. Louis, Missouri on Navy Contract NOW 66-0372-f, "F-4B/J Direct Lift Control." Work was administered under the direction of the Stability and Control Section, Airframe Division, Naval Air Systems Command.

The study presented herein began in July 1966, was concluded in December 1966, and represents the efforts of the Engineering Technology Division, the Aircraft Engineering Division, and the Automation Center of the McDonnell Company. Personnel of these divisions, in addition to the authors noted, made significant contributions to the study.

This final report concludes the work on Contract NOW 66-0372-f.

## ABSTRACT

An aerodynamic analysis and system design study for incorporation of Direct Lift Control (DLC) in the McDonnell F-4J airplane has been accomplished. Redesign of lift or control surfaces was not considered. Design of both a prototype and production configuration was conducted, with the prototype configuration having the capability of DLC system variation for optimization through flight testing. Design was carried out to the schematic drawing stage and word descriptions of all system changes required are included. The results of an analog computer study were utilized: to define the flap nominal position, deflection rate, and total travel required to obtain the specified incremental normal load factors ( $\pm .10$  or  $+ .13/- .07$ ); to determine DLC-Stabilator and DLC-Approach Power Compensation System (APCS) Interconnect requirements; and to investigate wave-off capabilities. It is shown that DLC incorporation in the F-4 airplane is feasible. Production incorporation may necessitate consideration of the required strength of the landing gear and backup structure, as well as wind-over-deck requirements for carrier operations, if flight evaluation of DLC shows that increased landing attitude or increased approach speed is required.

## TABLE OF CONTENTS

	<u>Page No.</u>
FOREWORD	i
ABSTRACT	ii
TABLE OF CONTENTS	iii
LIST OF ILLUSTRATIONS	v
LIST OF SYMBOLS	x
1. INTRODUCTION	1
2. DIRECT LIFT CONTROL SYSTEM CONCEPT	3
2.1 Objectives	3
2.2 DLC Surface Requirements	3
2.2.1 DLC Surface Selection	3
2.2.2 Nominal Deflection Requirements	4
2.3 Surface Deflection Rate Requirements	4
2.4 DLC-Stabilator Interconnect Requirements	5
2.5 DLC-APCS Interconnect Requirements	6
2.6 Effect of Load Factor Requirements on Approach Speed	7
2.7 Effect of Initial Conditions on DLC Response	7
2.8 Conclusions	7
3. DIRECT LIFT CONTROL SYSTEM DESIGN	37
3.1 General Description	37
3.2 Mechanical Design	37
3.3 Hydraulic Design	38
3.3.1 Description	38
3.3.2 New Components	38
3.3.3 Plumbing	39
3.3.4 DLC Flap Servo Cylinder Stability Analysis	39
3.4 Electronic Design	40
3.4.1 Electronic Interface	40
3.4.2 Electronic Systems Modifications for DLC Operation	41
3.5 Cockpit Design	41
3.5.1 Pilot Operating Sequence	41
3.5.2 Disengagement	42

	<u>Page No.</u>
3.6 Aircraft Changes to Incorporate	42
3.6.1 Prototype	42
3.6.2 Production	42
3.7 Failure Analysis	43
3.8 Conclusions	43
4. SUMMARY	55
5. REFERENCES	56
APPENDIX A - AERODYNAMIC DATA BASIS	57
APPENDIX B - ANALOG PROGRAM DESCRIPTION	60
APPENDIX C - ANALOG PROGRAM RESULTS	66

## LIST OF ILLUSTRATIONS

<u>Figure No.</u>	<u>Title</u>	<u>Page No.</u>
1	Model F-4J Three View	2
2	Model F-4J Effect of Nominal Flap Position on Load Factor Capability and Approach Speed	9
3	Model F-4J Pilot DLC Command/Incremental Flap Deflection Schedule	10
4	Model F-4J Effect of Flap Deflection Rate (Nominal Flap Setting of 27°)	11
5	Model F-4J Effect of Flap Deflection Rate (Nominal Flap Setting of 32°)	12
6	Model F-4J DLC-Stabilator Interconnect Requirements	13
7.a	Model F-4J Effect of DLC-Stabilator Interconnect (Analog Time History)	14
7.b	Model F-4J Effect of DLC-Stabilator Interconnect (Analog Time History)	15
8.a	Model F-4J Effect of DLC-Stabilator Interconnect (Nominal Flap Setting of 27°)	16
8.b	Model F-4J Effect of DLC-Stabilator Interconnect (Nominal Flap Setting of 27°)	17
9.a	Model F-4J Effect of DLC-Stabilator Interconnect (Nominal Flap Setting of 32°)	18
9.b	Model F-4J Effect of DLC-Stabilator Interconnect (Nominal Flap Setting of 32°)	19
10.a	Model F-4J Effect of Center of Gravity (Nominal Flap Setting of 27°)	20
10.b	Model F-4J Effect of Center of Gravity (Nominal Flap Setting of 27°)	21
11.a	Model F-4J Effect of Center of Gravity (Nominal Flap Setting of 32°)	22
11.b	Model F-4J Effect of Center of Gravity (Nominal Flap Setting of 32°)	23

<u>Figure No.</u>	<u>Title</u>	<u>Page No.</u>
12.a	Model F-4J Effect of Approach Power Compensation System (Analog Time History)	24
12.b	Model F-4J Effect of Approach Power Compensation System (Analog Time History)	25
12.c	Model F-4J Effect of Approach Power Compensation System (Analog Time History)	26
12.d	Model F-4J Effect of Approach Power Compensation System (Analog Time History)	27
13.a	Model F-4J Effect of Approach Power Compensation System (Nominal Flap Setting of 27°)	28
13.b	Model F-4J Effect of Approach Power Compensation System (Nominal Flap Setting of 27°)	29
13.c	Model F-4J Effect of Approach Power Compensation System (Nominal Flap Setting of 27°)	30
14.a	Model F-4J Effect of Approach Power Compensation System (Nominal Flap Setting of 32°)	31
14.b	Model F-4J Effect of Approach Power Compensation System (Nominal Flap Setting of 32°)	32
14.c	Model F-4J Effect of Approach Power Compensation System (Nominal Flap Setting of 32°)	33
15	Model F-4J Effect of Nominal Flap Position on Load Factor Capability and Approach Speed With DLC Stabilator Interconnect, Without APCS	34
16	Model F-4J Effect of Nominal Flap Position on Load Factor Capability and Approach Speed With DLC Stabilator Interconnect, With APCS	35
17	Model F-4J Effect of Nominal Flap Position on Angle- of-Attack Required to Maintain Approach Speed	36
18	Trailing Edge Flap System Installation	44
19	Hydraulic Schematic-Flap System With Drooped Ailerons and DLC	45
20	Trailing Edge Flap Servo Cylinder	46
21	Model F-4J Stability Analysis Model - DLC Flap Actuator	47

<u>Figure No.</u>	<u>Title</u>	<u>Page No.</u>
22	Power Actuator Stability Margin Comparison	48
23	DLC Electronic Interface Schematic	49
24	Modified Stick Grip for Forward Cockpit	50
A.1a	Model F-4J Analog Study Aerodynamic Data Basis	58
A.1b	Model F-4J Analog Study Aerodynamic Data Basis	59
B.1	Block Diagram-DLC Analog Computer Study	62
B.2a	Model F-4 DLC Analog Computer Wiring Diagram	63
B.2b	Model F-4 DLC Analog Computer Wiring Diagram	64
B.3	Analog Computer Installation	65
C.1a	Model F-4J Effect of Initial Flight Path Angle (Nominal Flap Setting of 27°, Analog Time History)	69
C.1b	Model F-4J Effect of Initial Flight Path Angle (Nominal Flap Setting of 27°, Analog Time History)	70
C.2a	Model F-4J Effect of Initial Flight Path Angle (Nominal Flap Setting of 32°, Analog Time History)	71
C.2b	Model F-4J Effect of Initial Flight Path Angle (Nominal Flap Setting of 32°, Analog Time History)	72
C.3a	Model F-4J Effect of Initial Flight Path Angle (Nominal Flap Setting of 27°, Without APCS)	73
C.3b	Model F-4J Effect of Initial Flight Path Angle (Nominal Flap Setting of 27°, Without APCS)	74
C.4a	Model F-4J Effect of Initial Flight Path Angle (Nominal Flap Setting of 32°, Without APCS)	75
C.4b	Model F-4J Effect of Initial Flight Path Angle (Nominal Flap Setting of 32°, Without APCS)	76
C.5a	Model F-4J Effect of Initial Flight Path Angle (Nominal Flap Setting of 27°, With APCS)	77
C.5b	Model F-4J Effect of Initial Flight Path Angle (Nominal Flap Setting of 27°, With APCS)	78

<u>Figure No.</u>	<u>Title</u>	<u>Page No.</u>
C.6a	Model F-4J Effect of Initial Flight Path Angle (Nominal Flap Setting of 32°, With APCS)	79
C.6b	Model F-4J Effect of Initial Flight Path Angle (Nominal Flap Setting of 32°, With APCS)	80
C.7a	Model F-4J Effect of Gross Weight (Nominal Flap Setting of 27°)	81
C.7b	Model F-4J Effect of Gross Weight (Nominal Flap Setting of 27°)	82
C.8a	Model F-4J Effect of Gross Weight (Nominal Flap Setting of 32°)	83
C.8b	Model F-4J Effect of Gross Weight (Nominal Flap Setting of 32°)	84
C.9A	Model F-4J Effect of Center of Gravity (Nominal Flap Setting of 27°)	85
C.9b	Model F-4J Effect of Center of Gravity (Nominal Flap Setting of 27°)	86
C.10a	Model F-4J Effect of Center of Gravity (Nominal Flap Setting of 32°)	87
C.10b	Model F-4J Effect of Center of Gravity (Nominal Flap Setting of 32°)	88
C.11a	Model F-4J Effect of Trim Velocity (Nominal Flap Setting of 27°)	89
C.11b	Model F-4J Effect of Trim Velocity (Nominal Flap Setting of 27°)	90
C.12a	Model F-4J Effect of Trim Velocity (Nominal Flap Setting of 32°)	91
C.12a	Model F-4J Effect of Trim Velocity (Nominal Flap Setting of 32°)	92
C.13	Model F-4J Wave-off Characteristics (Nominal Flap Setting of 27°)	93
C.14	Model F-4J Wave-off Characteristics (Nominal Flap Setting of 32°)	94
C.15a	Model F-4J Wave-off Characteristics (Analog Time History)	95

<u>Figure No.</u>	<u>Title</u>	<u>Page No.</u>
C.15b	Model F-4J Wave-off Characteristics (Analog Time History)	96
C.16	Model F-4J Wave-off Characteristics Summary	97
C.17	Model F-4J Single Engine Wave-off Characteristics	98
C.18	Model F-4J Failure Analysis-Effect of Pilot Control Correction, DLC Hardover-Upstream of Stabilator-Interconnect	99
C.19	Model F-4J Failure Analysis-Effect of Pilot Control Correction, DLC Hardover-Downstream of Stabilator-Interconnect	100
C.20	Model F-4J Failure Analysis-Effect of Pilot Reaction Time, DLC Hardover-Upstream of Stabilator-Interconnect	101
C.21	Model F-4J Failure Analysis-Effect of Pilot Reaction Time, DLC Hardover-Downstream of Stabilator-Interconnect	102
 <u>Table No.</u>		
1	Failure Analysis	51

## LIST OF SYMBOLS

<u>Symbol</u>	<u>Definition</u>	<u>Units</u>
APCS	Approach Power Compensation System	
AFCS	Automatic Flight Control System	
$\bar{c}$	Mean Aerodynamic Chord	Ft.
$C_D$	Drag Coefficient (D/qS)	
$C_{D\delta_s}$	Incremental Drag Coefficient Due to Stabilator Deflection	Deg. <sup>-1</sup>
$C_{D_{FP}}$	Drag Coefficient Due to Flap Deflection	
C.G.	Center of Gravity	% $\bar{c}$
$C_L$	Lift Coefficient (L/qS)	
$C_{L\delta_s}$	Incremental Lift Coefficient Due to Stabilator Deflection	Deg. <sup>-1</sup>
$C_{L_{FP}}$	Lift Coefficient Due to Flap Deflection	
$C_{L\dot{\theta}}$	Incremental Lift Coefficient Due to Pitch Rate	Rad. <sup>-1</sup>
$C_{L_{TRIM}}$	Trim Lift Coefficient	
$C_{m_{C.G.}}$	Pitching Moment Coefficient About the Center of Gravity ( $M_{C.G.}/qS\bar{c}$ )	
$C_{m\delta_s}$	Incremental Pitching Moment Coefficient Due to Stabilator Deflection	Deg. <sup>-1</sup>
$C_{m_{FP}}$	Pitching Moment Coefficient Due to Flap Deflection	
$C_{m\dot{\theta}}$	Incremental Pitching Moment Coefficient Due to Pitch Rate	Rad. <sup>-1</sup>
$C_{m\dot{\alpha}}$	Incremental Pitching Moment Coefficient Due to Angle of Attack Rate	Rad. <sup>-1</sup>

$C_{\mu}$	Momentum Coefficient	
D	Drag	Lb.
DLC	Direct Lift Control	
F	Force	Lb.
g	Acceleration Due to Gravity	ft/sec <sup>2</sup>
G.W.	Gross Weight	Lb.
GPM	Gallons Per Minute	
H	Altitude	Ft.
INTER.	DLC-Stabilator Interconnect	
$I_Y$	Aircraft Moment of Inertia About Y Axis	Slug-Ft <sup>2</sup>
$i_t$	Angle of Incidence of Centerline of Thrust; Referenced to Wing Root Chord	Deg.
KCAS	Knots Calibrated Airspeed	
L	Lift	Lb.
$M_{C.G.}$	Pitching Moment About the Center of Gravity	Ft.-Lb.
MIL	Military Power	
MTBF	Mean Time Between Failures	
m	Mass	Slugs
$N_z$	Normal Load Factor	g's
q	Dynamic Pressure	Lb/Ft <sup>2</sup>
S	Wing Area	Ft <sup>2</sup>
T	Thrust	Lb.
t	Time	Seconds
V	Velocity or Speed	Knots
$V_{PA}$	Approach Speed	Knots

$\Delta X$	Difference In Fuselage Station Between Aerodynamic Data Reference C.G. and Desired C.G.	Ft.
Z	Distance Perpendicular to the Flight Path	Ft.
$Z_T$	Moment Arm of the Thrust About the C.G.	Ft.
$\alpha_w$	Angle-of-Attack; Referenced to Wing Root Chord	Deg.
$\alpha_{w_{TRIM}}$	Trim Angle-of-Attack	Deg.
$\alpha_t$	Angle-of-Attack of Centerline of Thrust; $\alpha_t = \alpha_w + i_t$	Deg.
$\gamma$	Flight Path Angle	Deg.
$\Delta$	Incremental Value	
$\delta_{DLC}$	Pilot DLC Input	% Wheel
$\delta_{FN}$	Wing Leading Edge Flap Deflection	Deg.
$\delta_{FNOM.}$	Nominal Trailing Edge Flap Deflection	Deg.
$\dot{\delta}_{FP}$	Trailing Edge Flap Deflection Rate	Deg/Sec.
$\delta_{FP}$	Trailing Edge Flap Deflection	Deg.
$\delta_s$	Stabilator Deflection	Deg.
$\delta_A$	Drooped Aileron Deflection	Deg.
$\delta_{SINTER}$	Stabilator Interconnect Deflection	Deg.
$\theta$	Pitch Angle	Deg.
$\lambda$	Laplace Transform Variable	Sec. <sup>-1</sup>
$\rho$	Air Density	Slugs/Ft <sup>3</sup>

SUBSCRIPTS

0	Initial Value
2	Value After Two Seconds
5	Value After Five Seconds
PK	Peak Value
L.E.	Leading Edge
w	Wing
s	Stabilator

## 1. INTRODUCTION

It has long been recognized that one of the most exacting tasks required of a pilot is landing aboard an aircraft carrier. To be able to land safely and without damage to the airplane in a moving area only several times longer than the airplane's length is primarily dependent on a low approach speed and precise flight path control. In recent years developments such as boundary layer control, optical landing systems, angle-of-attack indexer, automatic throttle, improved arresting gear and landing gear have all contributed to the safety of operation and reduction of aircraft damage during landings. However, the United States Navy, desiring further improvement in this area, has initiated and sponsored considerable research and development concerning the problem of flight path control. Recent investigations by both the Navy and its contractors (References 1, 2, 3, and 4) concerned a new system of flight path control which shows considerable improvement for the configurations investigated. This system, called Direct Lift Control (DLC), differs from the conventional control in that the pilot manipulates the airplane's high lift devices rather than rotating the entire airplane to effect increases or decreases in aircraft lift. The airplane is flown at essentially a constant angle-of-attack while the high-lift devices are extended or retracted to maintain or correct the flight path. The major advantage of this system is the more rapid vertical response of the airplane which permits more precise control of the flight path.

The Navy requested, under Contract No. N0w 66-0372f, F-4B/J Direct Lift Control, that the McDonnell Company conduct, from both an aerodynamic and design standpoint, a feasibility study of the incorporation of a DLC system in the McDonnell F-4 airplane. Specifically, the basis for this study was the McDonnell F-4J configuration (drooped ailerons, slotted leading edge stabilator and permanently retracted wing leading edge inboard flap) as shown in Figure (1). No changes to present lift or control surfaces were considered. The fundamental system requirement from an aerodynamic standpoint was the ability of the DLC system to produce incremental normal load factors of either  $\pm 0.10$  or  $\pm 0.13/0.07$  "g". Evaluation of the adequacy of these DLC load factor capabilities for flight path control on the glide slope was not part of this study. Design studies were carried out to the schematic drawing stage and include word descriptions of all system changes required for both a prototype and a production configuration. Fundamentally, the prototype configuration has the ability to optimize the DLC system during flight testing. Flap deflection rate, travel and nominal position and DLC-Stabilator and/or DLC-APCS Interconnect requirements were also determined.

For the feasibility study reported herein, the effects of possible increases in approach speed or attitude on the required strength of the landing gear and back up structure were not evaluated. Production incorporation may also require investigation of the effects of increased wind-over-the-deck requirements on the overall carrier suitability if flight test evaluation of DLC indicates that increased landing attitude or approach speed is required.

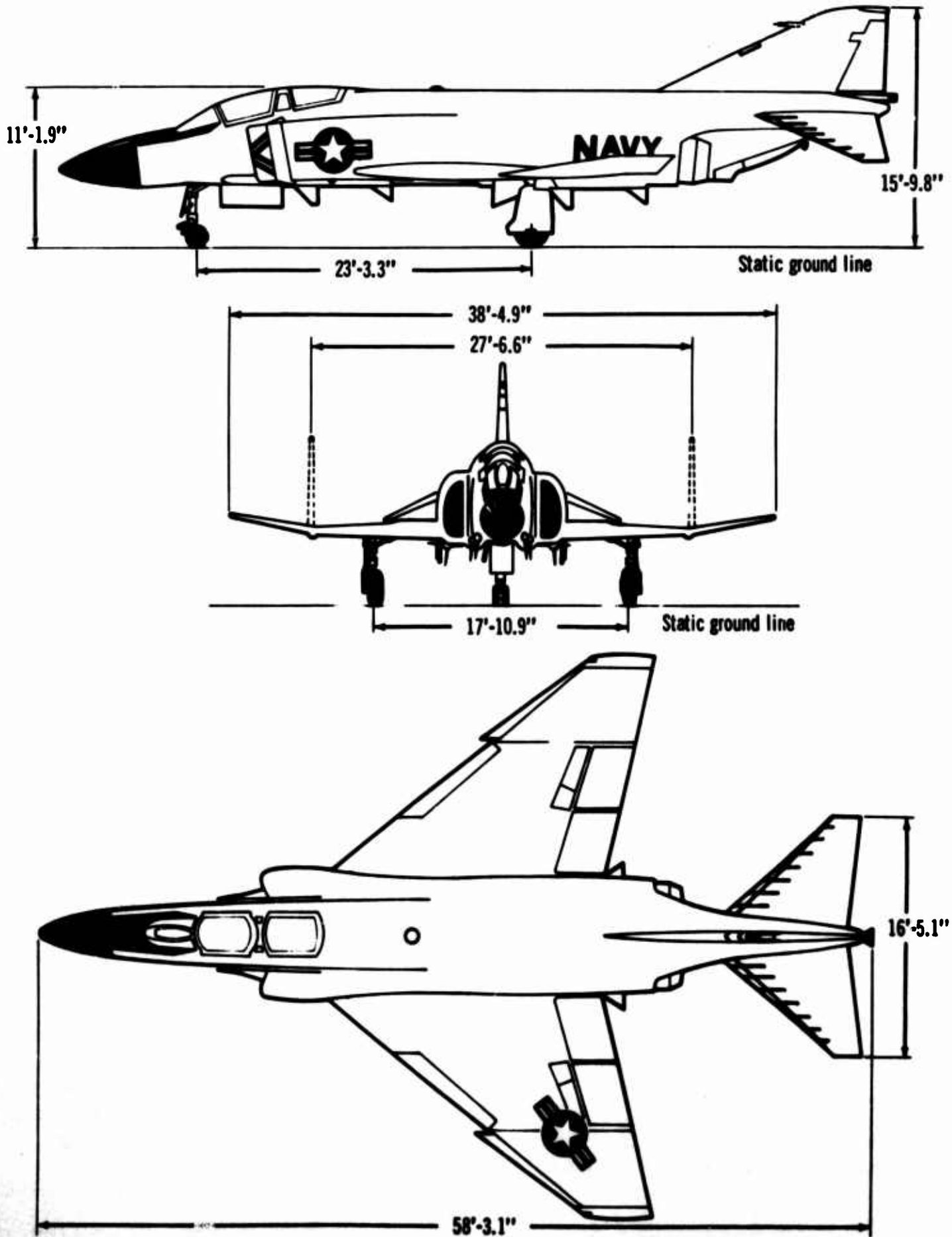


Figure 1 Model F-4J Three View

## 2. DIRECT LIFT CONTROL SYSTEM CONCEPT

### 2.1 Objectives

The incorporation of a DLC system in the McDonnell F-4J aircraft has as its primary objective the attainment of both a symmetrical  $\pm .10$  and an unsymmetrical  $+ .13/- .07$  "g" incremental normal load factor capability; evaluation of the adequacy of these DLC capabilities for flight path control was not an objective. These capabilities were obtained subject to the following ground rules and secondary objectives:

- (1) The DLC system would utilize the present F-4J aerodynamic lift or control surfaces; modification of present surfaces or incorporation of new surfaces would not be considered.
- (2) The DLC surface deflection rates would be sufficient to avoid compromising rapid aircraft response to DLC.
- (3) DLC surface induced pitching moments which result in undesirable pitch transient and angle of attack changes would be counteracted with a DLC-Stabilator Interconnect.
- (4) DLC surface induced drag which results in undesirable speed transients or changes would be counteracted with a DLC-Approach Power Compensation System (APCS) Interconnect.
- (5) The DLC system would not compromise the lateral control system or lateral control characteristics during DLC operation.

In analyzing the above objectives, considerable use was made of the analog program described in Appendix B. The results of this program are the basis for most of the substantiating data of this section of the report. The following sections describe the DLC system characteristics required to meet the objectives described above.

### 2.2 DLC Surface Requirements

The lift or load factor producing capabilities of the DLC surfaces and the specified load factor requirements combine to determine the surfaces required and their nominal or neutral position.

2.2.1 DLC Surface Selection - The lift, drag, and pitching moment characteristics of the trailing edge flaps, ailerons, and spoilers were determined from available wind tunnel and flight test data on both the "undrooped" and "drooped" aileron F-4B/J. These data show that utilizing either the ailerons alone, or in combination with the spoilers, would not result in a system capable of meeting the specified load factor requirements. However, the trailing edge flaps used alone are capable of meeting the specified requirements, and consequently, a system using the trailing edge flaps (hereafter referred to as flaps) was selected for DLC. The selection of the flaps for DLC has the added advantage that it does not compromise the present F-4J lateral control system or lateral control characteristics for the DLC configuration.

2.2.2 Nominal Deflection Requirements - The nominal flap deflections required to meet the specified load factor requirements were determined utilizing the aforementioned flap characteristics in conjunction with the analog computer program. The peak normal load factors were determined for a series of nominal flap positions with a maximum flap deflection of 60 degrees and minimum flap deflections from 24 to 12 degrees. From the results, which are shown in Figure (2), a nominal flap position of 27 degrees with a minimum flap deflection of 13 degrees was selected to meet the  $+0.13/-0.07$  "g" requirement, and a flap position of 32 degrees with a minimum flap deflection of 12 degrees was selected for the  $\pm 0.10$  "g" requirement. These nominal flap positions were maintained for the remainder of the study. The 3.5 degree glide slope approach speeds at 13 degrees wing angle-of-attack for nominal flap positions of 27 degrees and 32 degrees are 143.1 and 141.3 KCAS respectively. Figure (3) presents the relation which then exists between pilot DLC command and incremental flap deflection for the two nominal flap positions. It should be noted that the above data were obtained with flap induced pitching moment and drag equal to zero ( $\Delta C_{M_{F_P}} = 0$  and  $\Delta V = 0$ ), i.e., assumes perfect interconnect operation.

It will also be noted on Figure (2) that at the selected nominal and minimum flap deflections the load factor capabilities exceed the specified requirements, being  $+0.14/-0.08$  "g" and  $\pm 0.11$  "g". A "cushion" of  $0.01$  "g" was purposely included in order to insure meeting the specified load factor requirements when the effects of the flap induced pitching moment and drag and DLC-Stabilator/APCS Interconnects were introduced.

### 2.3 Surface Deflection Rate Requirements

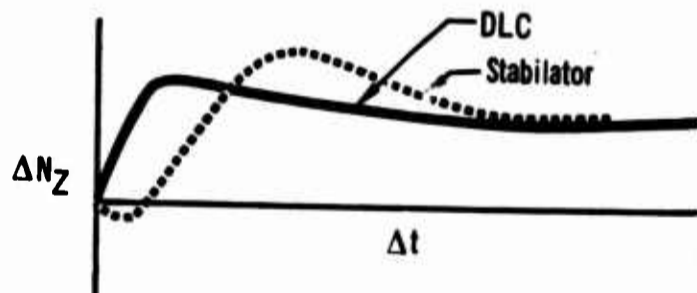
The flap deflection rate during DLC operation affects the rate of normal load factor increase, and, consequently, the altitude response characteristics of the DLC system. The flap deflection rate during DLC operation should be sufficient to insure that rapid aircraft response to DLC is not compromised. Initial estimates indicated a flap deflection rate of 75 degrees per second would be required to prevent any significant degradation in altitude response. During the analog program investigation of the effect of flap rate indicated negligible effect on peak normal load factor until rate limits of less than 20 degrees per second were imposed. In addition, as shown in Figures (4) and (5), noticeable reduction in altitude and attitude increments obtained after two and five seconds were not indicated until rate limits of less than 50 degrees per second were imposed. However, since reduction of flap rate requirements from 75 degrees per second to 50 degrees per second would not result in appreciable simplification in system design, the 75 degree per second requirement was maintained to insure optimum system performance.

It should be noted that the above investigation was conducted with flap induced pitching moments equal to zero. The pitch angle changes shown in Figures (4) and (5) are a result of flight path angle changes, i.e., the aircraft angle-of-attack remains essentially constant and changes in flight path angle result in corresponding pitch angle changes.

## 2.4 DLC-Stabilator Interconnect Requirements

The uncompensated pitching moment induced by flap deflection during DLC operation could result in undesirable pitch transients and angle-of-attack changes which would tend to nullify the incremental lift due to flaps. These moments must be counteracted by either the pilot or a DLC-Stabilator Interconnect if the full lift capabilities of the flaps are to be realized. The incremental stabilator positions required to counteract the flap induced pitching moments are presented in Figure (6) as a function of pilot DLC command and center of gravity location. Also shown are the schedules of incremental stabilator deflection versus DLC command selected for the DLC-Stabilator Interconnects. Figures (7.a) and (7.b) present typical time histories, with and without the DLC-Stabilator Interconnect, which demonstrate the adverse angle of attack change incurred due to uncompensated flap induced pitching moments.

It will be noted that the angle-of-attack change without DLC-Stabilator Interconnect nullifies the normal load factor due to DLC in less than two seconds. This raises the question, "Without DLC, what is the normal load factor and altitude response due to comparable pitching moments introduced with the stabilator at the same rate?" Conventional longitudinal control with the stabilator is characterized by an initial adverse load factor induced by the down load on the stabilator followed by the increase in load factor corresponding to the aircraft's response in pitch. Typical load factor responses to a step stabilator and DLC commands are compared below.



Since altitude changes are proportional to the areas under the curves, control with the stabilator requires longer time intervals to produce altitude changes comparable to those obtained with DLC. For short time intervals the advantage of DLC is apparent.

Figures (8.a), (8.b), (9.a), and (9.b) show the effect of the DLC Stabilator Interconnect on peak load factor and altitude and attitude increments; data with and without the interconnect are compared with data obtained with the pitching moment due to flaps equal to zero ( $\Delta C_{mfp} = 0$ ). The response obtained without an interconnect is significantly degraded from that obtained with an interconnect. The latter, in turn, is almost identical to the response obtained with ideal interconnect, i.e.,  $\Delta C_{mfp} = 0$ .

The DLC-Stabilator Interconnect schedules shown in Figure (6) were optimized for a C.G. of 29%  $\bar{c}$ . However, the data presented in Figures (10.a), (10.b), (11.a), and (11.b), which show the effect of C.G. location on peak load factor and altitude and attitude increments, indicate that interconnects optimized for a mean C.G. location should be acceptable for C.G. locations three percent either side of the selected C.G. These DLC-Stabilator Interconnect requirements are compatible with an integrated stabilator actuator with a  $\pm 2$  degree authority series servo.

## 2.5 DLC - APCS Interconnect Requirements

Operation of the DLC system results in an initial decrease in angle-of-attack when positive load factors are commanded. This decrease in angle-of-attack, with normal operation of the F4J APCS would result in a commanded decrease in engine thrust. Since the increased flap deflection necessary to produce the desired positive load factor results in greater drag, an increase in engine thrust is required. This incompatibility between the DLC system and the APCS required either extensive modifications to the present APCS or the addition of an interconnect signal. Of these two possibilities, the use of an interconnect signal was selected. The interconnect system requires only minor modifications within the APCS controller and leaves the Approach Power Compensation System unchanged for operation without DLC. The interconnect system developed during the analog computer study is of the form:

$$\frac{\Delta \text{ thrust command}}{\Delta \text{ DLC}} = \left( \frac{K_I}{\lambda} + \frac{K_p A}{\lambda + A} \right) \text{ pounds/degree}$$

For positive DLC commands, the system parameters which provide the best overall performance are:

$$K_I = 10.0 \text{ (lbs./sec. per deg.)}$$

$$K_p = 115.8 \text{ (lbs. per deg.)}$$

$$A = 1.0 \frac{1}{\text{sec.}}$$

$$\lambda = \text{Laplace Transform Variable (1/sec)}$$

Due to the nonlinear characteristics of the drag vs. flap deflection curve, the values of  $K_I$  and  $K_p$  are reduced to 69% of the above values for negative load factor commands.

The aircraft response characteristics following DLC inputs with and without the APCS operating are depicted in the time history traces of Figures (12.a) through (12.d). Without the APCS but with DLC-Stabilator Interconnect operating and assuming no power adjustment by the pilot, the airspeed diverges rapidly causing the incremental load factor to "bleed" back to zero. With the APCS and DLC-Stabilator Interconnect operating, the thrust changes commanded through the DLC-APCS Interconnect cause the airspeed and load factor to remain nearly constant. From the summary plots presented in Figures (13.a) through (13.c) it is apparent that APCS operation slightly improves the DLC response as measured in both peak load factor and altitude change after two and five seconds. The greatest improvement provided by the DLC-APCS Interconnect, however, is in the airspeed changes measured at two and five seconds following a DLC input. With the exception of the two-second value for positive inputs, all changes in airspeed with the DLC-APCS Interconnect operating are in the direction to improve the DLC altitude response i.e., positive load factor commands result in increasing speeds.

The results summarized in Figures (14.a) through (14.c) are essentially the same as those of Figures (13.a) through (13.c) with the exception that the nominal flap position is set at 32 degrees rather than at 27 degrees. It is apparent that the nominal flap position has a very small effect on the operation of the DLC-APCS Interconnect.

## 2.6 Effect of Load Factor Requirements on Approach Speed

The effect of load factor requirements and thus nominal flap positions on approach speed has already been demonstrated in Section 2.2. However, the data presented in that section were obtained with the flap induced pitching moment and drag set equal to zero. The inclusion of these effects and the off-setting effects of DLC-Stabilator and DLC-APCS Interconnects alter DLC response characteristics and permit selection of more optimum nominal flap positions with corresponding optimum approach speeds. Figure (15) presents load factor capability and corresponding approach speed as a function of nominal flap position for a DLC system with a DLC-Stabilator Interconnect but without DLC-APCS Interconnect. Figure (16) presents similar data for a DLC system with a DLC-Stabilator Interconnect and a DLC-APCS Interconnect. These data show that the specified load factor capabilities of  $+0.13/-0.07$  "g" and  $\pm 0.10$  "g" may be obtained with approach speeds of 141.0 KCAS and 139.0 KCAS respectively, with both DLC-APCS and DLC-Stabilator Interconnects. Substantial load factor capability is also available at nominal flap positions corresponding to even lower approach speeds.

It should be noted that the approach speeds presented in Figures (15) and (16) are for a -3.5 degree glide path with a trim angle of attack corresponding to the present F-4J approach angle of attack. If the use of DLC should permit higher angles-of-attack during approach, the approach speed corresponding to any nominal flap setting would be decreased. Figure (17) presents the angle of attack increase required to maintain the present F-4J full flap approach speed of 132 KCAS at 34,000 pounds. Although it may be possible to increase the approach angle of attack with DLC over that currently used, it is doubtful that the angle-of-attack for approach with DLC would be increased to these levels. Consequently, some degradation in approach speed with DLC may be experienced.

## 2.7 Effect of Initial Conditions on DLC Response

A complete summary of the incremental load factor, altitude, and attitude change capability of the DLC system is presented in Appendix C. These data show that the effect of flight path angle, center of gravity, gross weight, or trim airspeed on these capabilities is small. Additional data demonstrate that the DLC system can improve wave-off characteristics for two-engine approaches and that the use of the DLC nominal flap position for single engine approaches is acceptable.

## 2.8 Conclusions

The primary and secondary objectives noted in Section 2.1 for incorporation of a DLC system in an F-4J are attainable on a suitably modified aircraft.

(1) The specified incremental load factor requirements of + .13/- .07 "g" or  $\pm .10$  "g" may be obtained utilizing the trailing edge flaps with corresponding approach speeds, at 34,000 pounds gross weight; of 141.0 KCAS and 139.0 KCAS, respectively.

(2) The incremental stabilator deflections required to offset flap induced pitching moments are small and are within the capabilities of DLC-Stabilator Interconnect utilizing an integrated stabilator actuator with  $\pm 2$  degree authority series servo.

(3) The DLC-APCS Interconnect characteristics required to offset flap induced drag are compatible with the APCS with the stabilator interconnect planned for later McDonnell F-4J's.

(4) The DLC system does not compromise the lateral control system or lateral control system characteristics.

G.W. = 34,000 Lb.      C.G. at 29%  $\bar{c}$        $\gamma_0 = 0^\circ$        $\alpha_{wTrim} = 13^\circ$

- Notes: 1. Pitching moment due to incremental flap deflection,  $\Delta C_{m_{FP}}$ , set to zero.  
 2. No APCS; incremental velocity,  $\Delta V$ , held to zero.

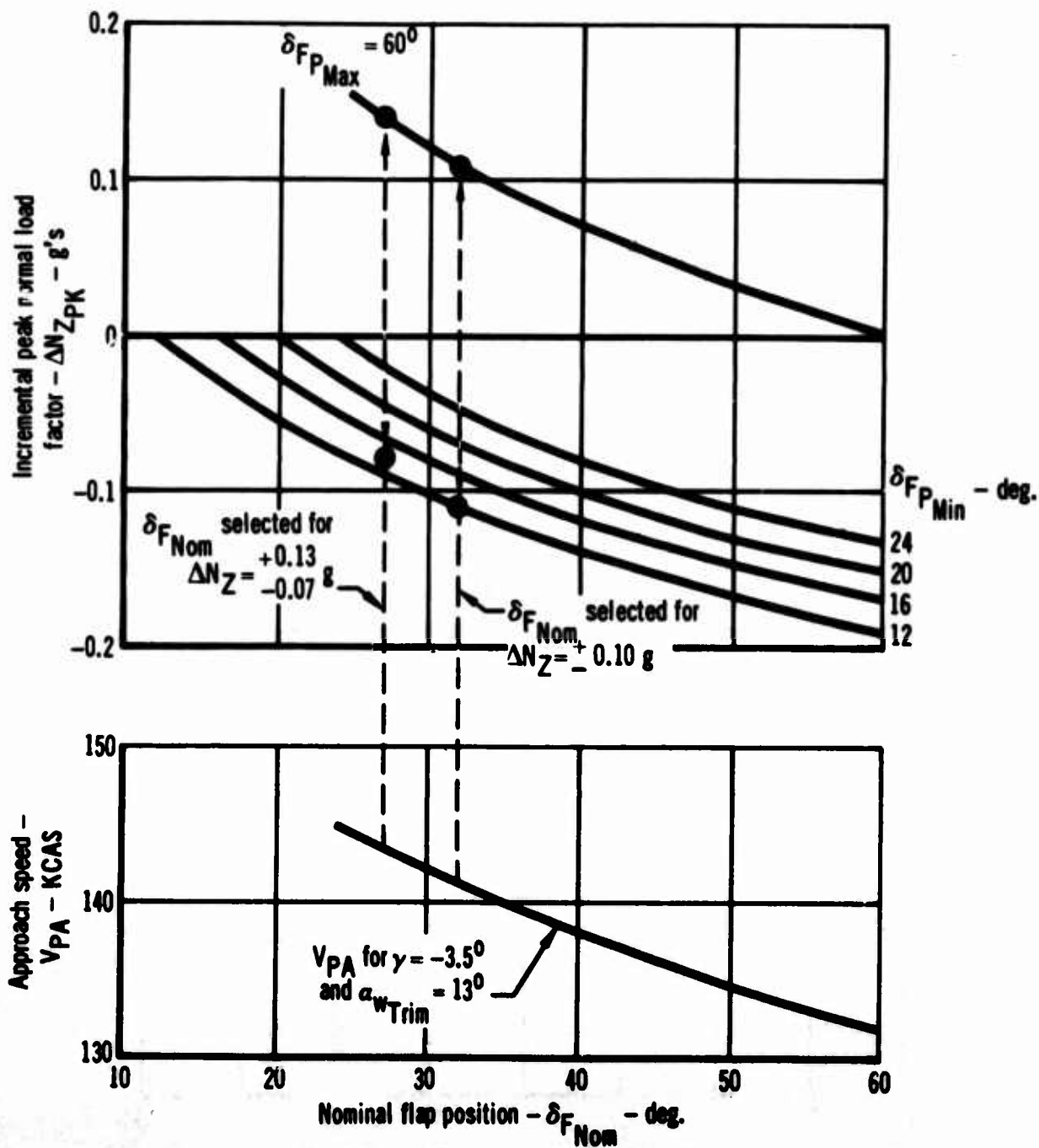
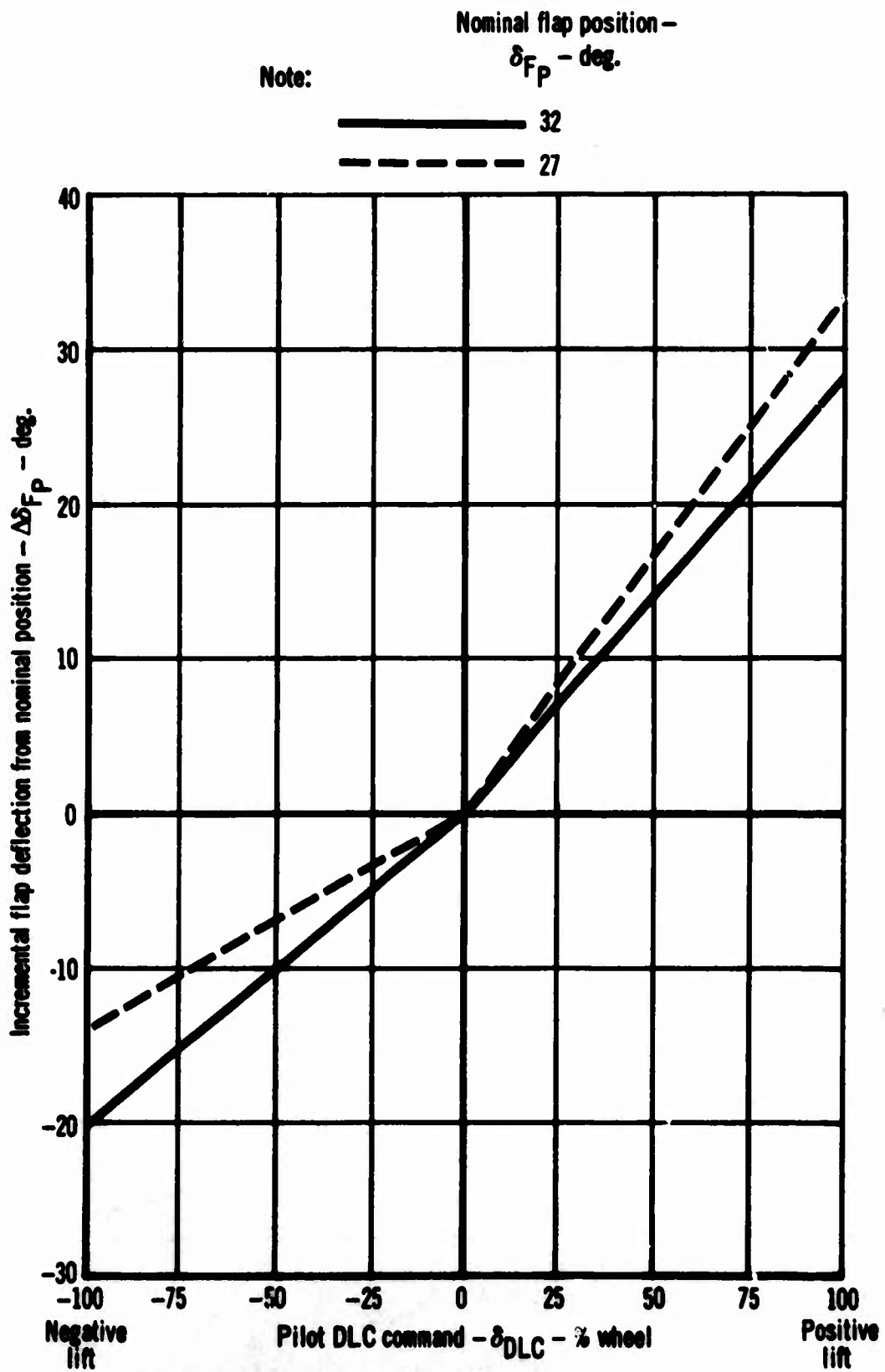


Figure 2 Model F-4J  
 Effect of Nominal Flap Position on  
 Load Factor Capability and Approach Speed



**Figure 3 Model F-4J**  
**Pilot DLC Command/Incremental Flap Deflection Schedule**

$\delta_{F_{Nom}} = 27^\circ$

$V_{Trim} = 142.0 \text{ KCAS}$

$\Delta C_{m_{FP}} = 0$

G.W. = 34,000 Lb.

$\alpha_{w_{Trim}} = 13^\circ$

$\Delta V = 0$

C.G. at 29%  $\bar{c}$

$\gamma_0 = 0^\circ$

— Five seconds  
 - - - Two seconds

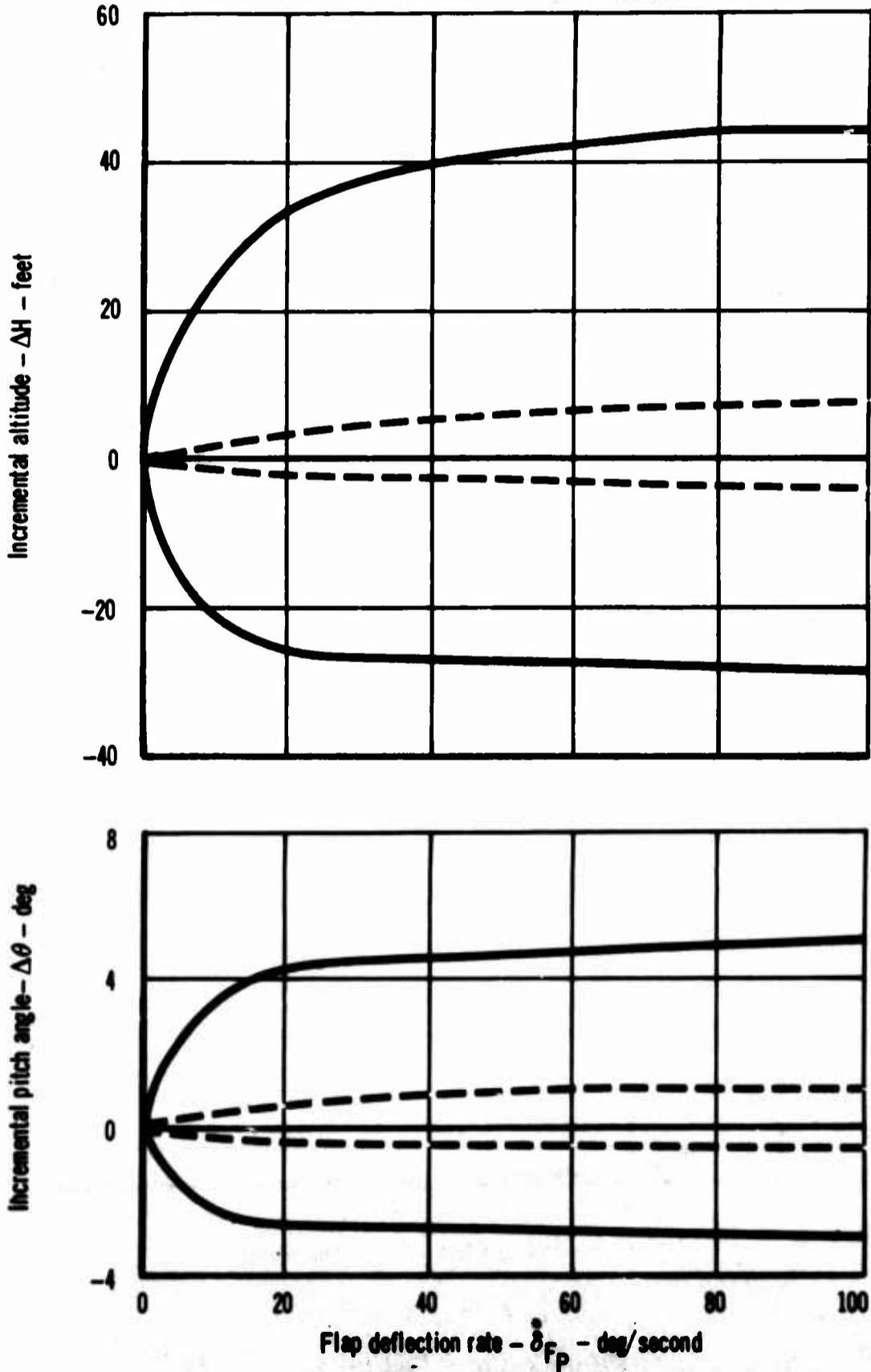


Figure 4 Model F-4J  
 Effect of Flap Deflection Rate

$\delta_{F_{Nom}} = 32^\circ$

$V_{Trim} = 140.0 \text{ KCAS}$

$\Delta C_{m_{FP}} = 0$

G.W. = 34,000 Lb.

$\alpha_{w_{Trim}} = 13^\circ$

$\Delta V = 0$

C.G. at 29%  $\bar{c}$

$\gamma_0 = 0^\circ$

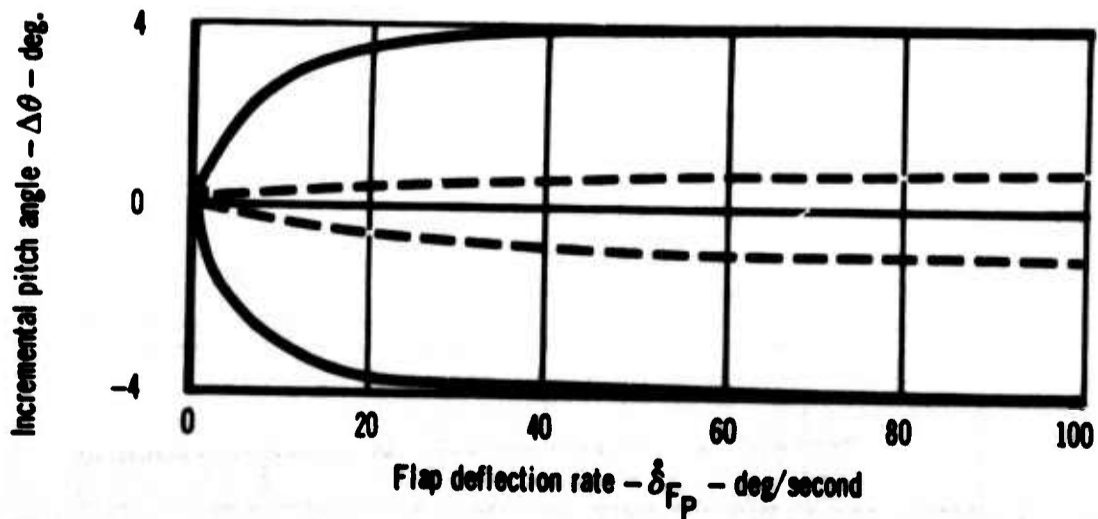
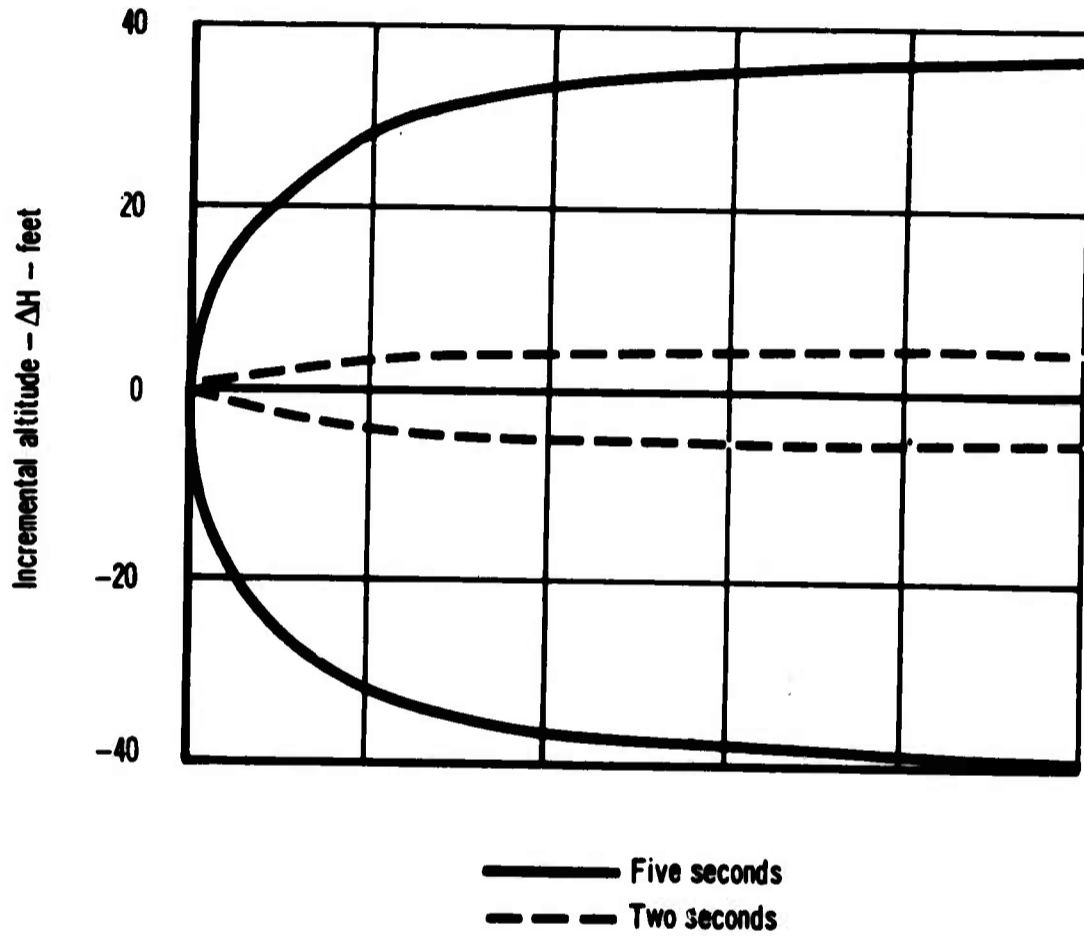


Figure 5 Model F-4J  
Effect of Flap Deflection Rate

Note: - - - - Required stabilator deflection  
 ————— Selected DLC-stabilator interconnect schedule

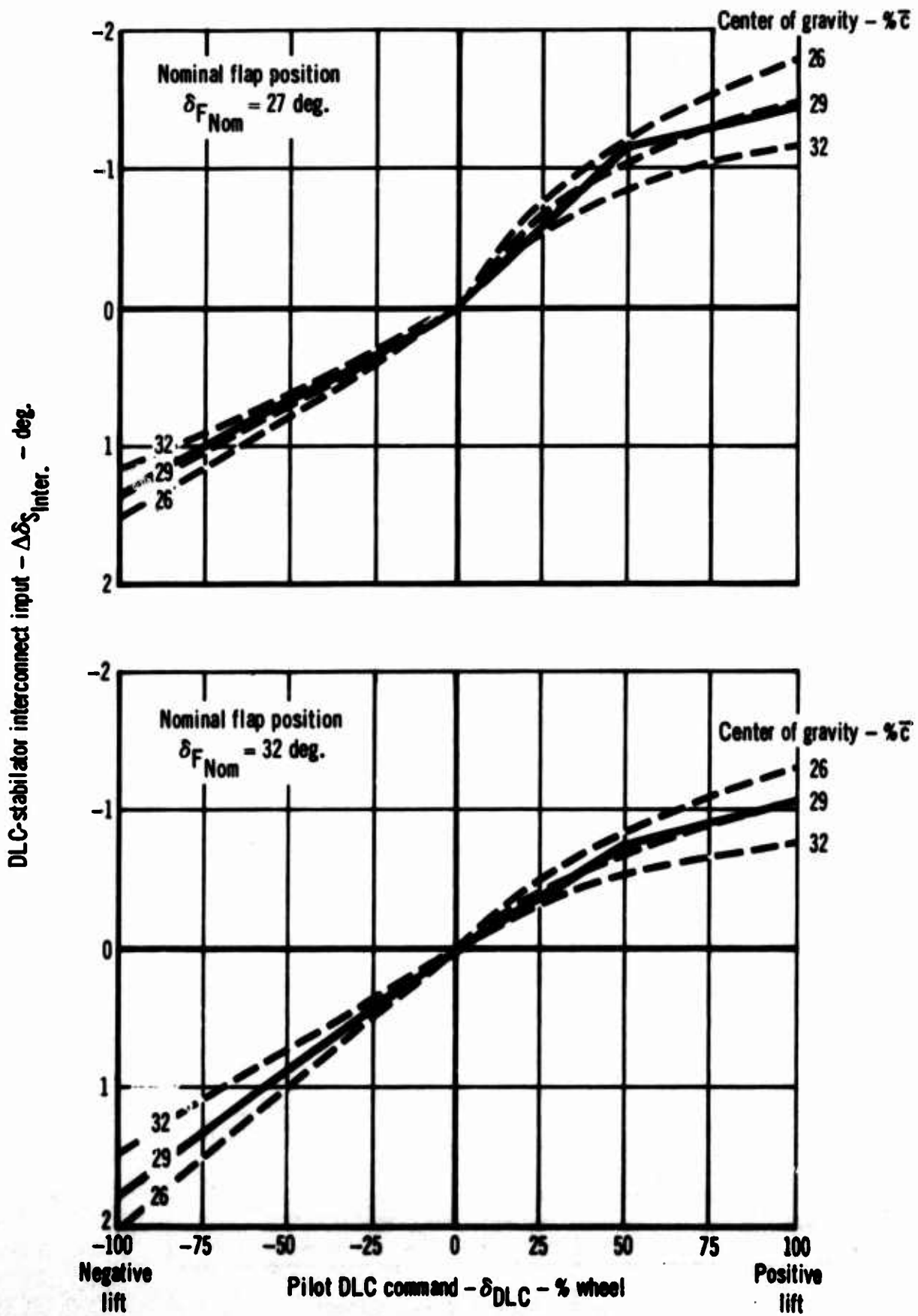


Figure 6 Model F-4J  
 DLC-Stabilator Interconnect Requirements

$\delta_{F \text{ Nom}} = 27^\circ$       C.G. at 29%  $\bar{c}$        $V_{\text{Trim}} = 142.0 \text{ KCAS}$   
 G.W. = 34,000 Lb.       $\alpha_{w \text{ Trim}} = 13^\circ$        $\gamma_0 = 0^\circ$   
 $\Delta V = 0$

No Interconnect

Pilot DLC command -  $\delta_{\text{DLC}}$  - 100% wheel (positive)

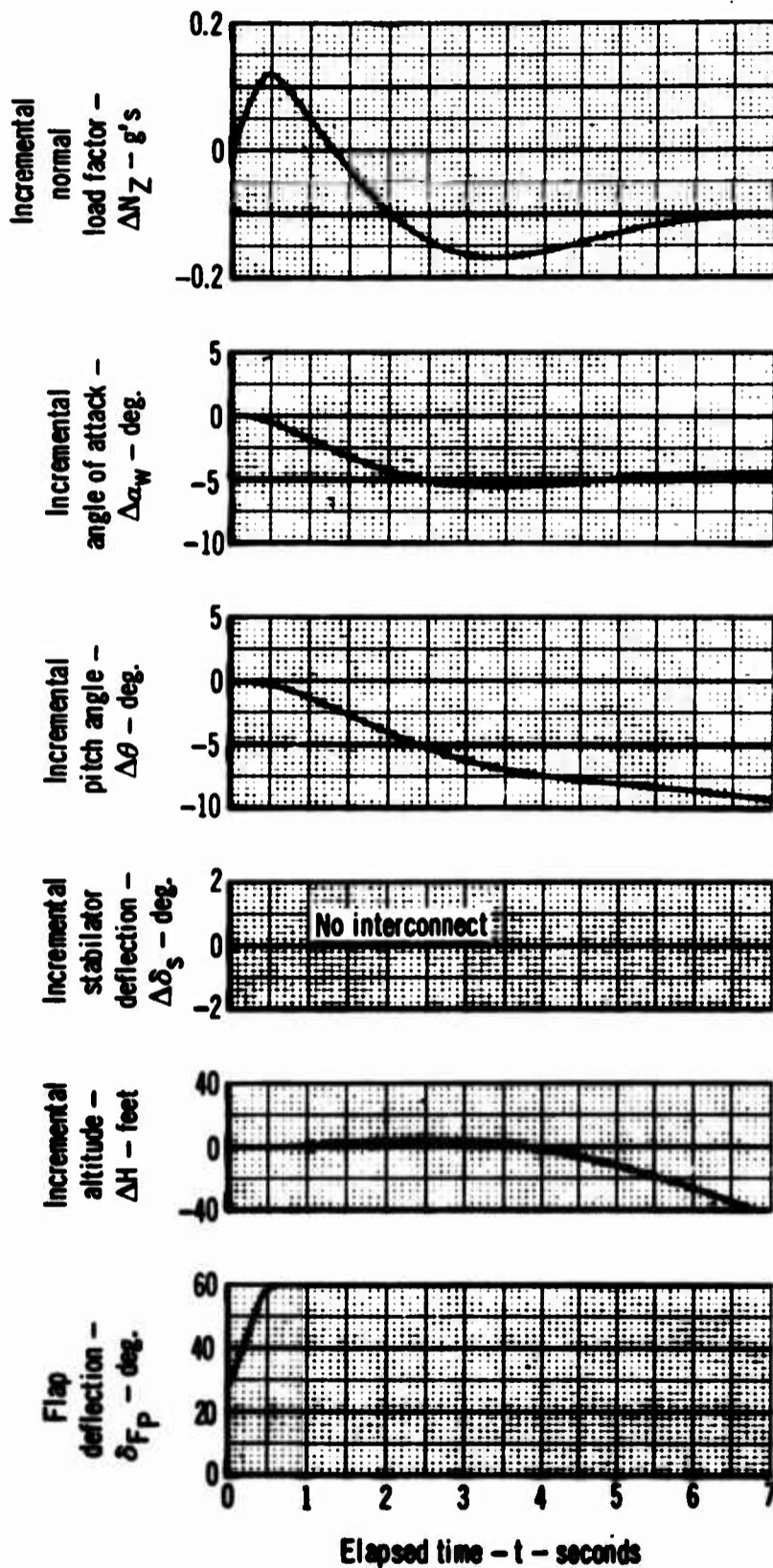


Figure 7.a Model F-4J  
Effect of DLC-Stabilator Interconnect

$\delta F_{Nom} = 27^{\circ}$       C.G. at 29%  $\bar{c}$        $V_{Trim} = 142.0$  KCAS  
 G.W. = 34,000 Lb.       $a_{wTrim} = 13^{\circ}$        $\gamma_0 = 0^{\circ}$   
 $\Delta V = 0$

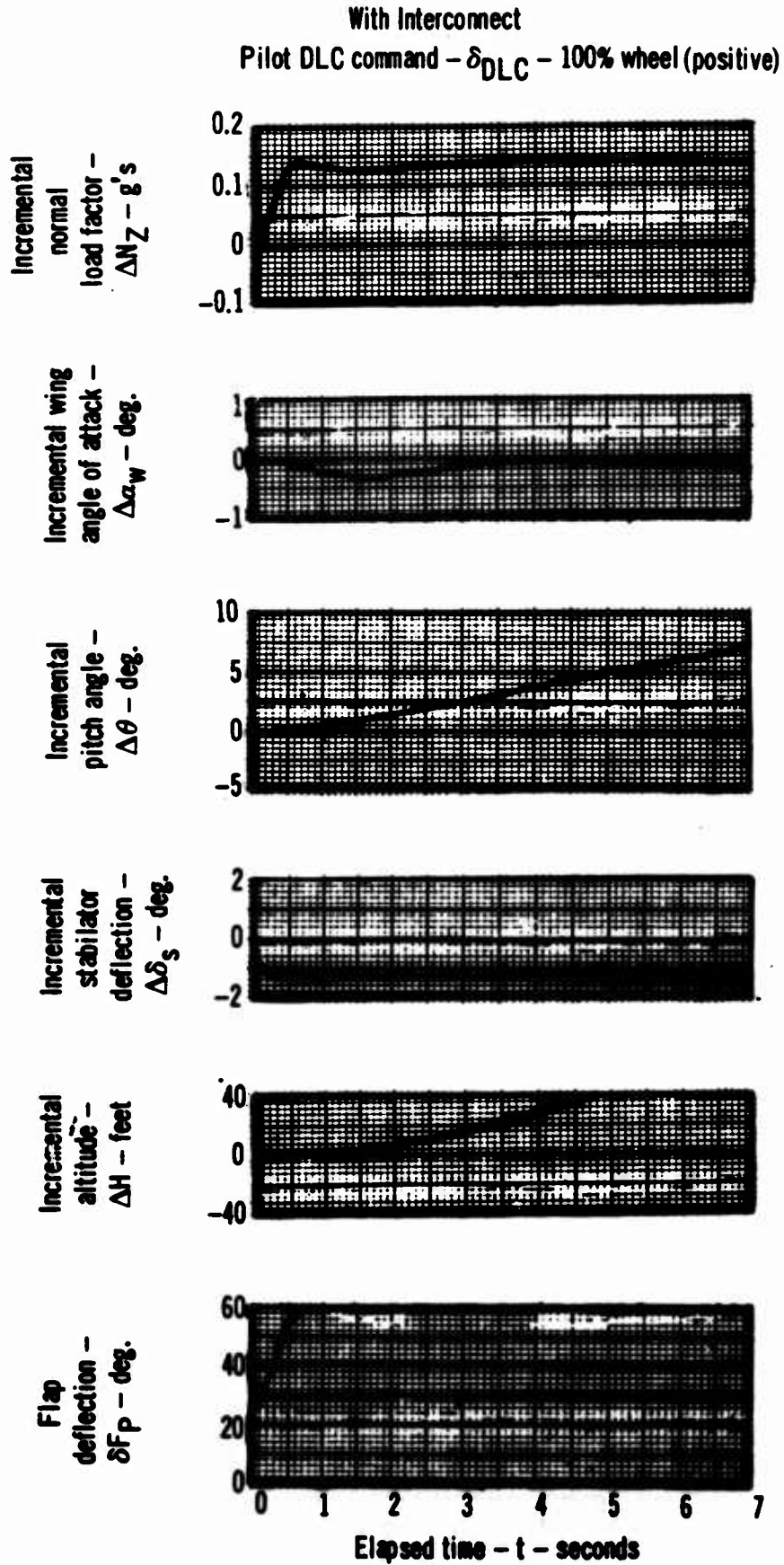


Figure 7.b Model F-4J  
Effect of DLC-Stabilator Interconnect

$$\delta_{F \text{ Nom.}} = 27^\circ; \gamma_0 = 0^\circ; \alpha_{w \text{ Trim}} = 13^\circ$$

Symbol	C.G. (% $\bar{c}$ )	G.W. (Lb.)	$V_{\text{Trim}}$ (KCAS)	APCS	Interconnect
————	29	34,000	142.0	$\Delta V=0$	In
-----	29	34,000	142.0	$\Delta V=0$	Out
.....	29	34,000	142.0	$\Delta V=0$	$\Delta C_{m_{FP}} = 0$

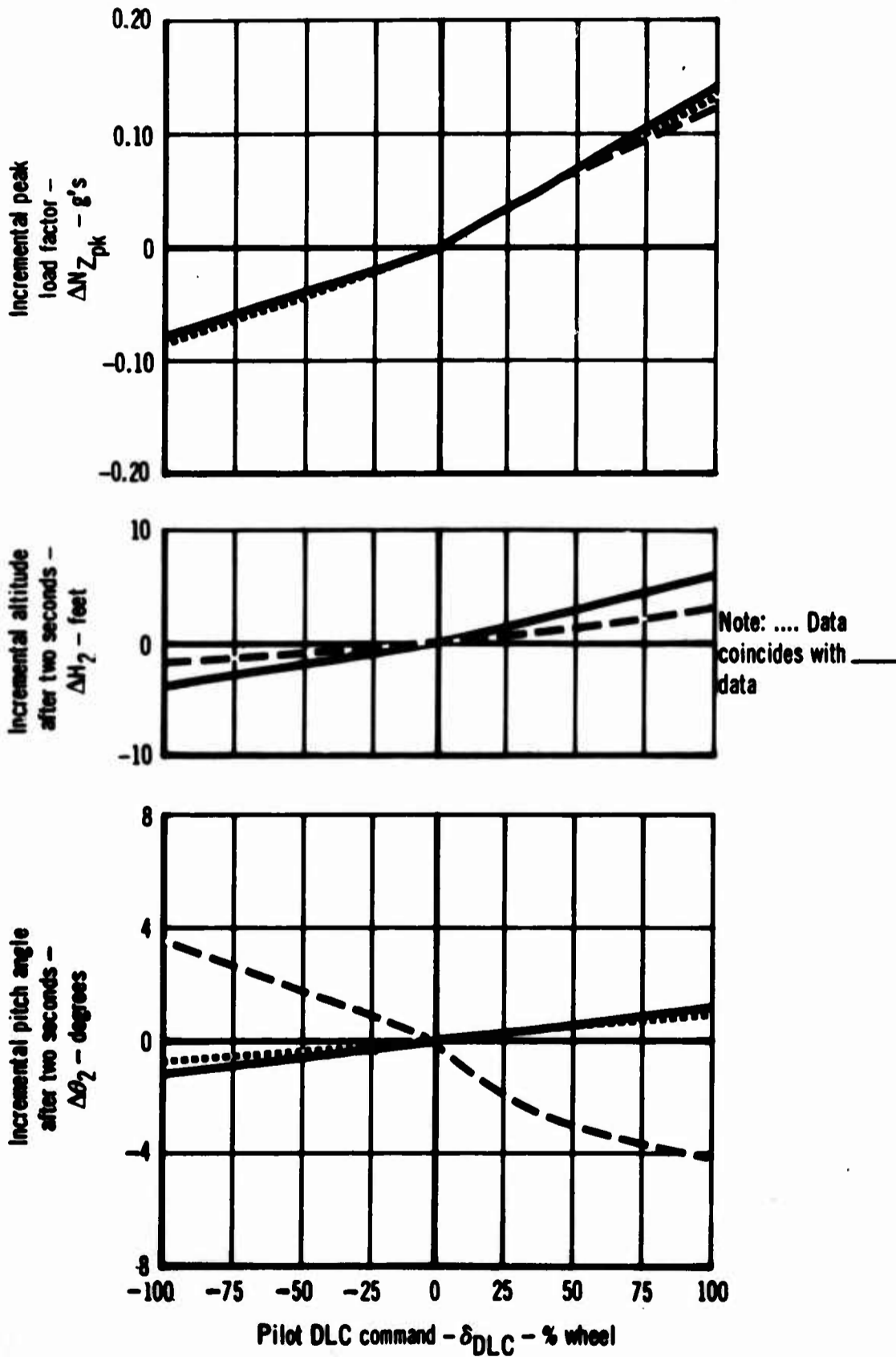


Figure 8.a Model F-4J  
Effect of DLC-Stabilator Interconnect

$$\delta_{F \text{ Nom.}} = 27^\circ; \gamma_0 = 0^\circ; \alpha_{w \text{ Trim}} = 13^\circ$$

Symbol	C.G. (%E)	G.W. (Lb.)	V <sub>Trim</sub> (KCAS)	APCS	Interconnect
—————	29	34,000	142.0	$\Delta V=0$	In
- - - - -	29	34,000	142.0	$\Delta V=0$	Out
.....	29	34,000	142.0	$\Delta V=0$	$\Delta C_{m_{FP}} = 0$

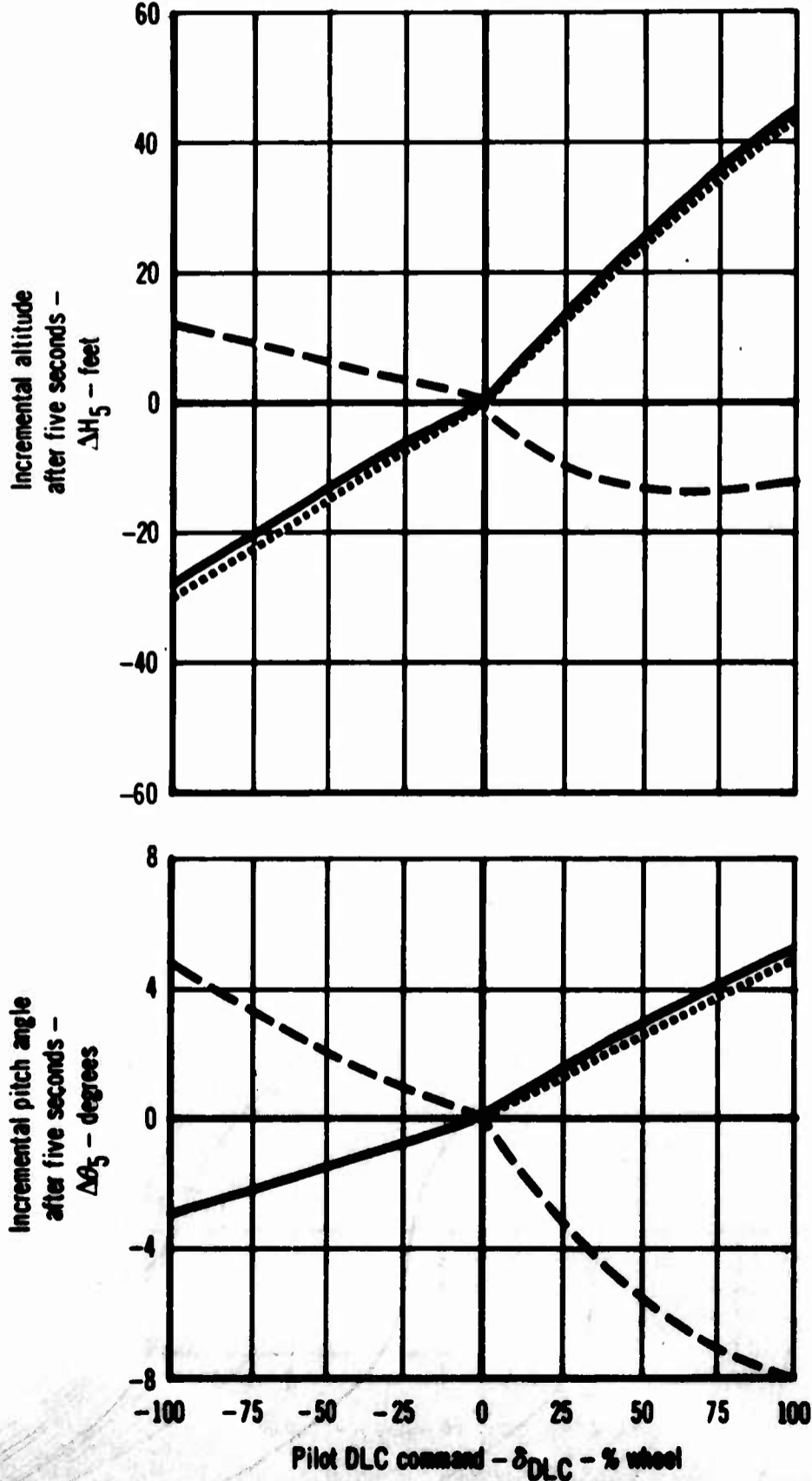


Figure 8.b Model F-4J  
Effect of DLC-Stabilator Interconnect

$$\delta_{F_{Nom.}} = 32^\circ; \gamma_0 = 0^\circ; \alpha_{w_{Trim}} = 13^\circ$$

Symbol	C.G. (%C)	G.W. (Lb.)	V <sub>Trim</sub> (KCAS)	APCS	Interconnect
—————	29	34,000	140.0	$\Delta V=0$	In
- - - - -	29	34,000	140.0	$\Delta V=0$	Out
.....	29	34,000	140.0	$\Delta V=0$	$\Delta C_{m_{Fp}} = 0$

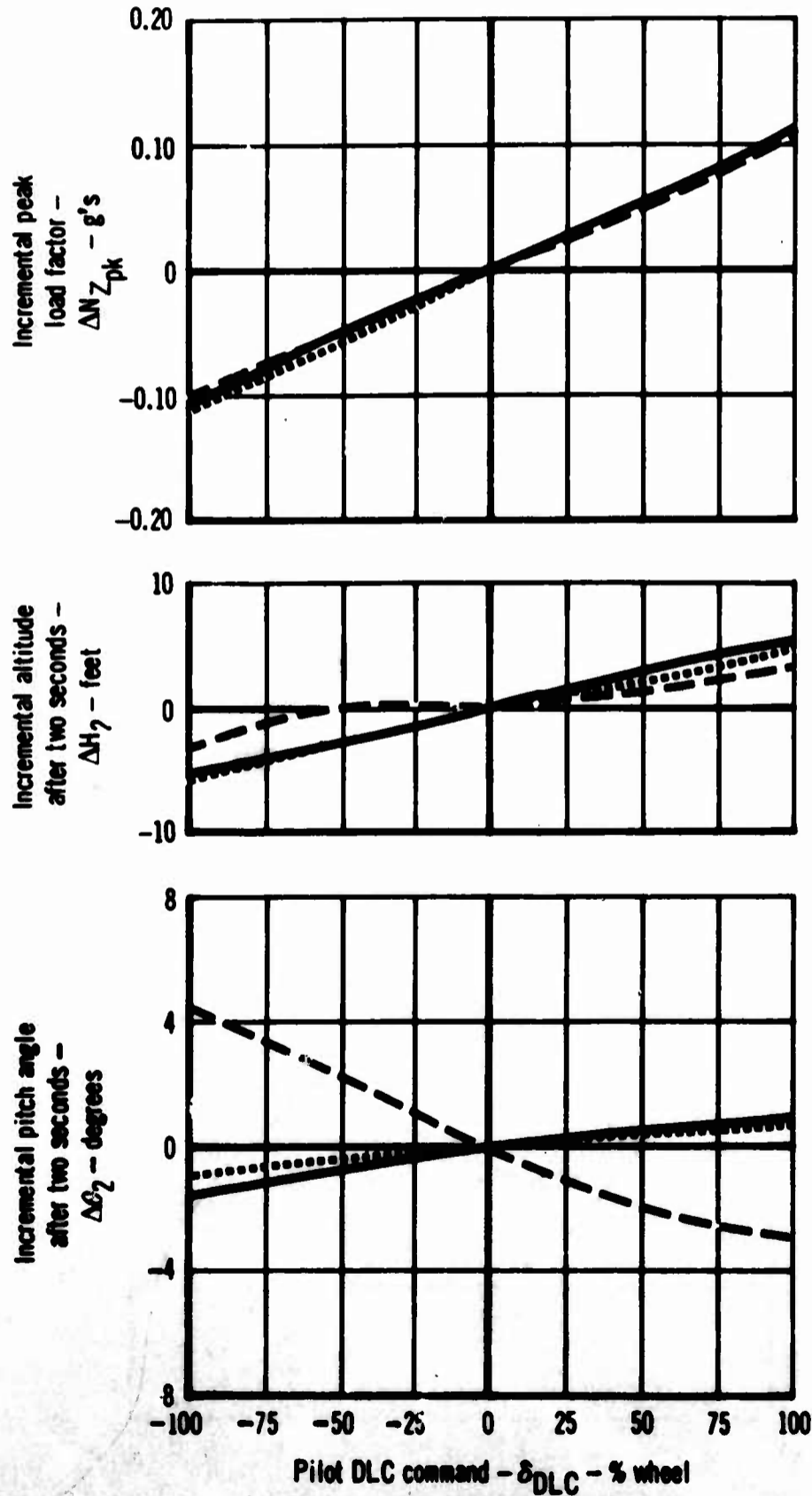


Figure 9.a Model F-4J  
Effect of DLC-Stabilator Interconnect

$$\delta_{F \text{ Nom.}} = 32^\circ; \gamma_0 = 0^\circ; a_{w \text{ Trim}} = 13^\circ$$

Symbol	C.G. (%C)	G.W. (Lb.)	V <sub>Trim</sub> (KCAS)	APCS	Interconnect
—————	29	34,000	140.0	$\Delta V=0$	In
- - - - -	29	34,000	140.0	$\Delta V=0$	Out
.....	29	34,000	140.0	$\Delta V=0$	$\Delta C_{m \text{ FP}}=0$

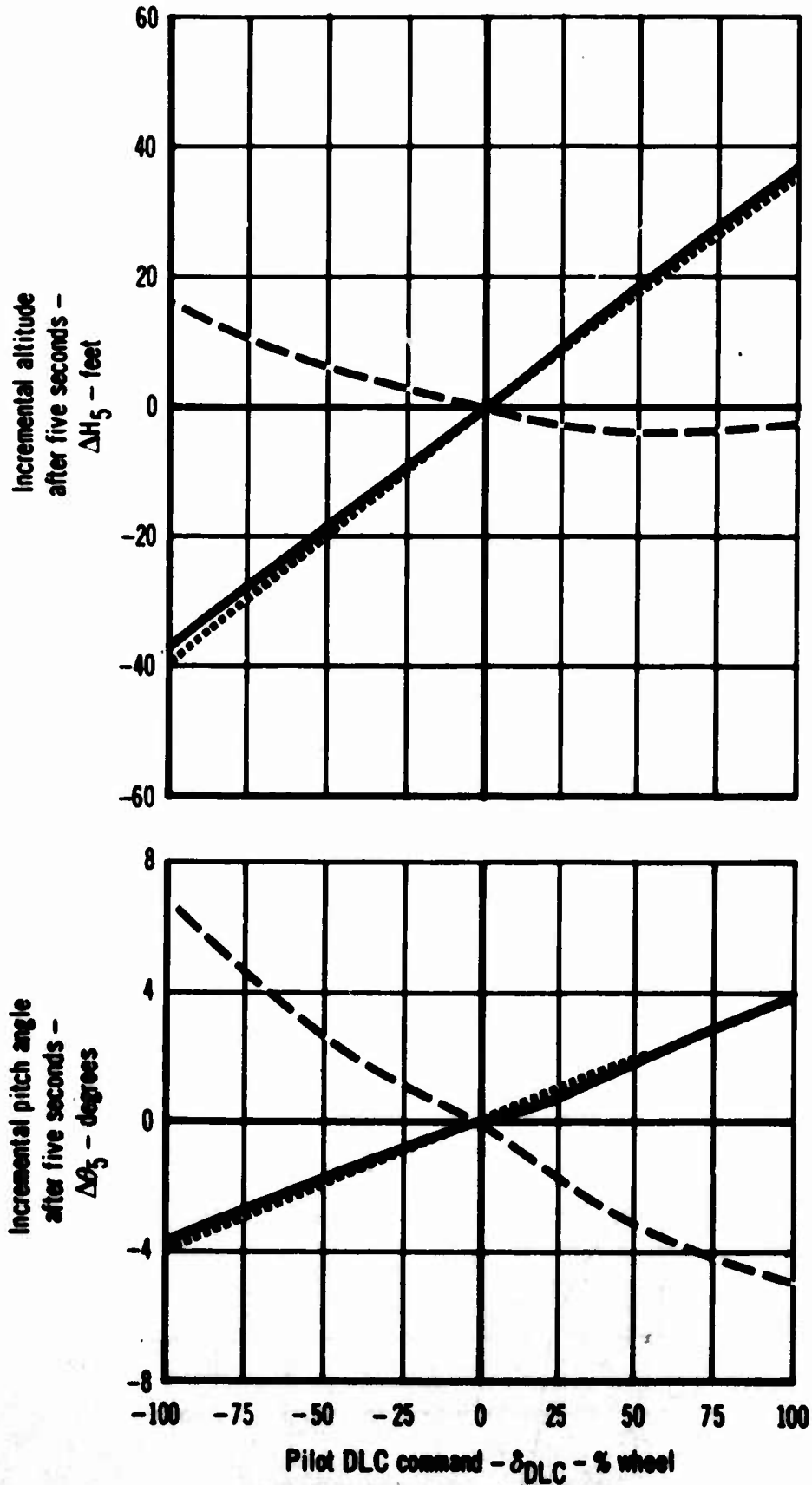


Figure 9.b Model F-4J  
Effect of DLC-Stabilator Interconnect

$$\delta_{F_{Nom.}} = 27^{\circ}; \gamma_0 = 0^{\circ}; a_{w_{Trim}} = 13^{\circ}$$

Symbol	C.G. (%E)	G.W. (Lb.)	V <sub>Trim</sub> (KCAS)	APCS	Interconnect
.....	26	34,000	143.4	$\Delta V=0$	In
————	29	34,000	142.0	$\Delta V=0$	In
-----	32	34,000	140.9	$\Delta V=0$	In

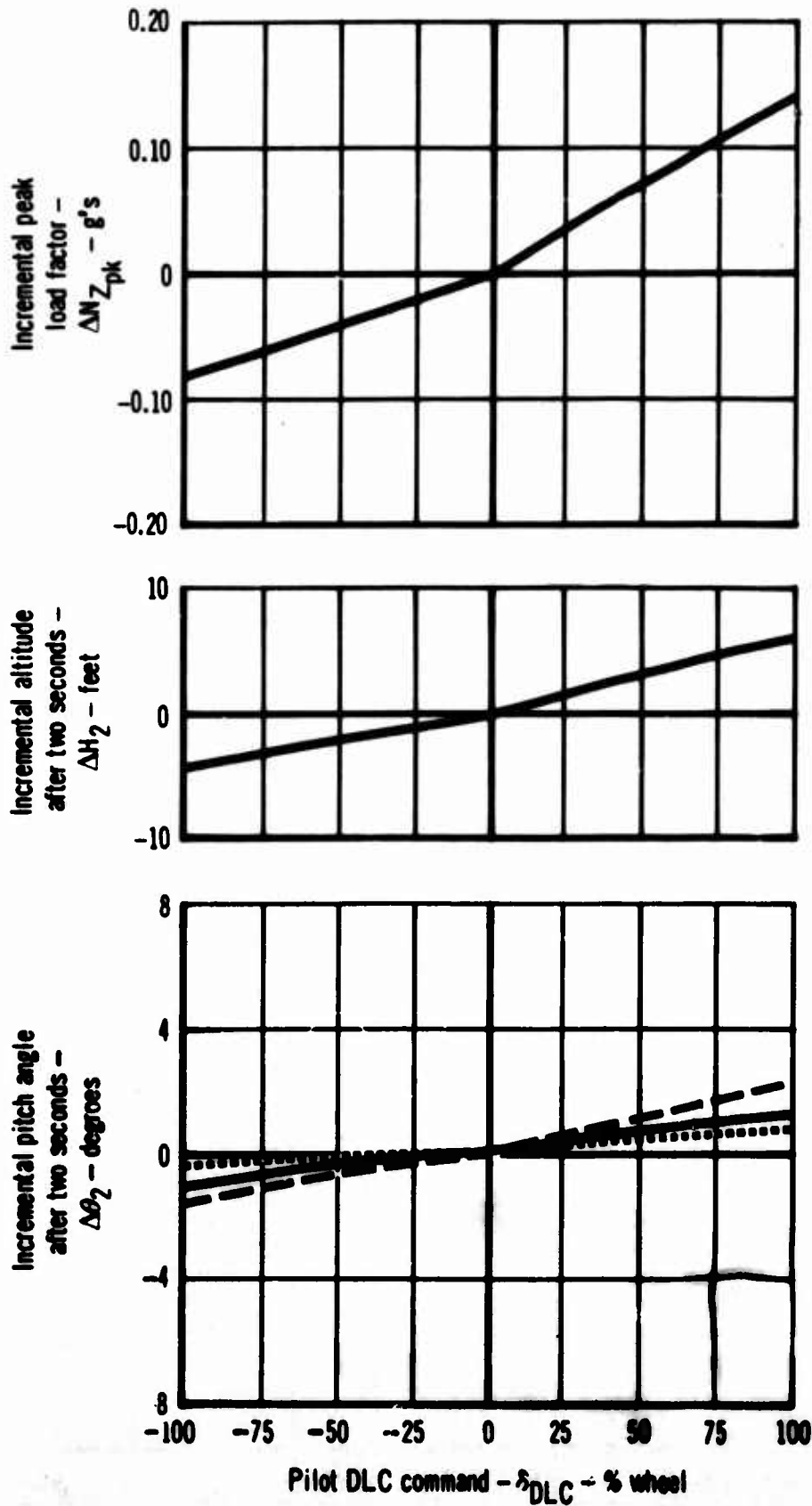


Figure 10.a Model F-4J  
Effect of Center of Gravity

$$\delta_{F_{Nom.}} = 32^\circ; \gamma_0 = 0^\circ; \alpha_{w_{Trim}} = 13^\circ$$

Symbol	C.G. (%C)	G.W. (Lb.)	V <sub>Trim</sub> (KCAS)	APCS	Interconnect
————	29	34,000	140.0	$\Delta V=0$	In
- - - -	29	34,000	140.0	$\Delta V=0$	Out
.....	29	34,000	140.0	$\Delta V=0$	$\Delta C_{m_{Fp}} = 0$

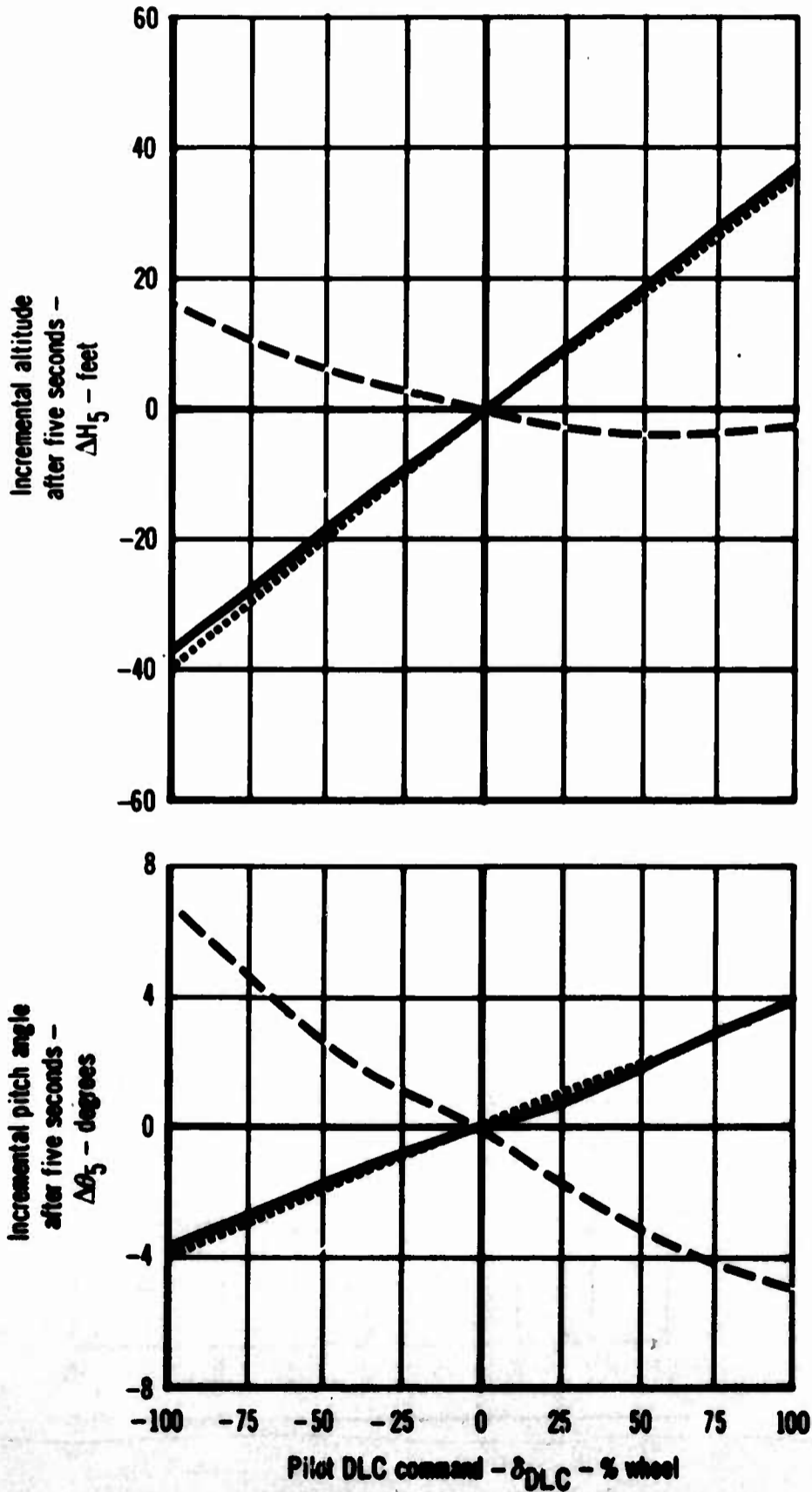


Figure 9.b Model F-4J  
Effect of DLC-Stabilator Interconnect

$$\delta_{F \text{ Nom.}} = 27^\circ; \gamma_0 = 0^\circ; \alpha_{w \text{ Trim}} = 13^\circ$$

Symbol	C.G. (% $\bar{c}$ )	G.W. (Lb.)	V <sub>Trim</sub> (KCAS)	APCS	Interconnect
.....	26	34,000	143.4	$\Delta V=0$	In
————	29	34,000	142.0	$\Delta V=0$	In
- - - -	32	34,000	140.9	$\Delta V=0$	In

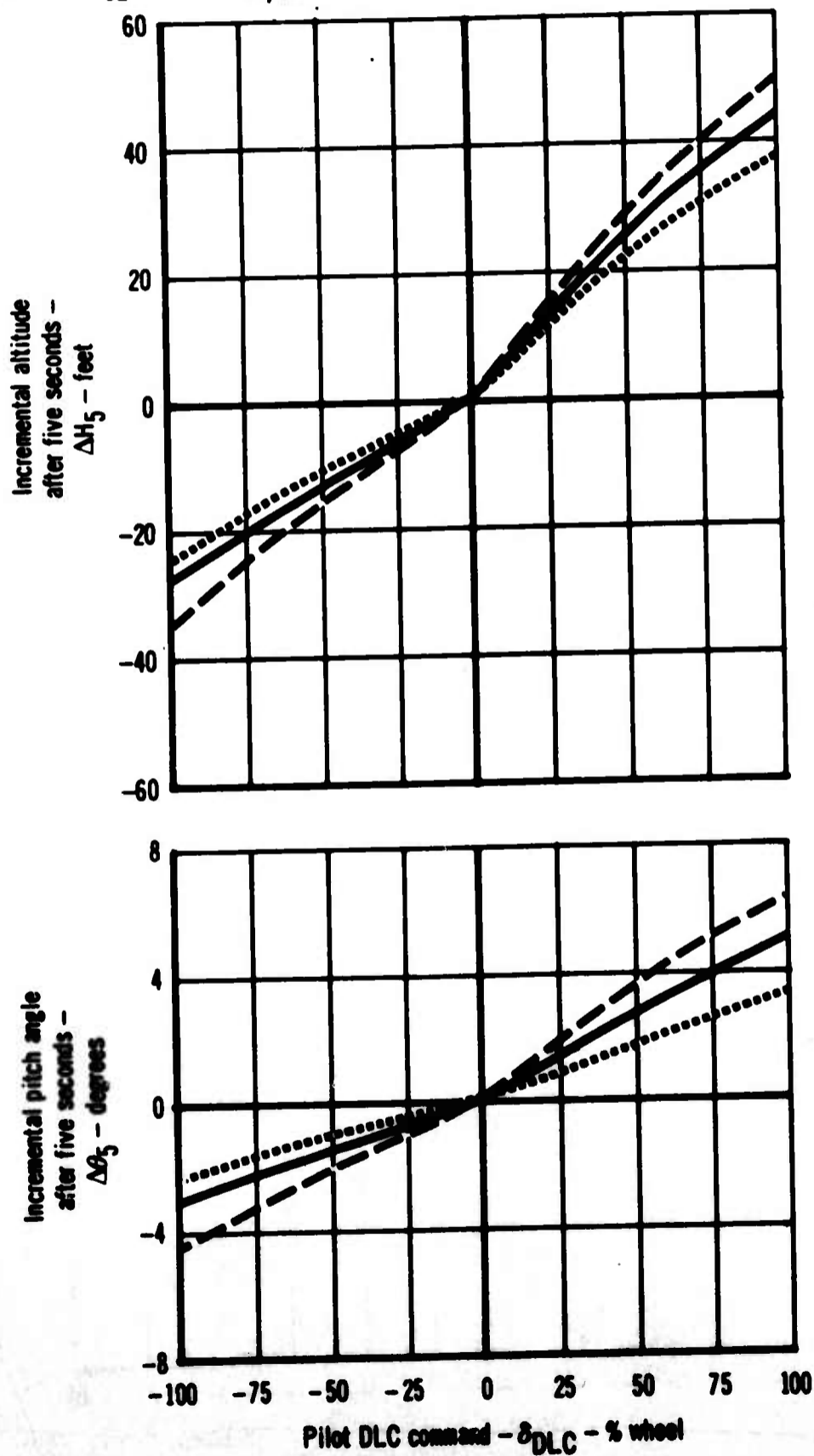


Figure 10.b Model F-4J  
Effect of Center of Gravity

$$\delta_{F_{Nom.}} = 32^\circ; \gamma_0 = 0^\circ; \alpha_{wTrim} = 13^\circ$$

Symbol	C.G. (% $\bar{c}$ )	G.W. (Lb.)	V <sub>Trim</sub> (KCAS)	APCS	Interconnect
.....	26	34,000	141.2	$\Delta V=0$	In
————	29	34,000	140.0	$\Delta V=0$	In
-----	32	34,000	138.9	$\Delta V=0$	In

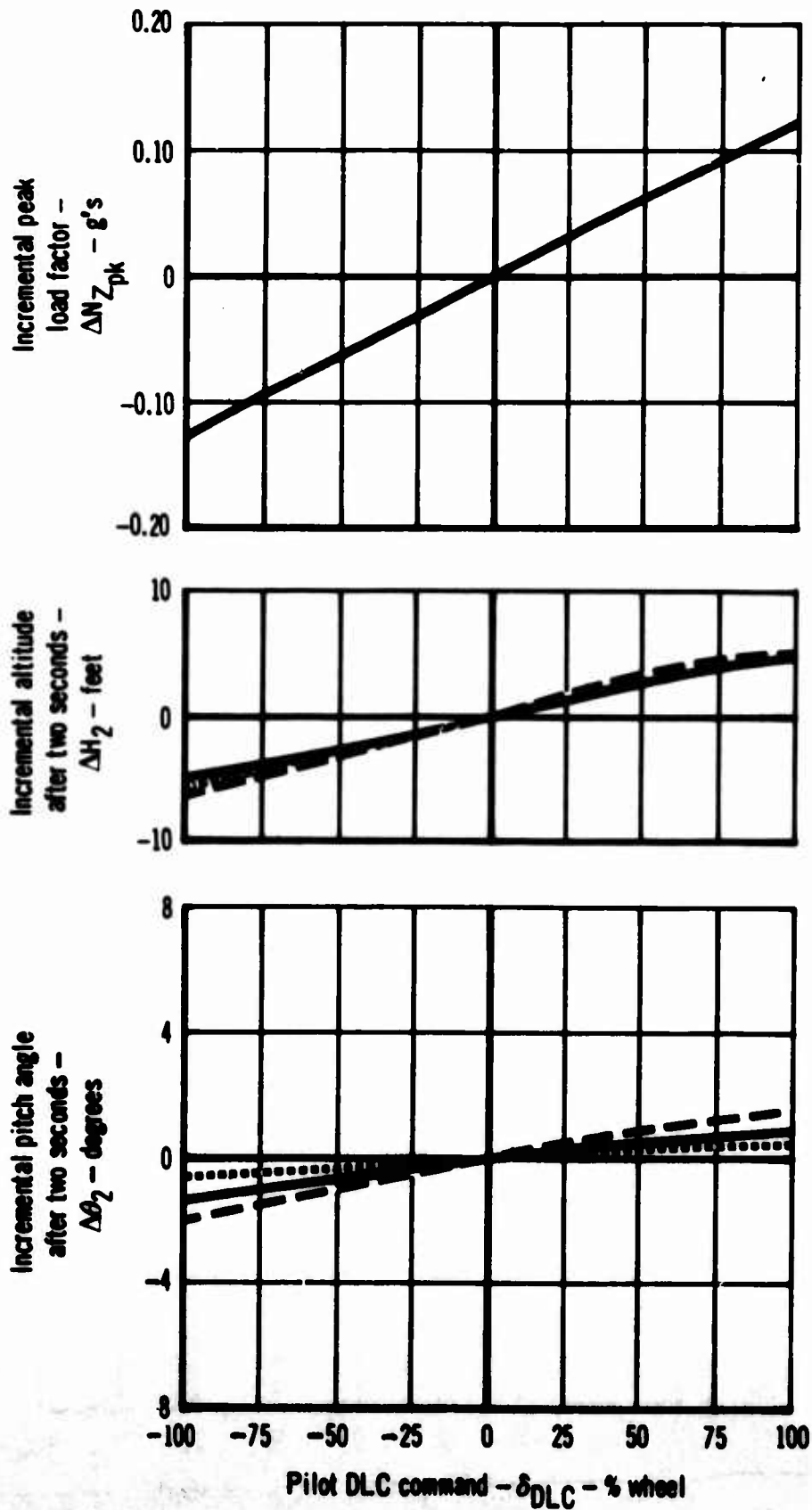


Figure 11.a Model F-4J  
Effect of Center of Gravity

$$\delta_{F \text{ Nom.}} = 32^\circ; \gamma_0 = 0^\circ; \alpha_{w \text{ Trim}} = 13^\circ$$

Symbol	C.G. (%C)	G.W. (Lb.)	V <sub>Trim</sub> (KCAS)	APCS	Interconnect
.....	26	34,000	141.2	$\Delta V=0$	In
————	29	34,000	140.0	$\Delta V=0$	In
-----	32	34,000	138.9	$\Delta V=0$	In

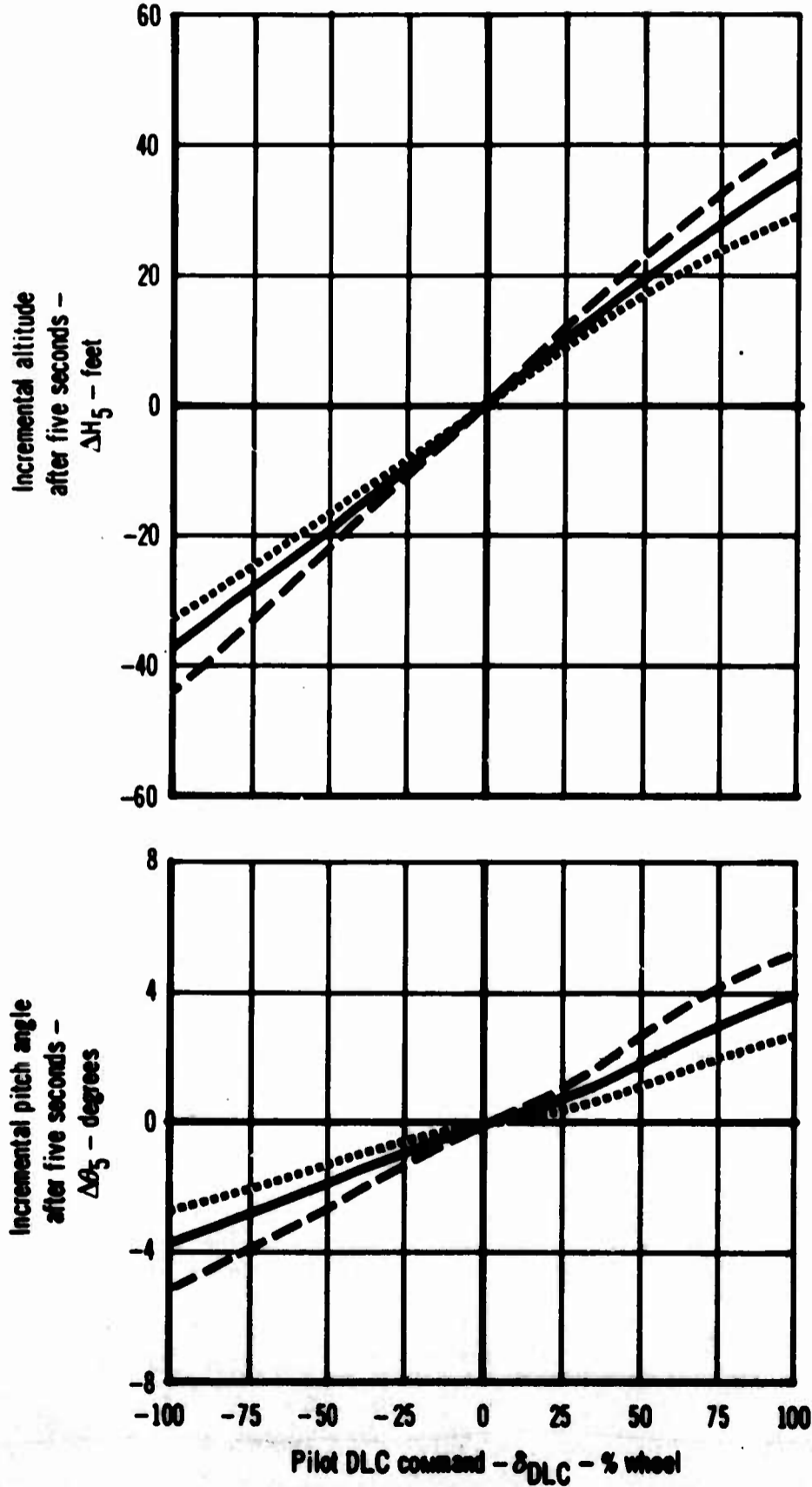
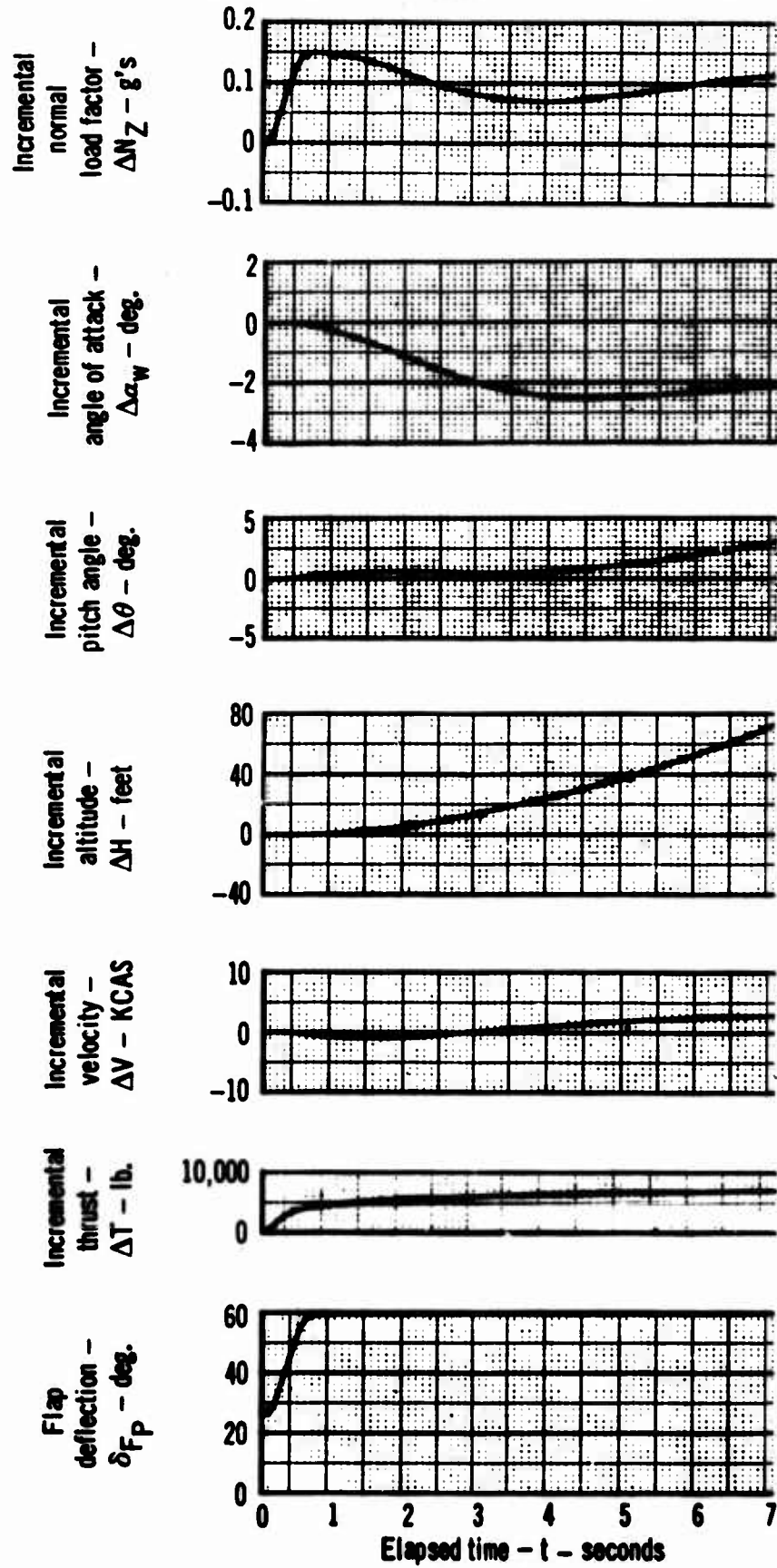


Figure 11.b Model F-4J  
Effect of Center of Gravity

$\delta_{F_{Nom}} = 27^\circ$                       C.G. at 29%  $\bar{c}$                        $V_{Trim} = 142.0$  KCAS  
 G.W. = 34,000 Lb.                       $\alpha_{w_{Trim}} = 13^\circ$                        $\gamma_0 = 0^\circ$

With APCS and DLC-stabilator interconnect  
 Pilot DLC command -  $\delta_{DLC}$  - 100% wheel (positive)



**Figure 12.a Model F-4J**  
**Effect of Approach Power Compensation System**

$\delta_{F \text{ Nom}} = 27^\circ$       C.G. at 29%  $\bar{c}$        $V_{\text{Trim}} = 142.0 \text{ KCAS}$   
 G.W. = 34,000 Lb.       $\alpha_{w \text{ Trim}} = 13^\circ$        $\gamma_0 = 0^\circ$

Without APCS but with DLC-stabilator interconnect  
 Pilot DLC command -  $\delta_{\text{DLC}}$  - 100% wheel (positive)

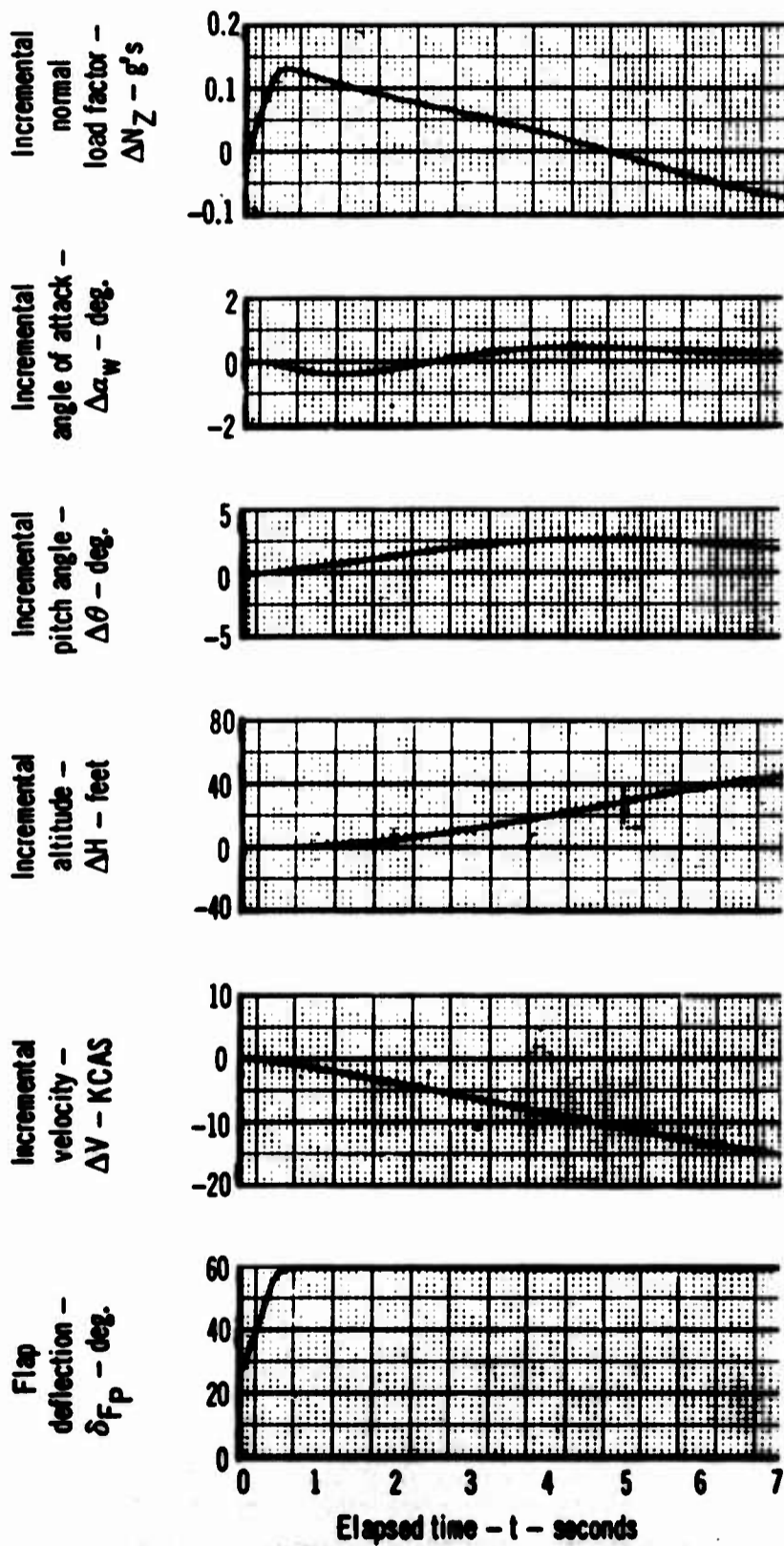


Figure 12.b Model F-4J  
 Effect of Approach Power Compensation System

$\delta_{F_{Nom}} = 27^\circ$       C.G. at 29%  $\bar{c}$        $V_{Trim} = 142.0$  KCAS  
 G.W. = 34,000 Lb.       $\alpha_{wTrim} = 13^\circ$        $\gamma_0 = 0^\circ$   
 With APCS and DLC-stabilator interconnect  
 Pilot DLC command -  $\delta_{DLC}$  - 100% wheel (negative)

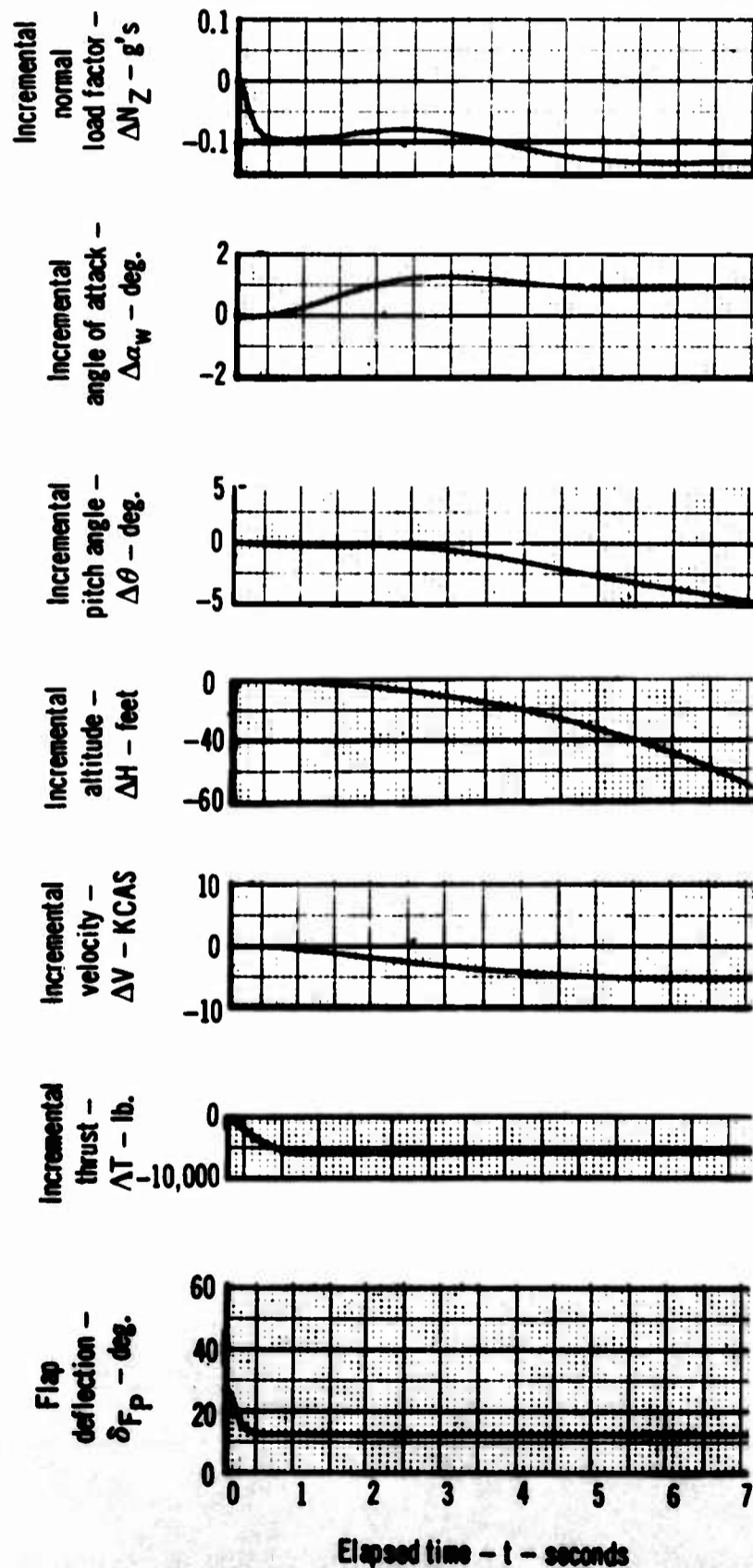


Figure 12.c Model F-4J  
Effect of Approach Power Compensation System

$\delta_{F\text{Nom}} = 27^\circ$       C.G. at 29%  $\bar{c}$        $V_{\text{Trim}} = 142.0$  KCAS  
 G.W. = 34,000 Lb.       $\alpha_{w\text{Trim}} = 13^\circ$        $\gamma_0 = 0^\circ$

Without APCS but with DLC-stabilator interconnect  
 Pilot DLC command -  $\delta_{\text{DLC}}$  - 100% wheel (negative)

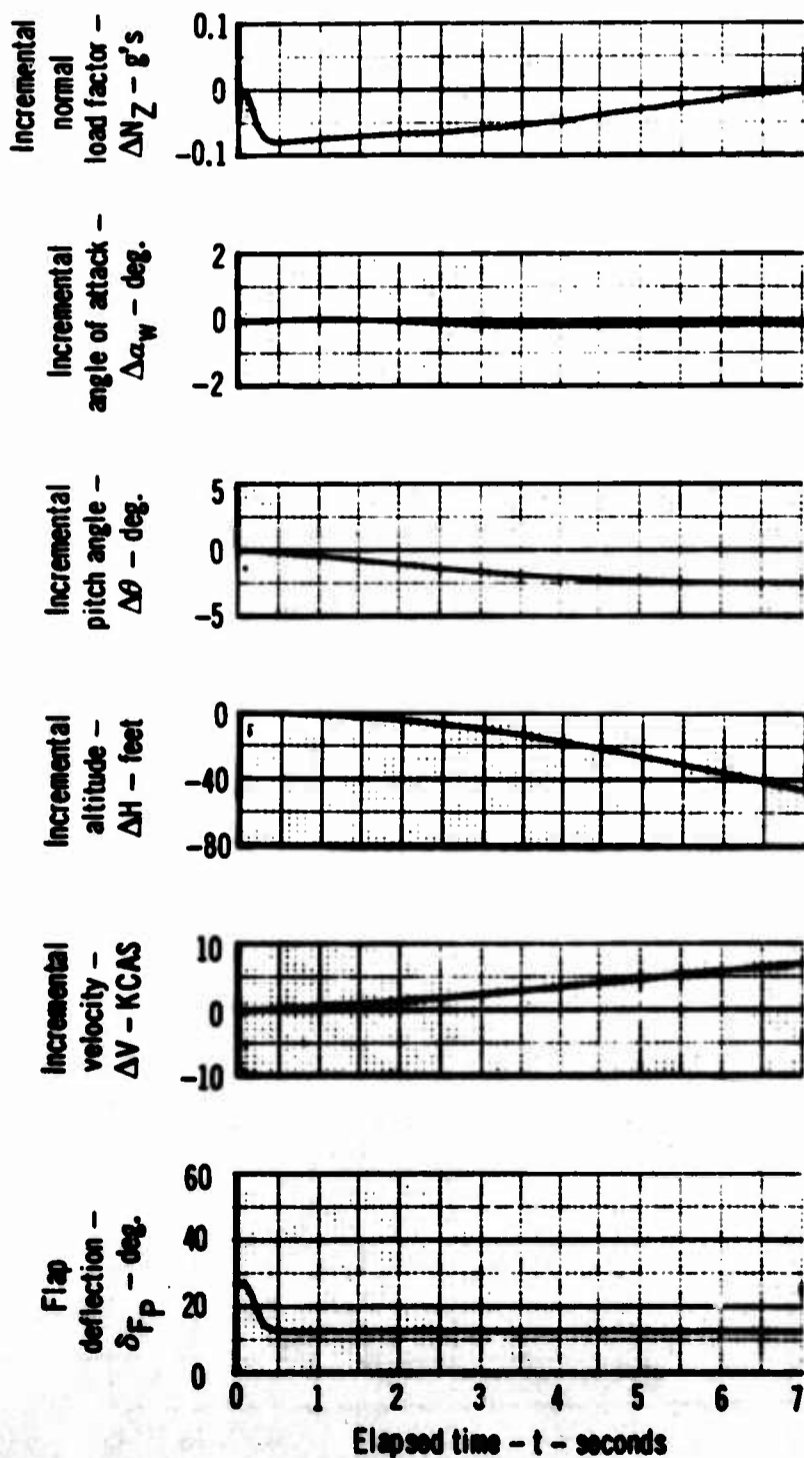


Figure 12.d Model F-4J  
 Effect of Approach Power Compensation System

$$\delta_{F_{Nom.}} = 27^{\circ}; \gamma_0 = 0^{\circ}; \alpha_{w_{Trim}} = 13^{\circ}$$

Symbol	C.G. (% $\bar{c}$ )	G.W. (Lb.)	$V_{Trim}$ (KCAS)	APCS	Interconnect
————	29	34,000	142.0	Out	In
- - - - -	29	34,000	142.0	In	In

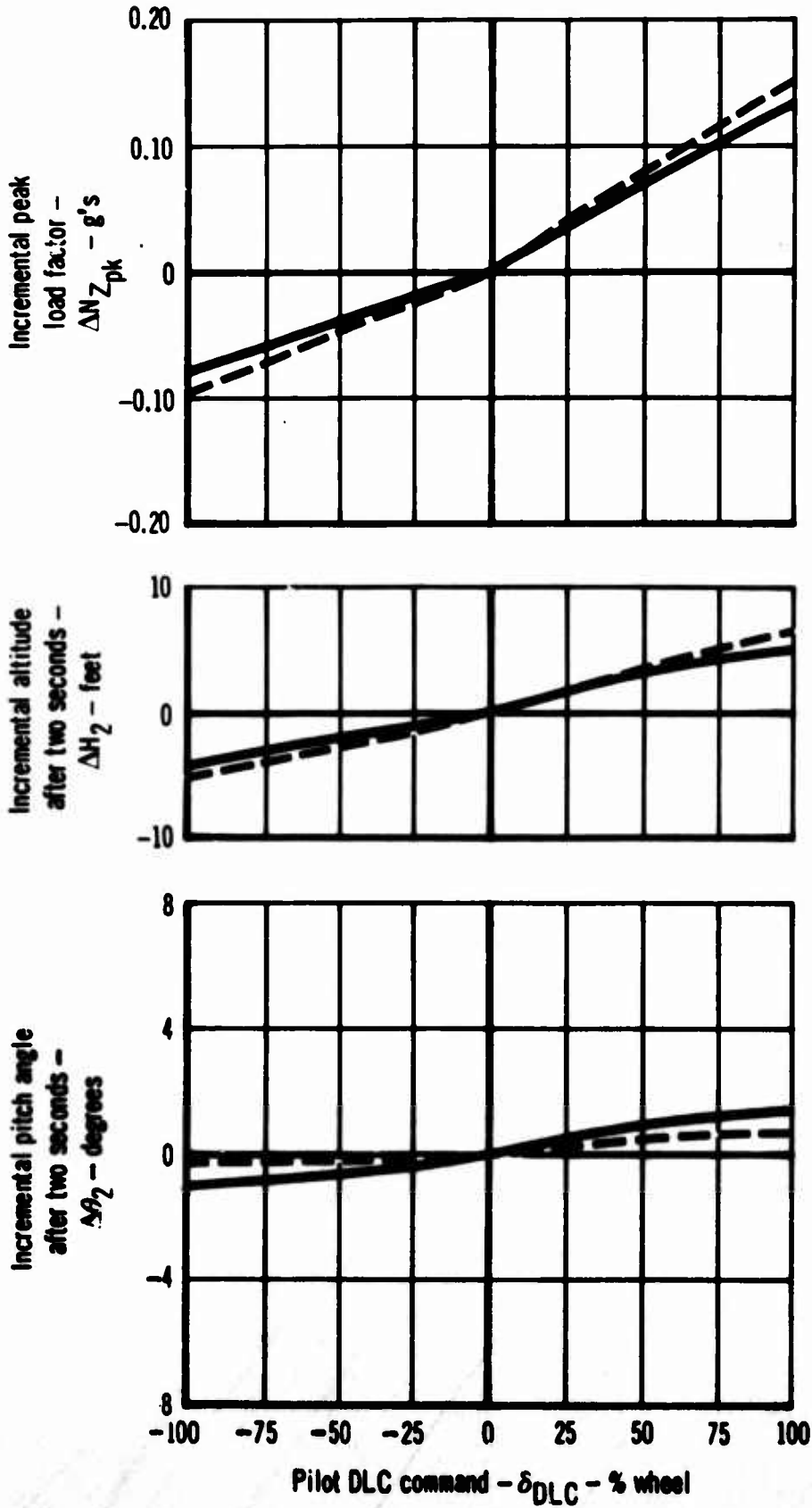


Figure 13.a Model F-4J  
Effect of Approach Power Compensation System

$$\delta_{F \text{ Nom.}} = 27^\circ; \gamma_0 = 0^\circ; \alpha_{w \text{ Trim}} = 13^\circ$$

Symbol	C.G. (%C)	G.W. (Lb.)	V <sub>Trim</sub> (KCAS)	APCS	Interconnect
————	29	34,000	142.0	Out	In
-----	29	34,000	142.0	In	In

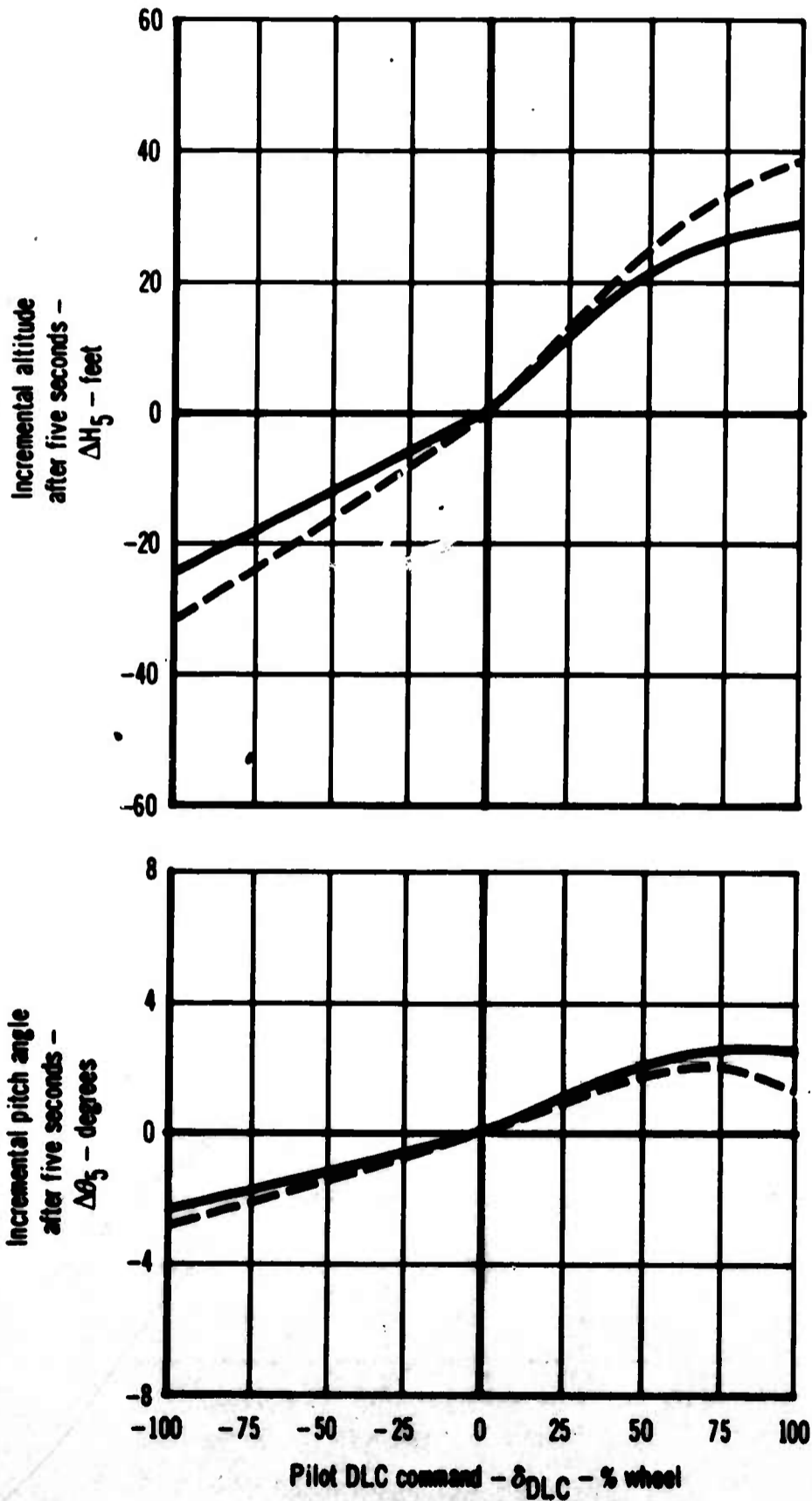


Figure 13.b Model F-4J  
Effect of Approach Power Compensation System

$$\delta_{F_{Nom.}} = 27^{\circ}; \gamma_0 = 0^{\circ}; \alpha_{w_{Trim}} = 13^{\circ}$$

Symbol	C.G. (% $\bar{c}$ )	G.W. (Lb.)	V <sub>Trim</sub> (KCAS)	APCS	Interconnect
—————	29	34,000	142.0	Out	In
- - - - -	29	34,000	142.0	In	In

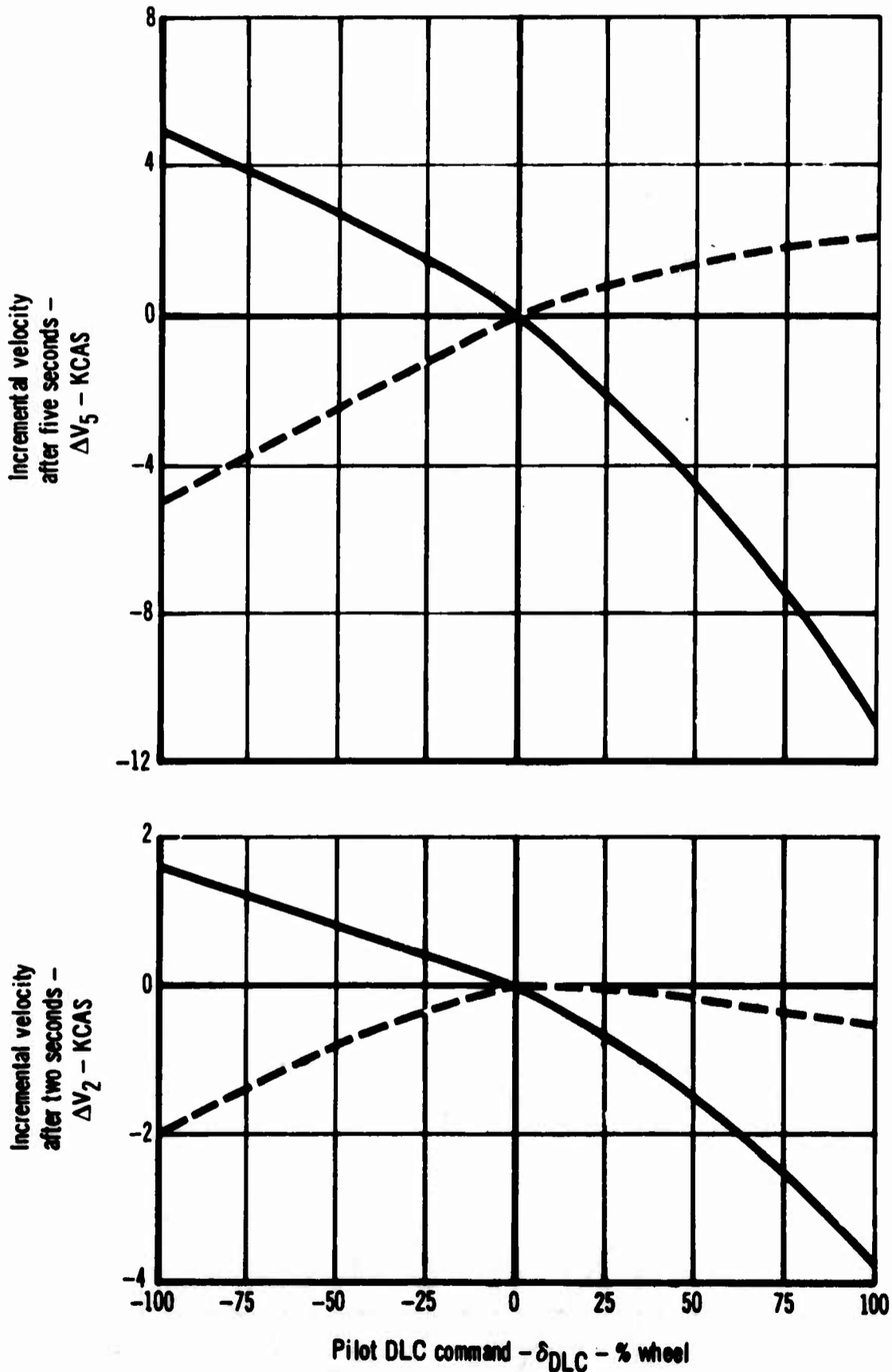


Figure 13.c Model F-4J  
Effect of Approach Power Compensation System

$$\delta_{F \text{ Nom.}} = 32^\circ; \gamma_0 = 0^\circ; \alpha_{w \text{ Trim}} = 13^\circ$$

Symbol	C.G. (%C)	G.W. (Lb.)	V <sub>Trim</sub> (KCAS)	APCS	Interconnect
—	29	34,000	140.0	Out	In
- - -	29	34,000	140.0	In	In

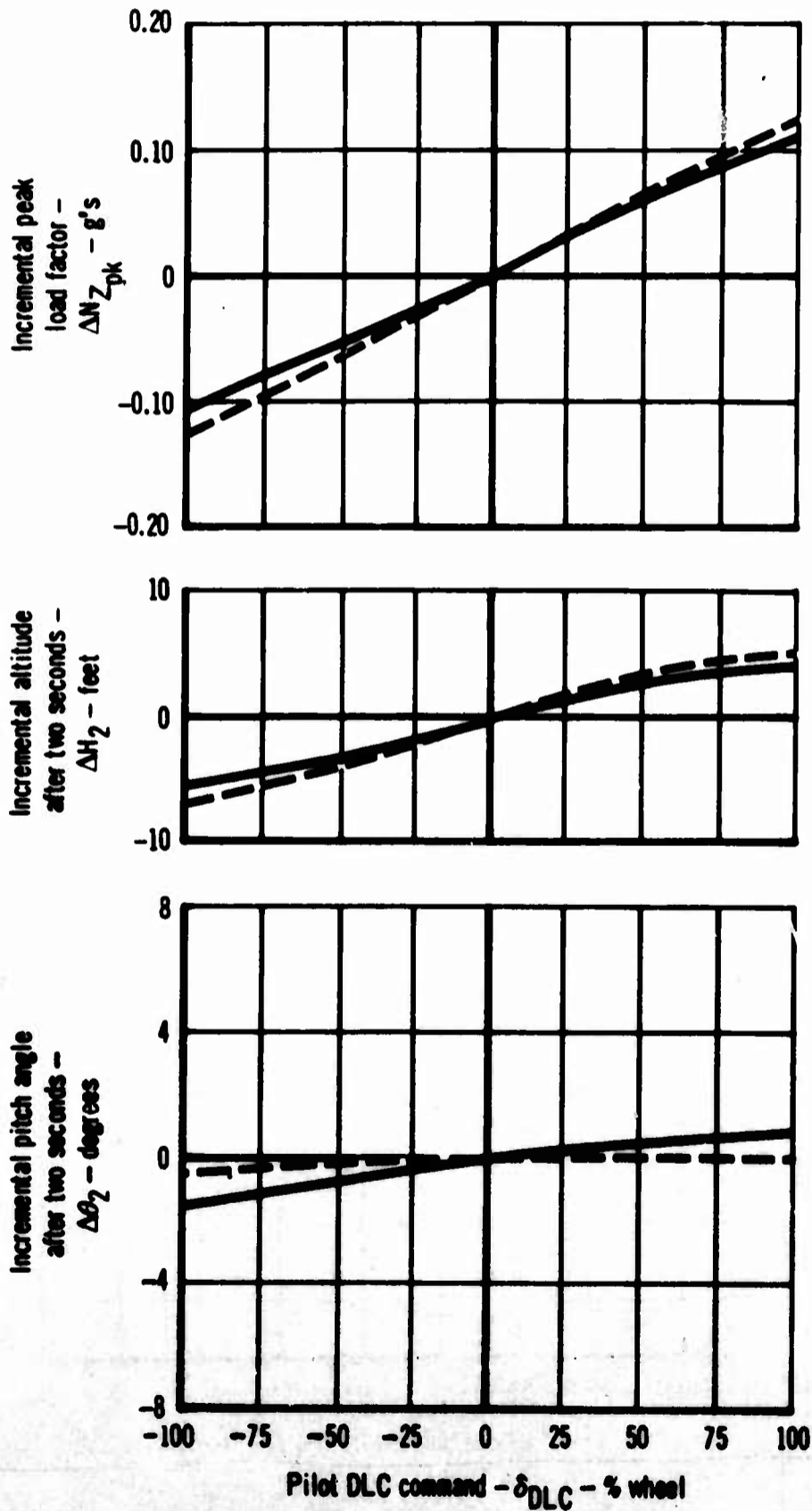


Figure 14.a Model F-4J  
Effect of Approach Power Compensation System

$$\delta_{F_{Nom.}} = 32^{\circ}; \gamma_0 = 0^{\circ}; \alpha_{w_{Trim}} = 13^{\circ}$$

Symbol	C.G. (% $\bar{c}$ )	G.W. (Lt.)	V <sub>Trim</sub> (KCAS)	APCS	Interconnect
————	29	34,000	140.0	Out	In
-----	29	34,000	140.0	In	In

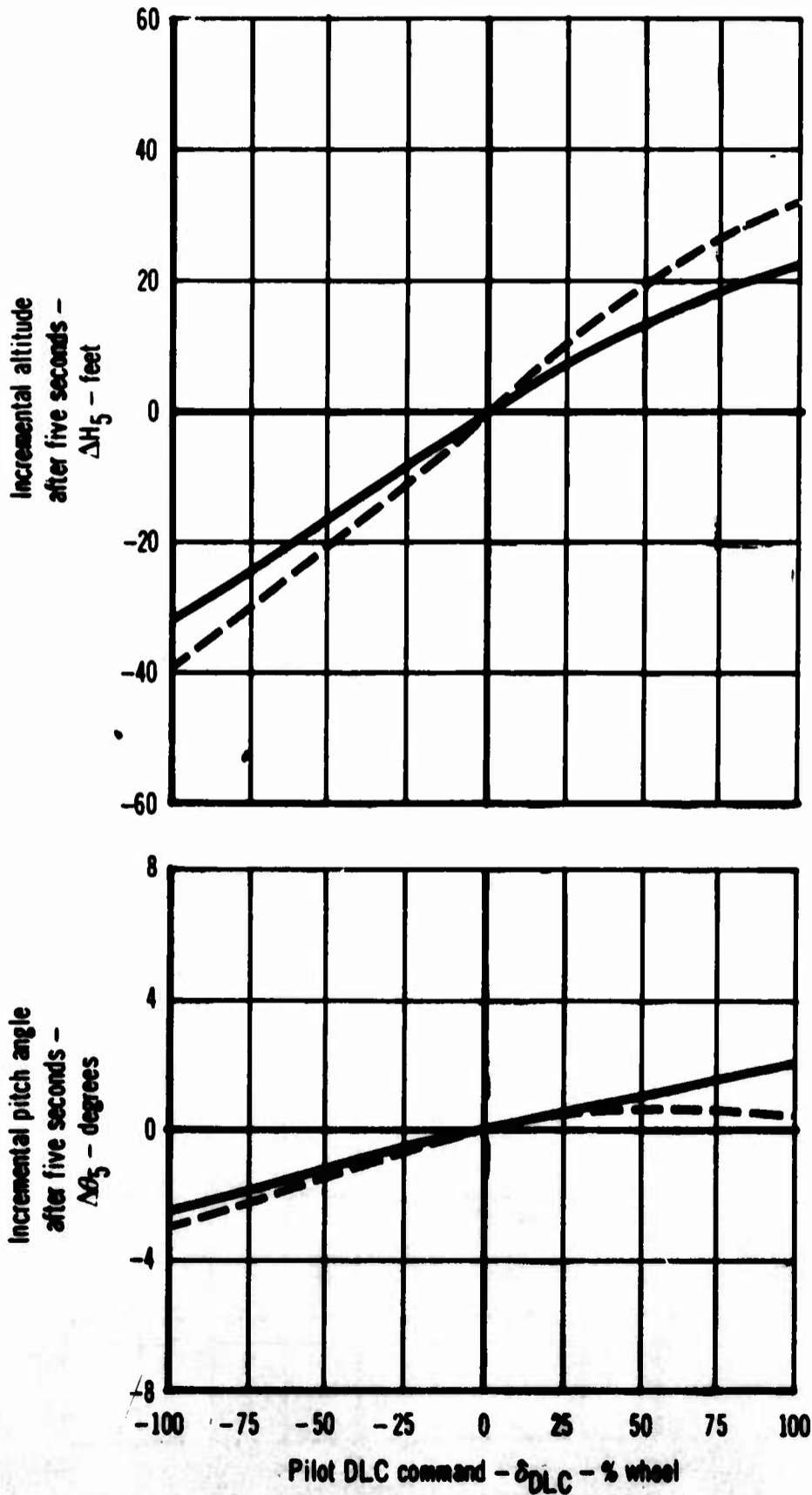


Figure 14.b Model F-4J  
Effect of Approach Power Compensating System

$$\delta_{F_{Nom.}} = 32^{\circ}; \gamma_0 = 0^{\circ}; \alpha_{w_{Trim}} = 13^{\circ}$$

Symbol	C.G. (%C)	G.W. (Lb.)	V <sub>Trim</sub> (KCAS)	APCS	Interconnect
—————	29	34,000	140.0	Out	In
- - - - -	29	34,000	140.0	In	In

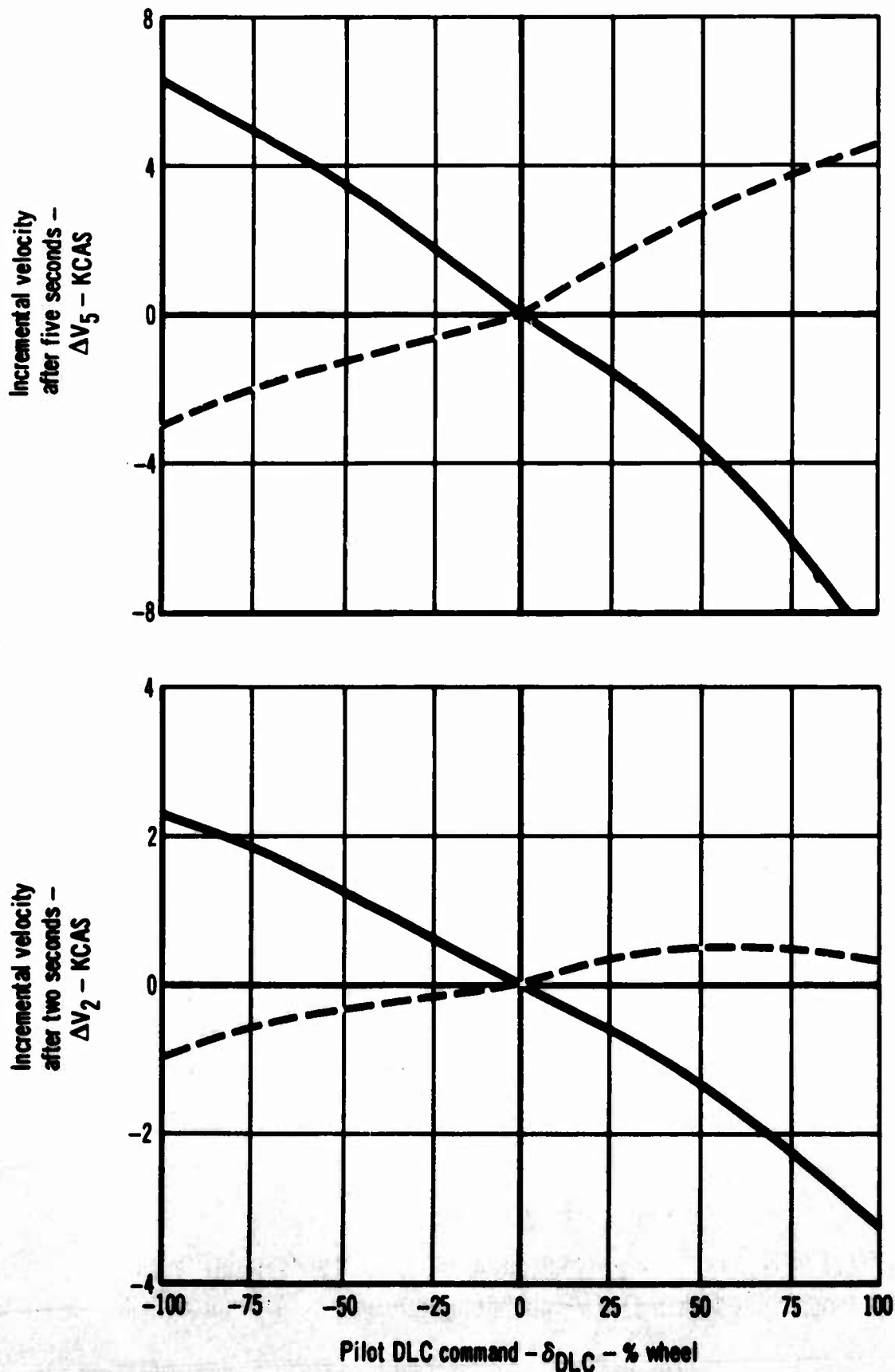


Figure 14.c Model F-4J  
Effect of Approach Power Compensation System

G.W. = 34,000 Lb.      C.G. at 29%  $\bar{c}$        $\gamma_0 = 0^\circ$        $\alpha_{wTrim} = 13^\circ$

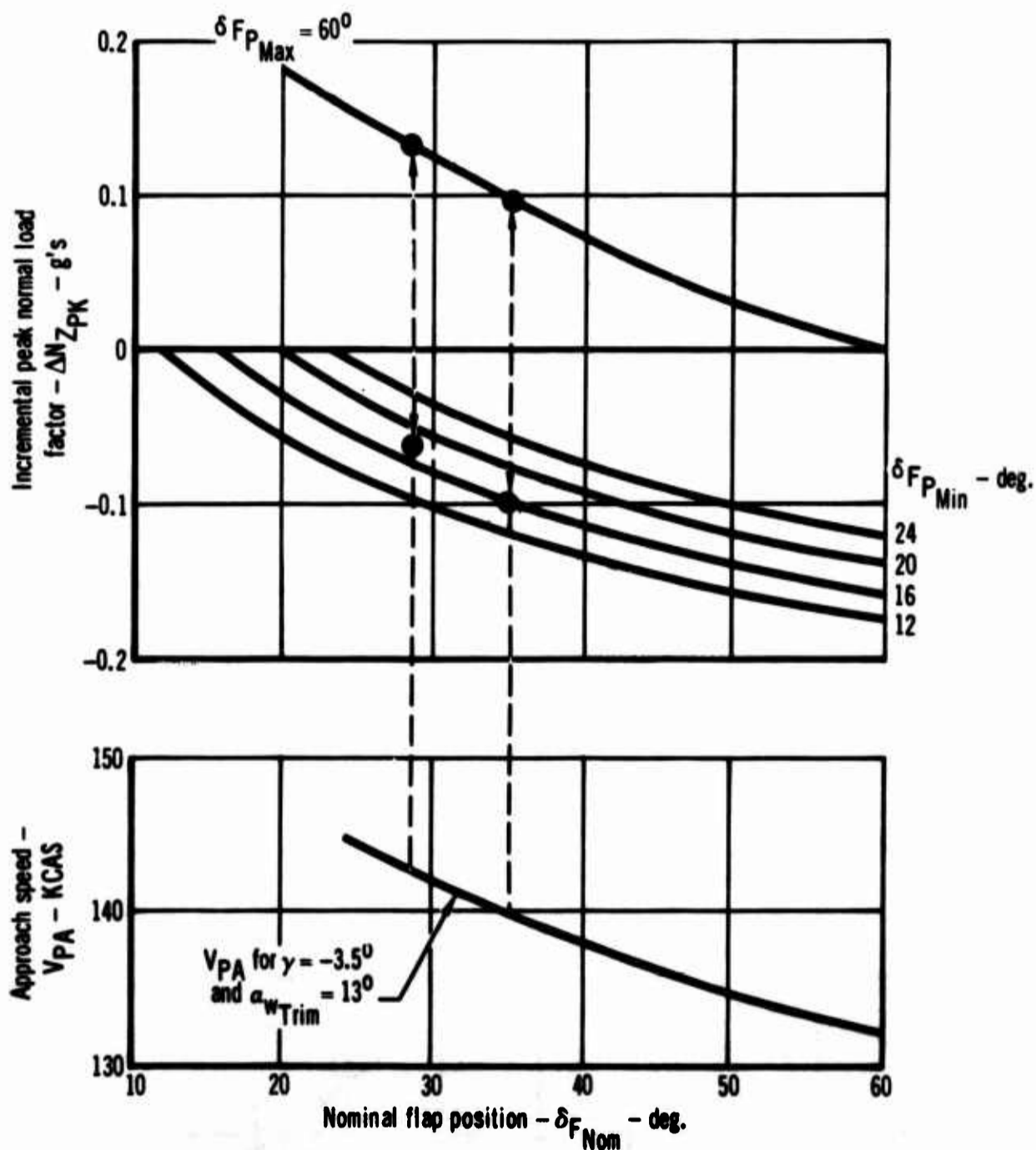
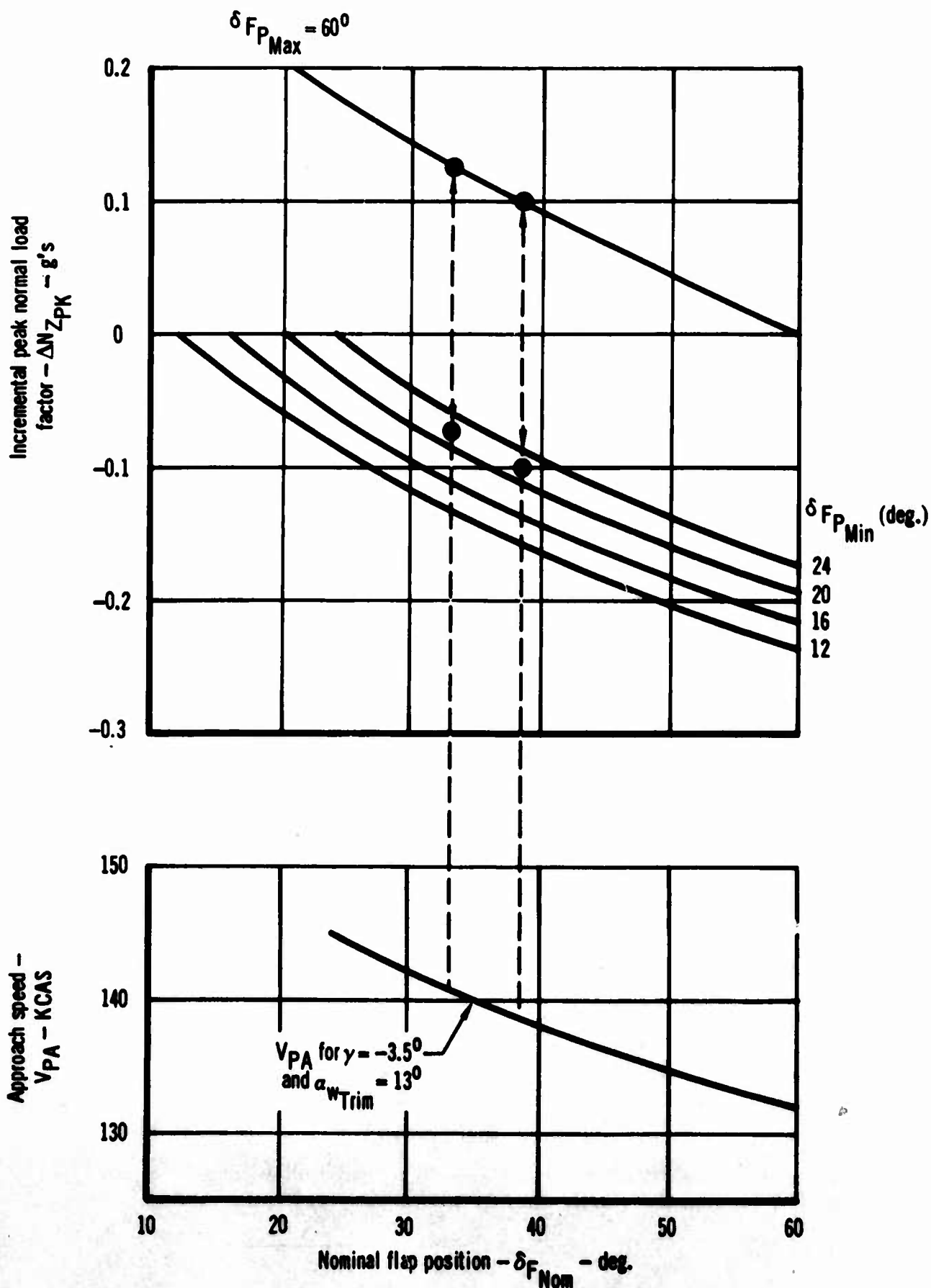


Figure 15 Model F-4J  
 Effect of Nominal Flap Position on Load Factor Capability and Approach Speed With DLC-Stabilator Interconnect, Without APCS

G.W. = 34,000 Lb.  
C.G. at 29%  $\bar{c}$

$\gamma_0 = 0^\circ$   
 $\alpha_{wTrim} = 13^\circ$



**Figure 16 Model F-4J**  
**Effect of Nominal Flap Position on Load Factor Capability and**  
**Approach Speed With DLC-Stabilator Interconnect, With APCS**

G.W. = 34,000 Lb. C.G. at 29% $\bar{c}$  Flight Path Angle =  $-3.5^\circ$

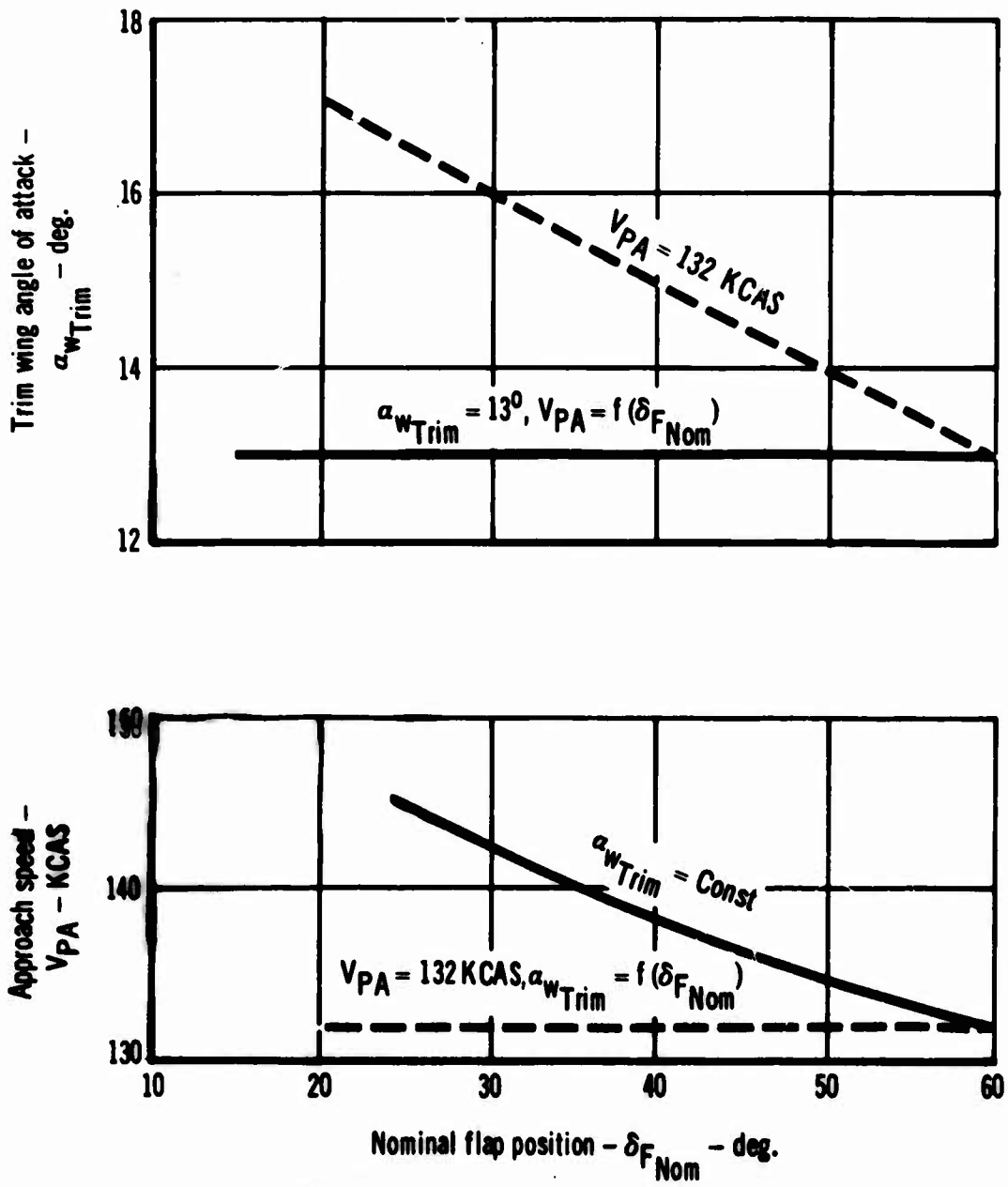


**Figure 17 Model F-4J**  
**Effect of Nominal Flap Position on Angle-of-Attack**  
**Required to Maintain Approach Speed**

### 3. DIRECT LIFT CONTROL SYSTEM DESIGN

#### 3.1 General Description

The system concept described in Section 2 is implemented by utilizing manually controlled trailing edge flap servo cylinders with appropriate electrical interconnects to the AFCS and APCS. The basic flap configuration in DLC mode is leading edge flaps extended (BLC on), trailing edge flaps at nominal DLC position, and ailerons drooped.

With no changes to the present leading edge flap subsystem, the trailing edge flap subsystem is used in a closed loop arrangement by attaching the cylinder piston rods to structure and the barrels to surface horns. For the normal flap mode the barrel-mounted servo valves receive mechanical inputs from an electrical actuator for positions preselected by the cockpit switch. As in present F-4 aircraft, the leading edge flaps go to fully extend position at "1/2" position of the trailing edge flaps, where they remain until the "UP" position is selected. System design makes "1/2" position a prerequisite for DLC mode in which mechanical inputs to the flap servo valves are generated by a servo actuator controlled by a transducer on the stick grip. The servo actuator inputs are transmitted to the flap servo valves by a mechanical system which also serves to synchronize the trailing edge flaps.

#### 3.2 Mechanical Design

The mechanical system for normal and DLC flap operation consists of an electrical actuator, a DLC servo actuator, a linkage to accept dual inputs, and a push-pull cable system to transmit inputs to the trailing edge flap cylinders as shown in Figure (18).

Trailing edge flap design parameters:

Normal flap deflection -  $0^\circ$ ,  $30^\circ$ , and  $60^\circ$ .

Normal flap deflection rate -  $10^\circ/\text{sec}$ . (approximately).

DLC flap deflection -  $10.5^\circ$  to  $60^\circ$ \*

DLC flap deflection maximum rate -  $75^\circ/\text{sec}$ .

\*Range shown is for prototype flight testing. DLC nominal is adjustable from 27 degrees to 37 degrees flap deflection. Production DLC nominal position and travel would be determined during flight test evaluation of prototype.

The electrical actuator provides the low rate normal flap inputs and the DLC nominal position. Up flap position is determined by integral up locks in the trailing edge flap cylinders. The half flap position and the DLC nominal position are determined by limit switches in the electrical actuator, and the full flap position by the trailing edge flap cylinders bottoming out. For the prototype system the DLC nominal position switch is adjustable through the range 27 degrees to 37 degrees flap deflection. The electrical actuator includes

a high breakout force spring cartridge to prevent damage to the trailing edge flap system in the event of a component failure or servo actuator hardover.

The DLC servo actuator provides the high rate input required for DLC and infinite selection of flap deflection within the DLC range. For the prototype system the upper flap deflection limit is adjustable. For the production version the upper flap deflection limit is determined by the DLC servo actuator ram bottoming out. The DLC 60 degrees flap deflection limit for both the prototype and the production systems is provided by the trailing edge flap cylinders bottoming out.

The linkage to accept dual inputs consists of a walking beam and bellcrank with a pivot for the walking beam. In normal mode the DLC servo actuator locks up mechanically to fix the walking beam lower pivot in line with the fixed pivot of the bellcrank. The electrical actuator then operates the linkage as a simple bellcrank to provide normal flap inputs. In DLC mode the electrical actuator locks up mechanically and fixes the bellcrank to provide the pivot point for the walking beam. The DLC servo unlocks and then operates the walking beam to provide DLC inputs.

A push-pull cable system transmits normal or DLC flap inputs from the linkage to the trailing edge flap servo cylinders and provides synchronization of the surfaces. Inherent backlash is not expected to cause stability problems since the mechanical system is open loop beyond the DLC servo actuator.

### 3.3 Hydraulic Design

3.3.1 Description - Figure (19) shows the proposed flap hydraulic system. The DLC trailing edge flap subsystem is compatible with the existing leading edge flap subsystem and no changes to the leading edge flap subsystem are required. The utility hydraulic system is utilized for normal power and the pneumatic system for emergency extension. For surface deflection rates of 75 degrees per second, approximately 6 GPM flow is delivered to each of the two trailing edge flap cylinders. Engine pump capacity is sufficient, with appreciable margin at carrier approach engine speeds, to supply this flow in addition to other utility services being operated. To enable employment of the existing solenoid selector valve (1) to control power to all flap cylinders, power for the trailing edge flap actuators is available from either of the leading edge flap control lines. Surface extension rate during air emergency operation is controlled by flow restrictor (24).

### 3.3.2 New Components

3.3.2.1 Trailing Edge Flap Servo Cylinder - The proposed new design utilizes the same bore, stroke and effective areas as the existing flap cylinders. Referring to Figure (20), it incorporates a segment type lock in its fully retracted position, and a switch, which operates upon lock engagement, to depressurize the flap subsystem. Two pistons, referred to as primary and secondary, are utilized to enable cylinder extension equivalent to 30 degrees of surface travel with admission of emergency air. The pistons are locked together during normal operation by a "ring-finger" type lock enclosed in the piston rod. Lock

release results from air pressure moving the spring loaded locking piston to a position enabling finger disengagement. Normal cylinder rate and direction of motion are controlled by the servo valve mounted on the barrel. The new cylinder is physically interchangeable with the existing cylinder.

3.3.2.2 DLC Servo Actuator - The DLC Servo Actuator is a closed loop unit integrating an electro-hydraulic valve, a main ram with a centering and locking device, and a transducer. Stroke of the main ram is sufficient to cover adjustment ranges of nominal DLC flap position for prototype flight testing.

3.3.2.3 Stabilator Power Cylinder - The DLC Stabilator Interconnect requires a  $\pm 2$  degree authority series servo for the stabilator surface control. For the prototype, the  $\pm 2$  degree stabilator authority in stabilator power cylinder SCD 32-69007-23 will be utilized for the DLC-Stabilator interconnect with external wiring changes. For production, a redesigned stabilator power cylinder will be required. Redesign will revise the integrated valve package to include a DLC series servo with  $\pm 2$  degree authority while retaining the  $\pm 1/2$  degree authority series servo utilized for stability augmentation and the existing parallel servo function.

3.3.3 Plumbing - Flexible plumbing to the new trailing edge flap cylinder is redesigned for compatibility with port locations, valve operation, and mechanical input to the valve. It consists of a scissors swivel arrangement to the pressure port, a flexible hose to the air emergency port, and two pressure and volume balanced extension units for the return and dump ports. Pressure and return lines are 1/2 inch from valve (1) to the junction point of entering each wing, and 3/8 inch from the junction to the cylinders. Generally, existing line routings are utilized.

3.3.4 DLC Flap Servo Cylinder Stability Analysis - The addition of a mechanical input valve converts the present flap actuator into a closed loop position control device. This required that the closed loop stability characteristics be examined to assure stable operation of the modified system. The analysis model used in this study is presented in Figure (21). The valve gain of the proposed system was assumed linear from neutral to full flow with system structural estimates for the original flap actuator being used in this analysis.

Results of this stability analysis are presented in Figure (22) and indicate that an adequate stability margin will exist for the proposed flap actuator installation. The stability criterion shown in Figure (22) is developed in Reference (7) and is in the form of a non-dimensional plot of valve gain divided by system frequency versus the total effective back-up spring rate divided by cylinder-surface coupling spring rate. The stability margins for various damping ratio values of the equivalent mass-spring damper actuator load are shown as dashed lines. The solid line represents a level of damping which is consistent with current aircraft construction methods and has been found adequate to define power cylinder stability margins for past McDonnell aircraft. For comparison purposes, the stability characteristics of other F-4 power actuator installations are shown. It is apparent that an adequate stability margin exists for the proposed flap actuator design.

### 3.4 Electronic Design

The electronic interface between the various aircraft systems, and the modifications required in the electronic systems, for the DLC mode of operation are described below.

3.4.1 Electronic Interface - Figure (23) shows the electronic interface required for flap positioning and for DLC operation.

Normal flap positions are controlled by the flap control switch which energizes the flap solenoid selector valve and the flap electrical screw jack actuator (FESA) via logic circuits. The flap control switch is a three position switch located in the pilot's cockpit. When the flap control switch is moved to either the "DOWN" or "1/2" position the leading edge flaps and the drooped ailerons are moved to the full down position and the trailing edge flaps are moved to the "DOWN" or "1/2" position. The flap solenoid selector valve remains energized to maintain hydraulic pressure on the actuators in "DOWN" or "1/2" positions. When the switch is moved to the "UP" position, the leading and trailing edge flaps are moved to the "UP" position and the drooped ailerons are moved to undroop position. Each flap has a limit switch which opens when the flap reaches its up position. The switches are connected in parallel so that the flap solenoid selector valve is de-energized and hydraulic pressure is removed from all flap actuators when all of the flaps are in the up position.

To operate the flaps in the DLC mode, the flap control switch must be in the "1/2" position and the DLC engage switch, located in the pilot's cockpit, must be in the "ENGAGED" position. This is a solenoid held switch which requires power to maintain its engaged position. Power is available only after "1/2" position has been selected on the normal flap selector switch. This feature helps preclude inadvertent DLC engagement. When the DLC mode is engaged, the FESA, which is controlled by relays and limit switches, moves to the nominal DLC position and causes the trailing edge flaps to move to the nominal DLC position. The nominal DLC position is varied by moving S4, the DLC nominal position switch on the prototype FESA.

When the FESA reaches the nominal DLC position, the DLC solenoid selector valve is energized, which admits hydraulic pressure to the DLC servo actuator. The DLC servo actuator then moves the flaps about the nominal DLC position per commands from the pilot's inputs to the stick grip thumb wheel. Rotation of the stick control wheel a maximum of 20 degrees in the forward direction from its mid position causes flaps-up movement, and the aft direction a maximum of 20 degrees causes flaps-down movement. It is spring loaded to return to its mid-position so that if the pilot releases force on the wheel, the flaps will move to their nominal DLC position.

To prevent the flaps from being damaged by excessive air loads, a flap blow-up switch is incorporated in the flap control circuit which causes an automatic retraction of the flaps when the aircraft airspeed is above 230 knots.

The DLC mode of flap operation may be disengaged by moving the flap control switch to the "UP" or "DOWN" position, by moving the DLC engage switch to the "OFF" position, or by operating the paddle emergency disconnect switch on the control stick. DLC disengagement will result automatically by the flap blow-up switch at 230 knots when increasing airspeed.

### 3.4.2 Electronic Systems Modifications for DLC Operation

3.4.2.1 Automatic Flight Control System - The AFCS Control Amplifier requires an additional input into the stabilator servo amplifier which involves adding a resistor and a DLC mode relay (K8 in Figure 23). An additional servo amplifier is required for the new DLC servo actuator which is installed in the AFCS control amplifier assembly.

3.4.2.2 Approach Power Compensation System - The DLC-APCS Interconnect transfer function described in Section 2.5 is incorporated in the APCS Control Computer through the addition of an RC network and a DLC mode relay (K9 in Figure (23)) in the input to the signal summing amplifier of the APCS.

3.4.2.3 Stick Grip - The stick grip requires the addition of a potentiometer which is positioned by the thumb wheel.

3.4.2.4 DLC Signal Distribution Unit - This new electronic unit provides logic relays for the operation of the DLC solenoid selector valve and the FESA. The unit also contains a command servo which provides the command signals from the stick grip to the flaps, stabilator, and APCS. This command servo allows the independent variation in the transfer functions between the pilot commands and the flaps, stabilator, and APCS for flight test evaluations. Depending on the results of the flight tests, the command servo may be eliminated in the production version and the command signals for the flaps, stabilator, and APCS will be provided directly from the stick grip.

### 3.5 Cockpit Design

Cockpit control of the DLC mode of the flap system is accomplished by an energizing switch and a spring centered wheel control on the forward cockpit stick grip. The energizing switch is located near the existing flap control switch assembly. The stick grip wheel control proposed for both prototype and production is shown in Figure (24). This location requires utilization of the lower L/H pad for the nose steering switch location. Location of the DLC control wheel as shown is considered optimum by a number of McDonnell pilots. The DLC Signal Distribution Unit required for prototype only is mounted in the aft cockpit on the right hand side of the seat. This location enables easy accessibility required during prototype flight testing.

#### 3.5.1 Pilot Operating Sequence

3.5.1.1 Normal Flap Mode - No change to the existing switch operating procedure is required.

#### 3.5.1.2 DLC Flap Mode

3.5.1.2.1 Prototype - Pilot is required to place normal flap switch in "1/2" position and DLC switch in "ENGAGE" position. This results in electrical actuator moving flaps from "1/2" position to nominal DLC flap position, after which the DLC Servo Actuator solenoid valve and the DLC stick grip input transducer are energized. Pilot has the option of turning on the stability augmentation system which results in the DLC-Stabilator Interconnect being activated and the stabilator integrated series servo with  $\pm 2$  degree authority being energized and turning on APCS which results in DLC-APCS Interconnect being activated.

3.5.1.2.2 Production - Production operating sequence will be established after prototype flight testing.

3.5.2 Disengagement - Normal disengagement of the DLC flap mode is accomplished by operating the DLC energizing switch. Emergency disengagement is provided by operating either the AFCS disengage switch on the stick grip or the normal flap switch from "1/2" position to either "UP" or "DOWN". Automatic disengage results when the airspeed exceeds 230 knots by the flap blow up switch.

### 3.6 Aircraft Changes to Incorporate

#### 3.6.1 Prototype

3.6.1.1 Structural - In the area of the mechanical system, access panels are required in the left and right hand engine compartment firewalls, redesign of keel web stiffener at Fuselage Station 346.92 is necessary, holes for routing the mechanical system over the engines and in the wing are required, and support brackets are necessary. Minor structural modifications are needed for tubing and wiring, such as addition of support brackets, plate nuts and holes in webs. A mounting bracket is required in the aft cockpit for the signal distribution unit, and minor structural modification is necessary in the forward cockpit for mounting the DLC energizing switch.

3.6.1.2 Hydraulic - Existing flap components that are not required for DLC are removed if the space they occupy is needed for the DLC system. These components include two flow dividers, two shuttle valves, three flow restrictors and approximately 64 feet of 1/4 inch tubing. A solenoid valve in the L/H wing is moved to the fuselage. Tube routing will be adequate but not designed to production standards.

3.6.1.3 Electrical - New wiring is added, without revision of the existing wire bundles, for the sake of expediency.

#### 3.6.2 Production -

3.6.2.1 Structural - Redesign for production includes removal of all unused plate nuts, clips, and brackets and more efficient design of structure that is modified for the prototype.

For this feasibility study, the effects of a possible increase in approach speed and/or attitude on the required strength of the landing gear and back-up structure were not evaluated. Therefore, in addition to the foregoing structural considerations, production incorporation may require investigation of the effects of increased engaging speed and/or increased wind-over-deck requirements on the overall carrier suitability.

3.6.2.2 Hydraulic - Production changes include optimum tube routing and removal of all unnecessary components and tubing.

3.6.2.3 Electrical - Production changes include revising wire bundles, routing, and supports to production standards.

### 3.7 Failure Analysis

Table (1) lists assumed failures and results. Based on single failure concept, no failure will prevent extending the flaps normally or by emergency air to an angle of at least 30 degrees for the trailing edge flaps and full down for the leading edge flaps and drooped ailerons. New components selected are similar to those with exceptionally good mean time between failures (MTBF) ratings. The internal locks used in the trailing edge flap actuator are proven through McDonnell experience. The piston segment type uplock has been used in the Model F-4 since initial production. The ring-finger lock has been used by McDonnell in landing gear systems in several models. The flap application for this lock need operate only for emergency, resulting in low life cycle requirements. Appendix C, Section C.3, discusses analog studies conducted to evaluate consequences of two representative type failures.

### 3.8 Conclusions

The DLC system design described above can easily be incorporated in a production F-4B (with drooped ailerons) or a F-4J aircraft for prototype installation and flight testing. The design of the basic components for the production system is not materially different from those used for the prototype.

The final prototype DLC installation as developed during flight testing would be functionally identical to the production design. Pilot operated controls proposed for DLC are simple and convenient.

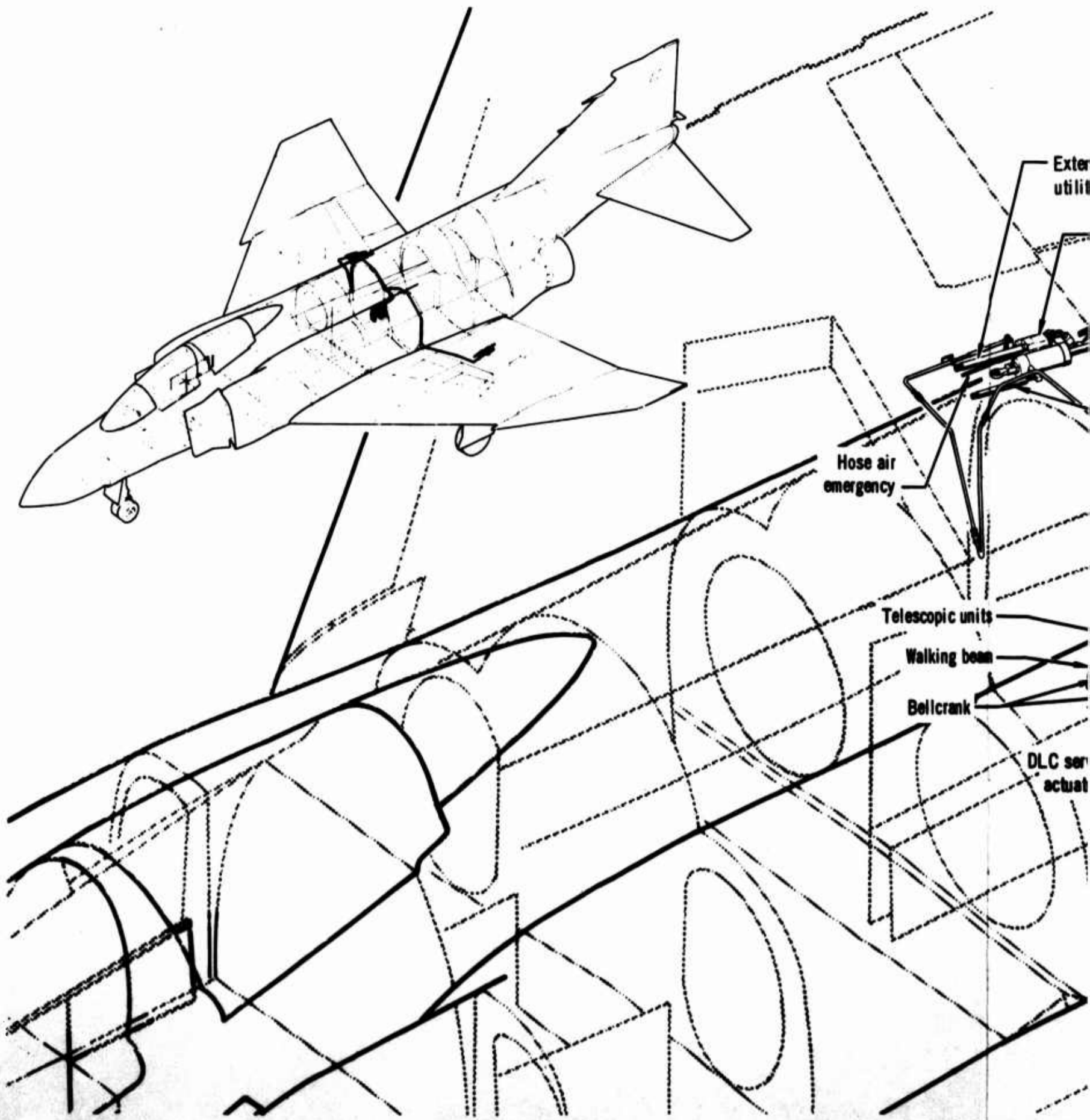
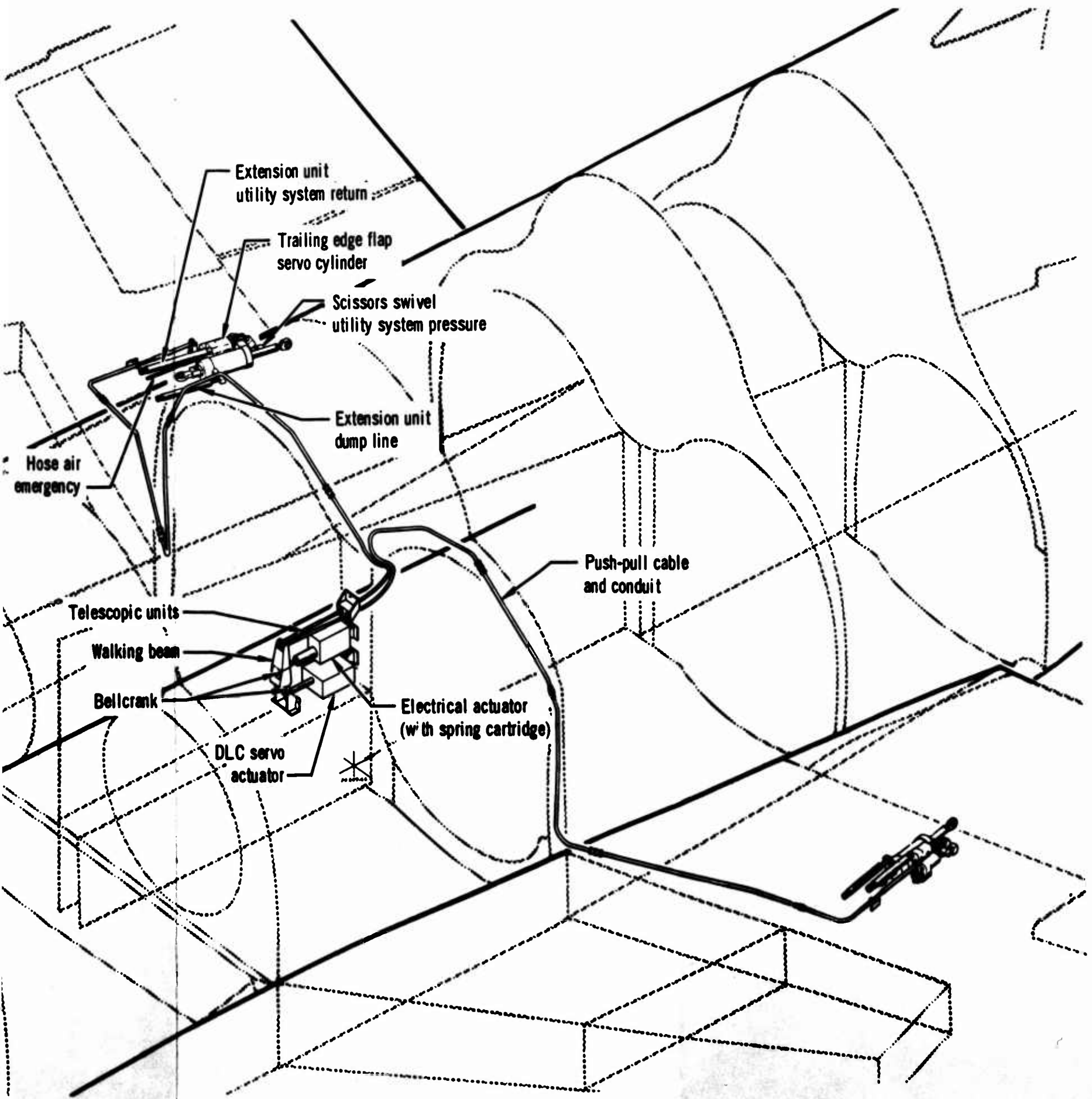
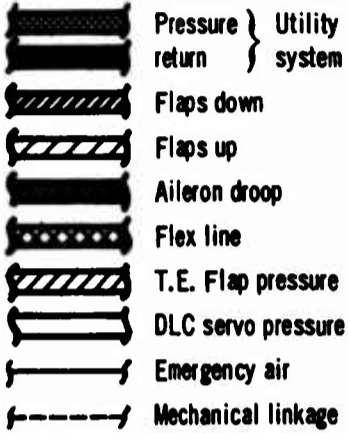


Figure 18 Trailing Edge Flap System Installation

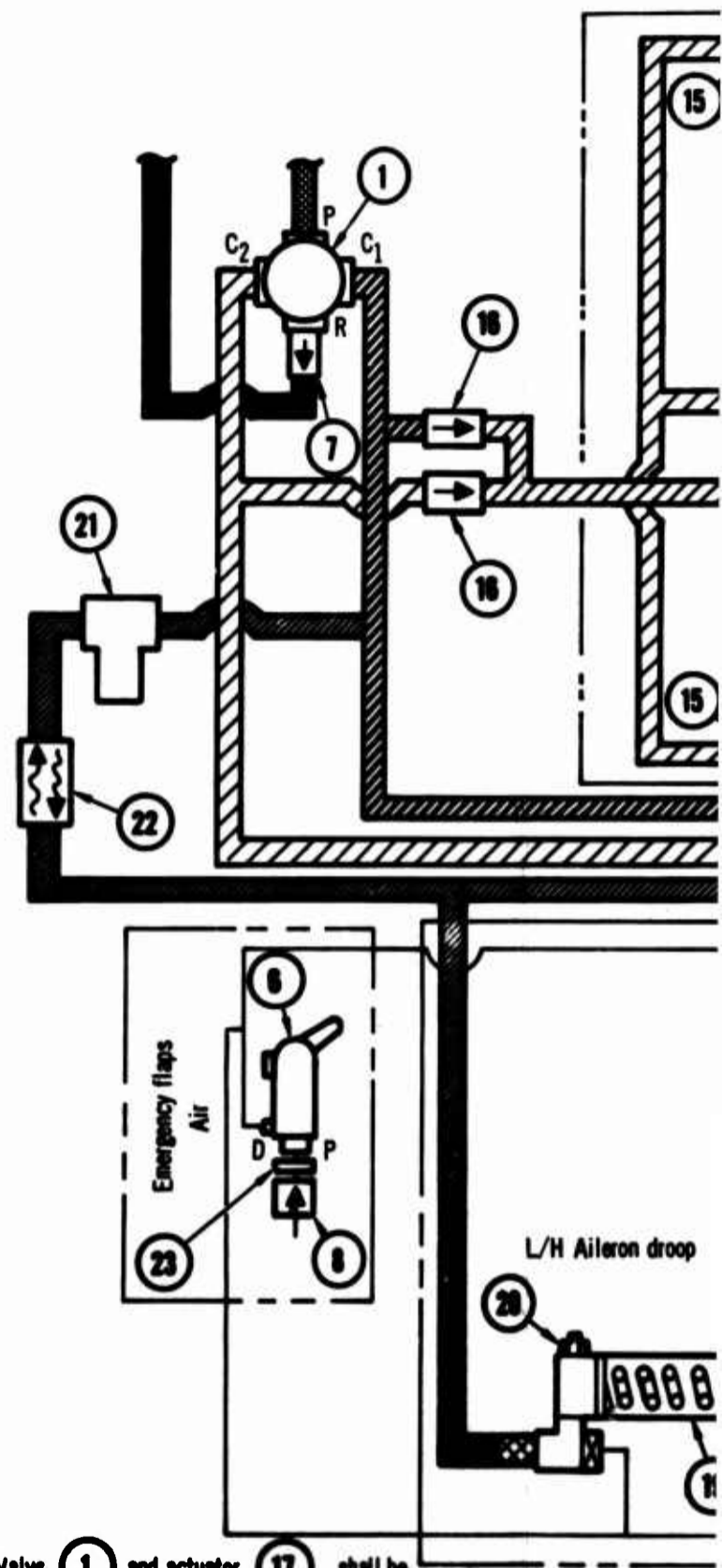
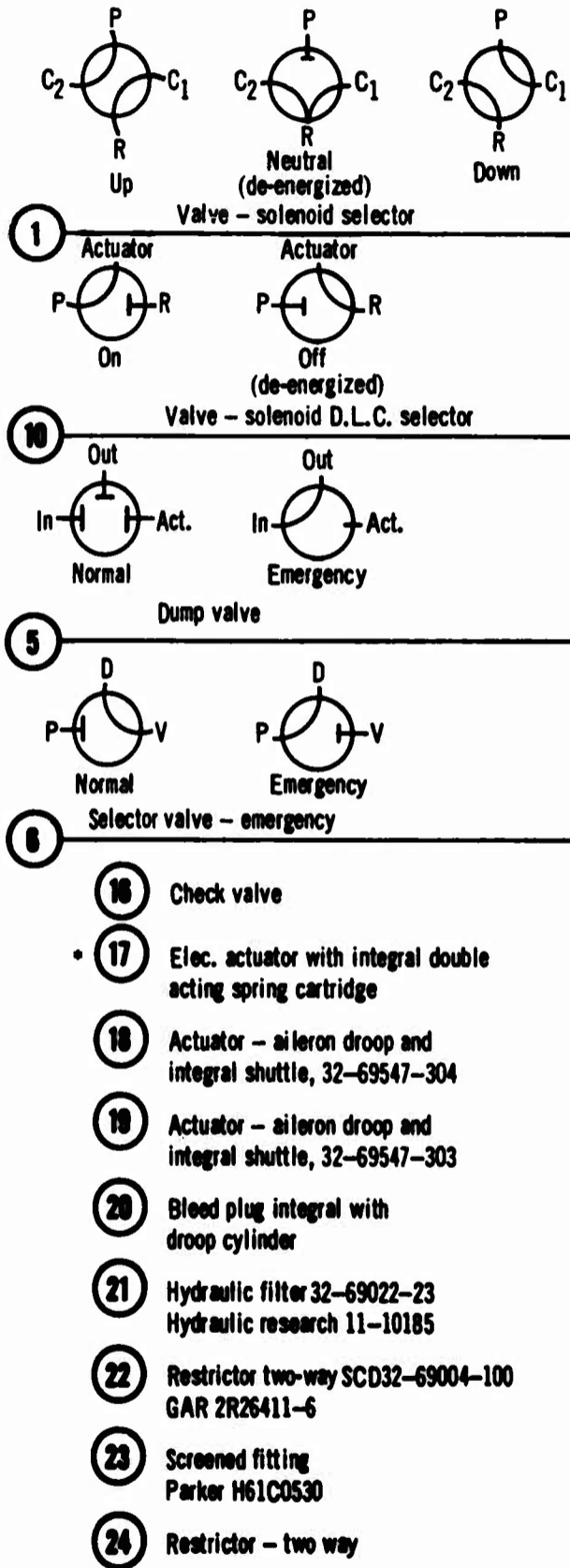
ber 1967



Legend

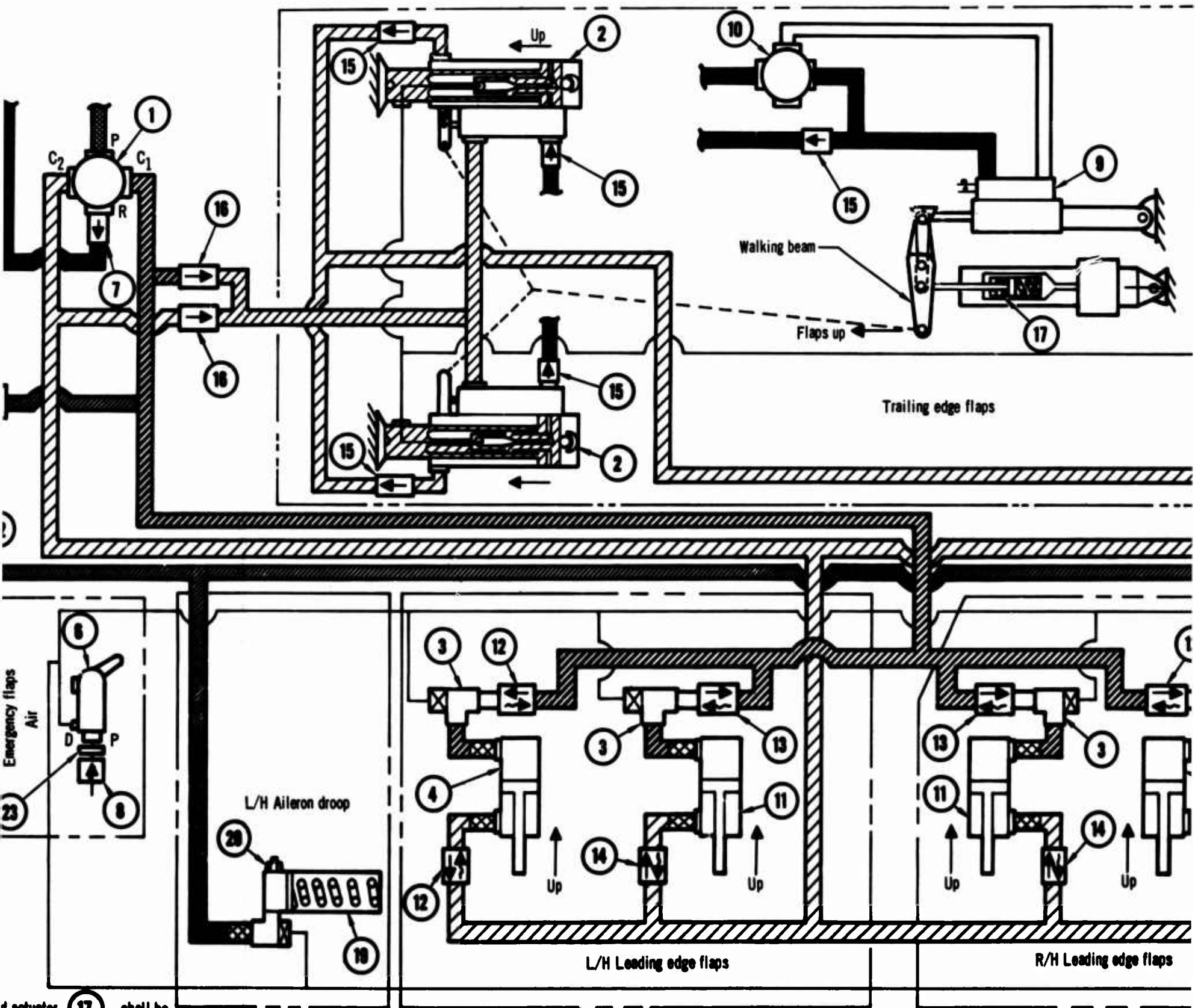


- φ 1 Valve - solenoid selector
- φ 2 T.E. Flap - DLC actuator
- 3 Shuttle valve - GAR 25V041
- 4 Actuator - L.E. flap outboard  
SCD 32-69034-3  
Mfg 32-69570-1 ozone
- 5 Dump valve - pressure oper.  
7-U-7138 Ronson hydraulic
- 6 Valve - emergency air sel. (32-72308)  
Kidde 870447
- 7 Check valve - integral with selector valve
- 8 Check valve - pneumatic  
Kidde 93296
- 9 DLC servo actuator with centering and locking device
- φ 10 Valve - solenoid selector
- 11 Actuator - L.E. flap  
SCD 32-69552-3 Mfg 32-69553-303
- 12 Restrictor - one way  
SCD 32-69004-59, GAR IR36411-59
- 13 Restrictor - one way  
SCD 32-69004-63, GAR IR3642-63
- 14 Restrictor - one way  
SCD 32-69004-57, GAR IR3642-57
- 15 Check valve



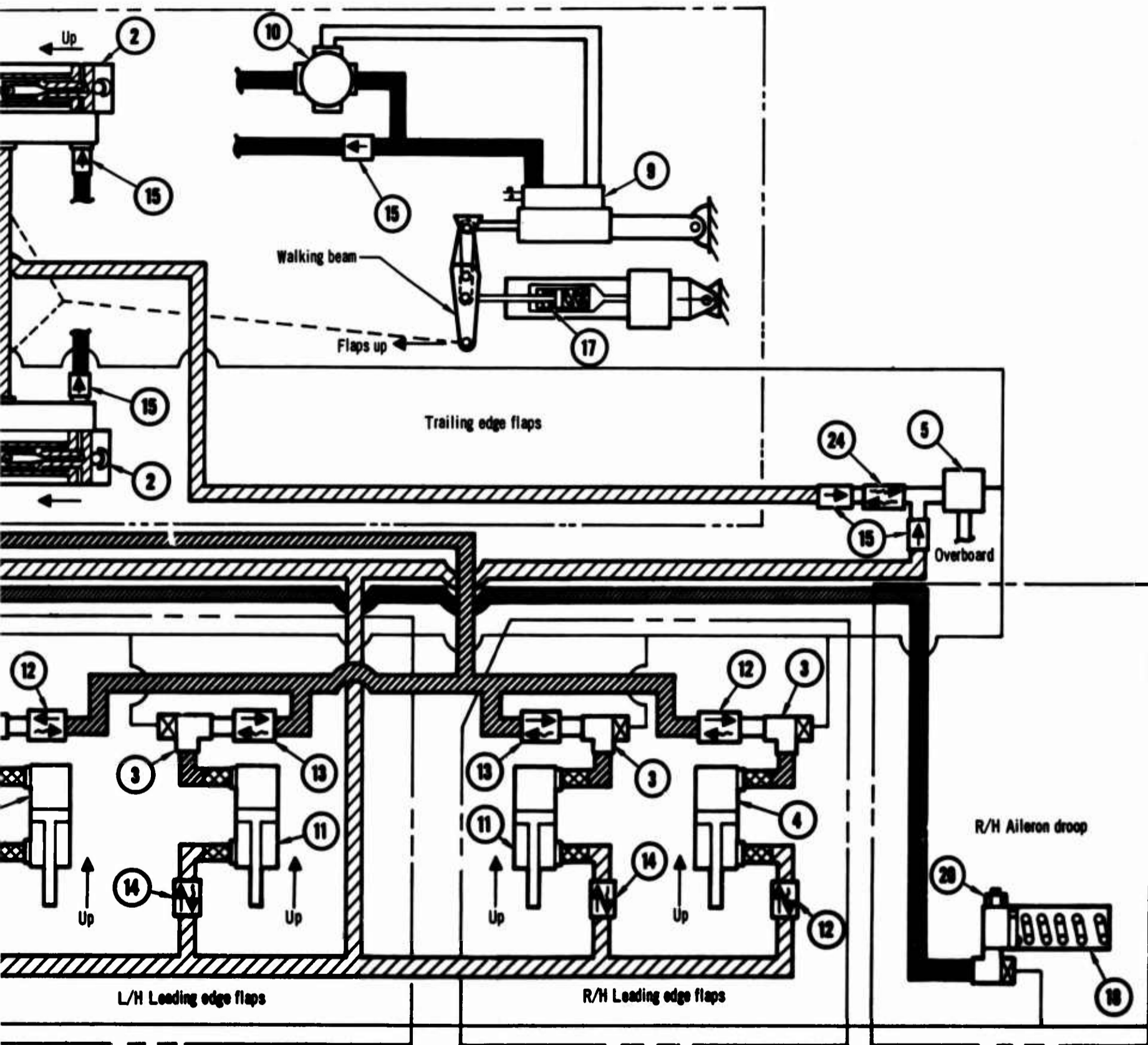
Valve 1 and actuator 17 shall be on separate circuit breakers

- φ Modified components
- New components



actuator (17) shall be  
circuit breakers  
components





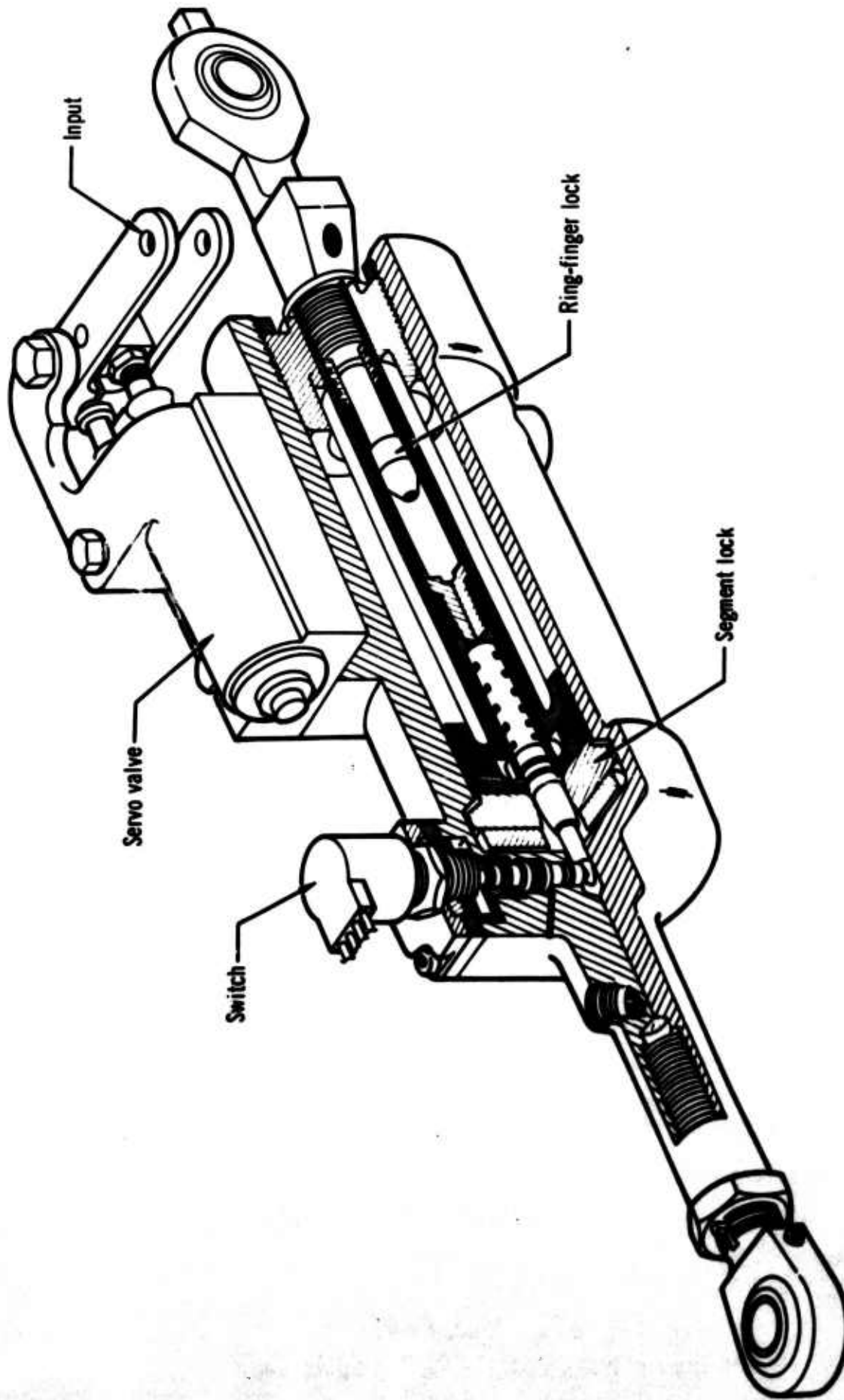
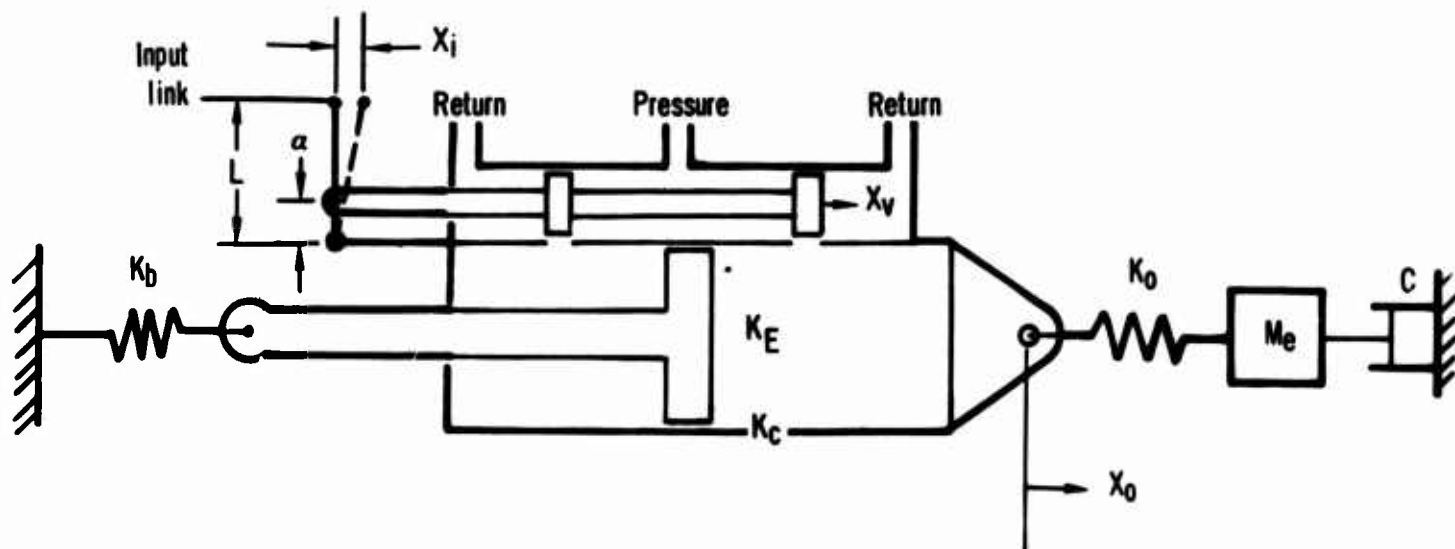


Figure 20 Trailing Edge Flap Servo Cylinder



- $A_{Ave}$  Average piston area (in.<sup>2</sup>)
- $X_i$  input displacement relative to cylinder (in.)
- $X_o$  Output displacement (in.)
- $X_v$  Valve displacement relative to cylinder;  $X_v = \left(\frac{a}{L}\right) X_i$  (in)
- $K_b$  Back-up structure spring rate (lb/in.)
- $K_o$  Cylinder-surface coupling spring rate (lb/in.)
- $M_e$  Surface effective mass (lb-in.<sup>2</sup>)
- $C$  System damping factor (lb/in./sec)
- $C_c$  Critical damping factor (lb/in./sec)
- $K_E$  Oil compressibility spring rate (lb/in.)
- $K_d$  Spring rate of springs whose deflections result in a valve opening (lb/in.)
- $\frac{1}{K_d} = \frac{1}{K_b} + \frac{1}{K_E} + \frac{1}{K_c}$
- $K_o$  Spring rate of springs whose deflections do not result in a valve opening (lb/in.)
- $K_c$  Spring rate of actuator cylinder (lb/in.)
- $K_\Sigma$  Total system spring rate (lb/in.)
- $\omega_\Sigma$  System natural frequency  $\omega_\Sigma = \sqrt{\frac{K_\Sigma}{M_e}}$  (rad/sec)
- $G$  Valve gain; flow per unit input arm displacement (in.<sup>3</sup>/sec/in.)

For DLC flap actuator:

$G = 31.9 \text{ in.}^3/\text{sec/in.}$        $K_b = 128,100 \text{ lb/in.}$        $K_c = 390,600 \text{ lb/in.}$

$A_{Ave} = 4.03 \text{ in.}^2$

$\omega_\Sigma = 143.5 \text{ rad/sec}$

**Figure 21 Model F-4J**  
**Stability Analysis Model - DLC Flap Actuator**

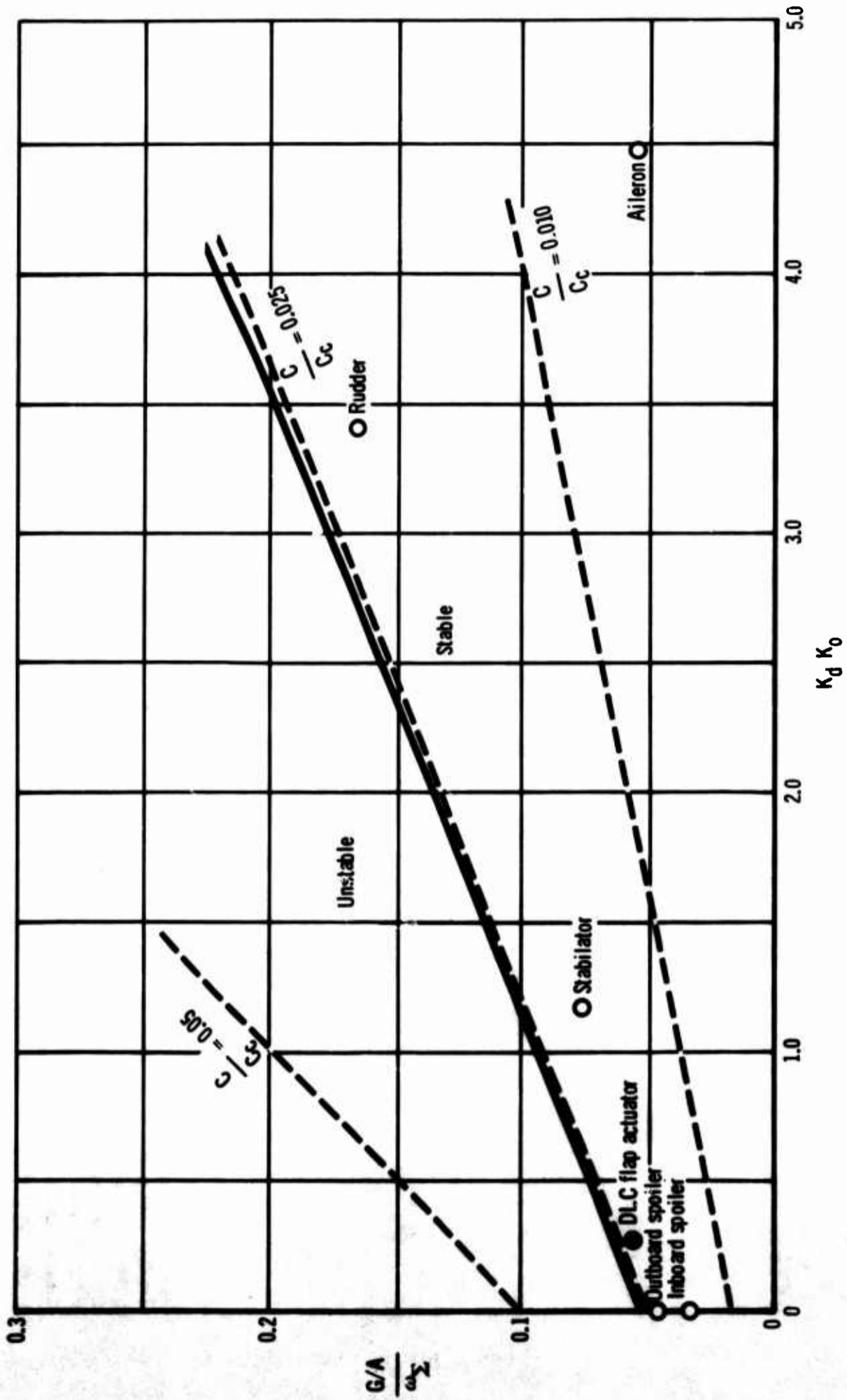


Figure 22  
Power Actuator Stability Margin Comparison



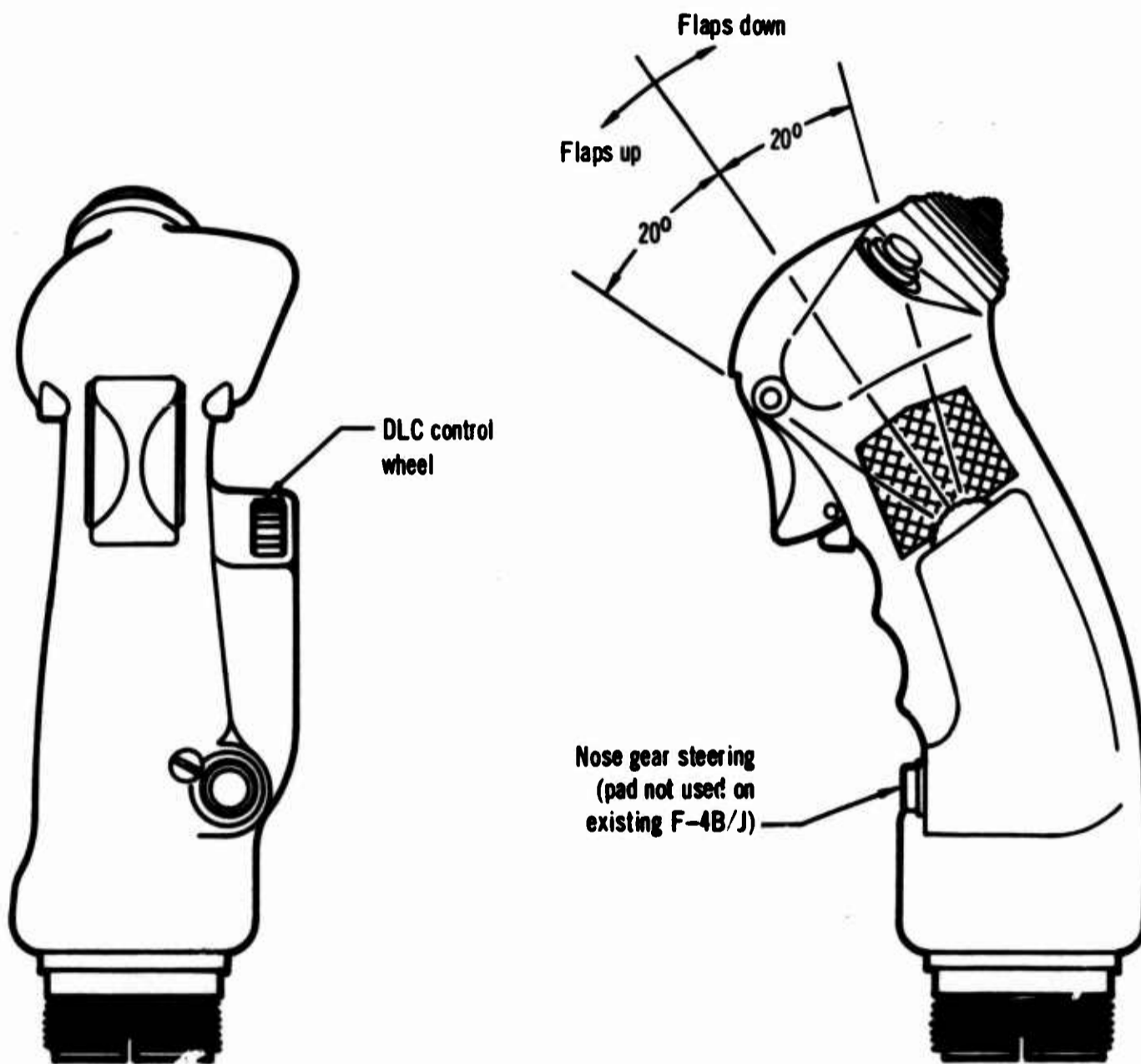


Figure 24 Modified Stick Grip for Forward Cockpit

TABLE I  
FAILURE ANALYSIS (Sheet 1 of 4)

System Component	Assumed Failure	Condition	Results	Remarks
DLC Electro-Hydraulic Servo Actuator (9)	Hardover signal - hydraulic or electric origin	DLC mode - extends to 60°	Inoperative - extends symmetrically.	Electric hardover signals are reduced by utilizing 2-wire servo.
		Normal mode	Operative after DLC disengagement to all normal positions.	Disengage by operating AFCs emergency disconnect switch on stick. Power off centering and mechanical lock provided in DLC servo (9).
		DLC mode retracts to 13°	Inoperative - retracts symmetrically.	
		Normal mode	Operative after DLC disengagement to all normal positions.	
		DLC mode	Erratic - should be disengaged.	
		Normal mode	Loss of positive pivot point for actuator (17). Erratic flap positioning with symmetry. Position of servo (9) dependent upon relative friction levels in servo and mechanical system.	Unlikely type of failure.
		Emergency mode	Operative	
		DLC mode	Operative until hydraulic system is failed by loss of fluid.	Routine maintenance procedure should detect overboard leakage long before system fails.
		Normal mode	Operative until hydraulic system is failed by loss of fluid.	
		Uplock does not operate	Inoperative	
DLC mode	Inoperative			
Normal mode	Operative			
Emergency mode	Operative until hydraulic system fails			
Trailing Edge Flap Actuator (2)	Total failure of "O" ring on secondary piston	DLC mode	Operative until hydraulic system fails	
		Normal mode	Operative until hydraulic system fails	
		Emergency mode	Operative	

TABLE I  
FAILURE ANALYSIS (Sheet 2 of 4)

System Component	Assumed Failure	Condition	Results	Remarks
	Small leak at "O" ring on primary piston (retract side)	DLC mode Normal mode	Operative until hydraulic system fails by loss of fluid Operative until hydraulic system fails by loss of fluid	Routine maintenance should detect prior to failure.
	Total failure of "O" ring on primary piston	DLC mode Normal mode	Operative in extend direction. System would soon fail if operated to retract. Operative to extend. In attempted retraction, probably would not lock with surfaces assuming trail position. Nose flaps will not retract.	
	Jammed servo valve spool on one side	Emergency mode Jammed in neutral position DLC mode Normal mode	Operative Inoperative Surface on opposite side will move a few degrees until mechanical interconnect cancels input motion. Operative	Very unlikely to occur
		Emergency mode Jammed in extend position DLC mode Normal mode	Inoperative Will extend to 60°	
		Jammed in retract position DLC mode Normal mode Emergency mode	Inoperative Inoperative Operative	Spring cartridge in (17) prevents damage to mechanical input system.
	Limit switch on actuator	Does not operate subsequent to uplock engagement DLC mode Normal mode	Operative Operative. Hydraulic pressure retained in cylinder in up and locked position.	Solenoid valve (10) is continuous duty

TABLE I  
FAILURE ANALYSIS (Sheet 3 of 4)

System Component	Assumed Failure	Condition	Results	Remarks
Electrical Screw-jack Actuator (17)	Broken wire or mechanically jammed	Failed at zero flap angle position DLC mode	Inoperative	
		Normal mode	Inoperative	
		Emergency mode	Operative	
	Limit switches for DLC nominal position and 1/2 flap position fail to operate.	Failed at 20° flap position DLC mode	Inoperative	
		Normal mode	Inoperative	
		Emergency mode	Operative	
Solenoid Valve (1)	Will not energize	Failed at 40° flap position DLC mode	Inoperative	Operative to full retract and full extend only.
		Normal mode	Inoperative	
		Emergency mode	Operative	
	Will not de-energize Jammed in flaps up position	DLC mode	Inoperative	
		Normal mode	Inoperative	
		Emergency mode	Operative	
Solenoid Valve (10)	Jammed in flaps down position	DLC mode	Inoperative	Servo in hydraulic neutral with lock disengaged
		Normal mode	Inoperative	
		Emergency mode	Operative	
	Will not energize	DLC mode	Inoperative	
		Normal mode	Operative	
		Emergency mode	Operative	
Will not de-energize	DLC mode	Inoperative		
	Normal mode	Operative		
	Emergency mode	Operative		

TABLE I  
FAILURE ANALYSIS (Sheet 4 of 4)

System Component	Assumed Failure	Condition	Results	Remarks
Dump Valve (5)	Leaks in closed position	DLC mode	Operative until hydraulic system fails	Unlikely to occur.
		Normal mode	Operative until hydraulic system fails	
DLC Input Transducer	Will not open when air pressure is applied	DLC mode	Operative	
		Normal mode	Operative	
AFCS Equipment for Stabilator Interconnect	No signal to DLC servo (9).	DLC mode	Inoperative	
		Normal mode	Operative	
APCS Equipment for Throttle Interconnect	Lack of signal to move stabilator. Incorrect signal.	DLC mode	Pilot moves stick manually.	
		DLC mode	Pilot overrides.	
DLC Signal Distribution Unit (Prototype Only)	Lack of signal to move throttles. Incorrect signal.	DLC mode	Pilot moves throttles manually.	Also DLC may be disengaged.
		DLC mode	Pilot overrides.	
	Hardover signal	DLC mode	Pilot overrides	
		Normal mode	Operative	

Notes:

1. Numbers in parentheses refer to Figure 19.
2. This analysis considers only single failures.

## 4. SUMMARY

As a result of the design and analysis study reported herein, the following summary is presented.

The McDonnell F-4J aircraft can be fitted with a DLC system which will provide either a  $\pm .10$  "g" or  $+ .13/-07$  "g" normal acceleration through pilot-controlled flap deflections. Prototype aircraft structural changes required to incorporate this capability are minor. Aircraft system changes which will be required include a redesigned flap actuation and control system, the addition of interconnect signals to the stability augmentation system and approach power compensation system, and minor hydraulic design changes to the integrated stabilator power actuator. The lateral control system and lateral control characteristics are not affected by the DLC system installation. To maintain the same approach angle-of-attack which is currently used in the F-4J aircraft, an increase in approach speed of 7.0 to 9.0 knots is required by DLC incorporation.

The analysis performed does not permit, and was not intended to permit, a decisive evaluation of the merits of incorporating DLC in the F-4J. Flight test evaluation of the DLC system would be required to determine its effects on the carrier suitability of the F-4J.

5. REFERENCES

- (1) Ling Temco Vought, Vought Aeronautics Division, Department No. 2-53310/4R-175, "Direct Lift Control as a Landing Approach Aid in the F-8C Airplane, Simulator and Flight Tests," 31 December 1964.
- (2) Douglas Aircraft Company, Inc., Aircraft Division, Report No. LB-31253, "Simulator Study of Direct Lift Control During Carrier Landing Approaches," 8 April 1963.
- (3) Drake, Douglas E., "Direct Lift Control During Landing Approaches," (Douglas Aircraft Company, Inc.), AIAA Paper 65-316, 29 July 1965.
- (4) Naval Air Test Center, Technical Report No. FT-51R-65, "Evaluation of the Direct Lift Control System Installed in the F-8C Airplane, Final Report," 13 August 1965.
- (5) McDonnell Report No. 9842, "Model F/RF-4B-C Aerodynamic Derivatives," 22 September 1965.
- (6) McDonnell Report No. 9842, Addendum I, "Model F-4 Aerodynamic Derivatives, F-4K/M Addendum," 31 May 1966.
- (7) McDonnell Report No. 6591, "Model F4H Airplane - Servo Mechanism Analysis of Power Cylinders," 30 August 1960.

## APPENDIX A

## AERODYNAMIC DATA BASIS

The data basis used for aerodynamic analysis and in the analog computer program during this study is based on wind tunnel data modified to reflect available "drooped" and "undrooped aileron" McDonnell F-4 flight test data. In developing this basis, particular emphasis was placed on matching demonstrated angle of attack, velocity, thrust, and trim stabilator characteristics and relationships at or near the present F-4J approach angle of attack of 13 degrees. The resulting basis is presented in Figures (A.1a) and (A.1b). It should be emphasized that this basis is applicable only for wing angles of attack at or near 13 degrees.

Additional aerodynamic derivatives required for the analog computer program were obtained from References (5) and (6) and are quoted below for reference.

$$\begin{array}{ll}
 C_{m\dot{\theta}} = -.0435/\text{deg} & C_{m\delta_s} = -.1375/\text{deg} \\
 C_{m\dot{\alpha}} = -.0165/\text{deg} & C_{L\delta_s} = .0095/\text{deg} \\
 C_{L\dot{\theta}} = .0435/\text{deg} & C_{D\delta_s} = -.0025/\text{deg}
 \end{array}$$

The above parameters are not totally independent of angle of attack. However, since the angle of attack variation from 13 degrees was small, the above nominal values were selected and held constant throughout the analog study.

Other aircraft physical characteristics used in the analog computer study were obtained from Reference (5) and are quoted for reference.

$$\begin{array}{ll}
 I_y = 131,525 \text{ Slug-Ft}^2 & i_t = 4.25 \text{ deg.} \\
 \bar{c} = 16.05 \text{ Feet} & Z_T = .916 \text{ Feet} \\
 S = 530 \text{ Ft}^2 &
 \end{array}$$

$\delta_{FN} = 0^\circ/60^\circ/60^\circ, \delta_s = -8^\circ, \delta_{FP} = 30^\circ, C_{LE} = 0.019, \delta_A = 16.5^\circ$

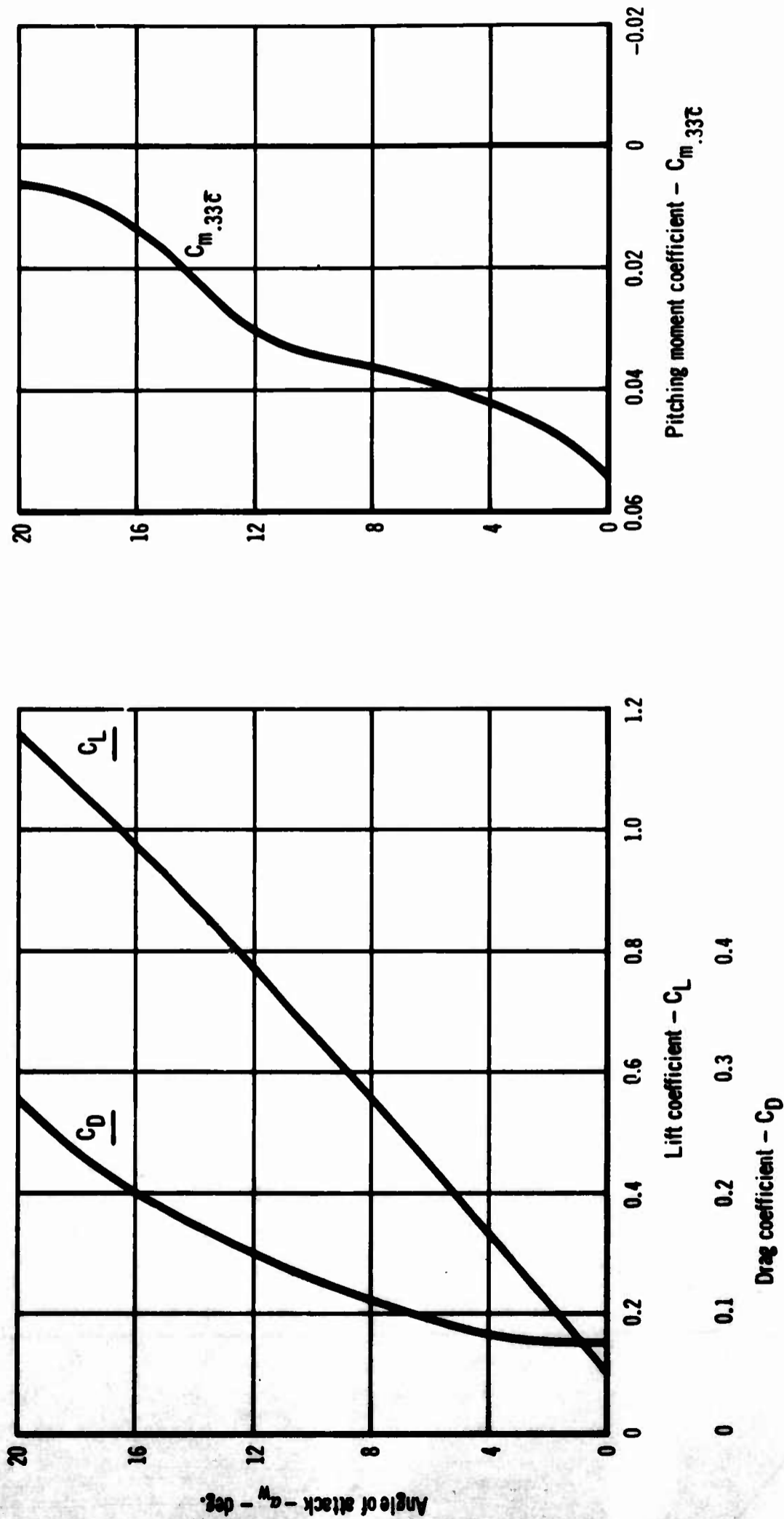


Figure A.1a Model F-4J  
Analog Study Aerodynamic Data Basis

$$\delta_{FN} = 0^\circ/60^\circ/60^\circ, \delta_S = -8^\circ, C_{\mu_{LE}} = 0.019, \delta_A = 16.5^\circ$$

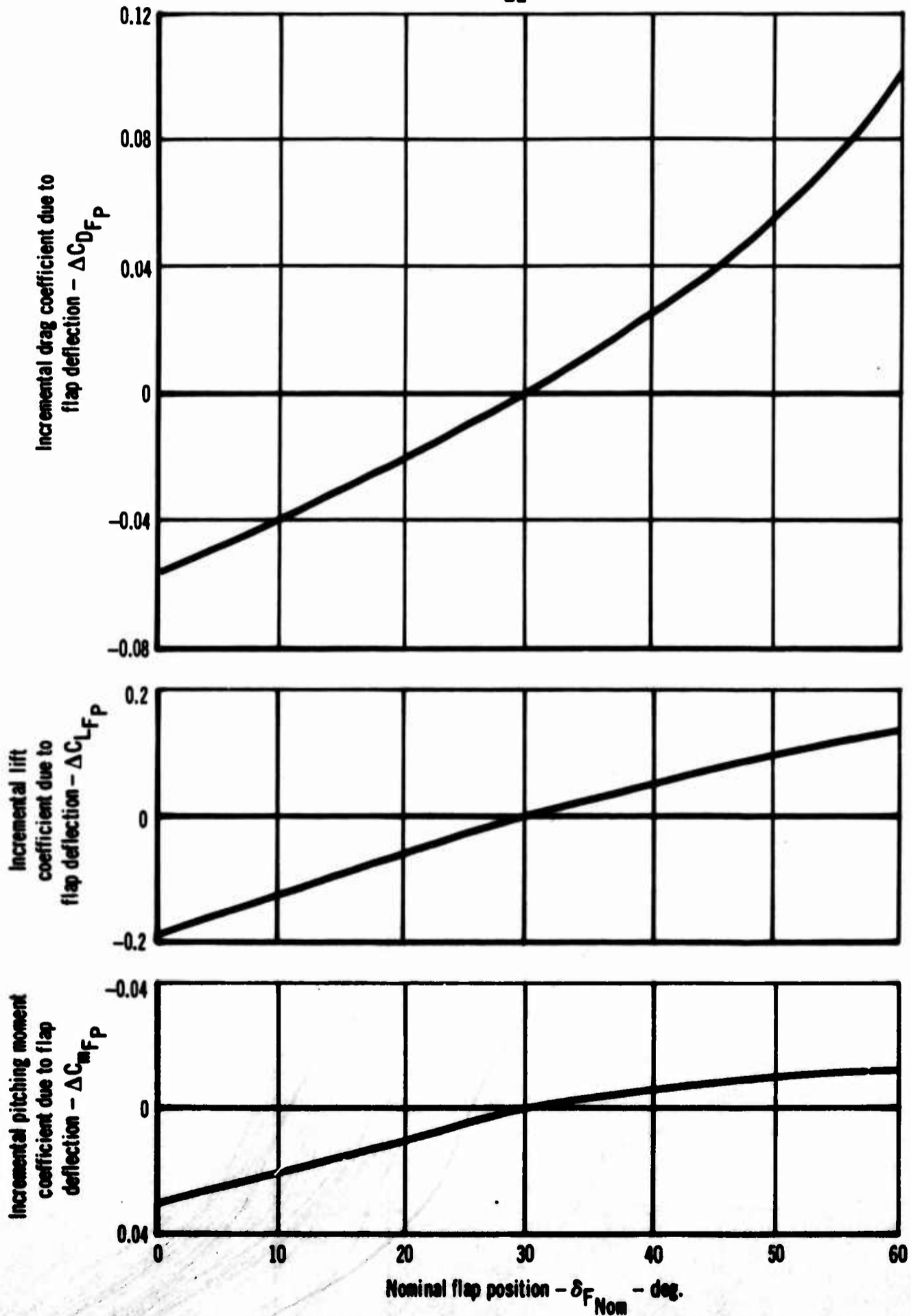


Figure A.1b Model F-4J  
Analog Study Aerodynamic Data Basis

## APPENDIX B

## ANALOG COMPUTER PROGRAM DESCRIPTION

A three-degree-of-freedom analog computer program was utilized during the course of the Direct Lift Control (DLC) study. The basic airframe equations of motion and supplementary equations used in the program are as follows:

## Basic Airframe

$$\Sigma F_x = 0 \quad (1)$$

$$m\dot{V} = \frac{\rho V^2 S}{2} (C_D + C_{D\delta_s} \Delta\delta_s + \Delta C_{DFP}) - \frac{W\gamma}{57.3} + T \cos(\alpha_{wTRIM} + \Delta\alpha + i_t)$$

$$\Sigma F_z = 0 \quad (2)$$

$$mV\dot{\gamma} = 57.3 \left[ \frac{\rho V^2 S}{2} (C_L + C_{L\delta_s} \Delta\delta_s + \Delta C_{LFP}) - W + \frac{\rho V S \bar{c}}{4} C_{L\dot{\theta}} \dot{\theta} + T \sin(\alpha_{wTRIM} + \Delta\alpha + i_t) \right]$$

$$\Sigma MCG = 0 \quad (3)$$

$$I_y \ddot{\theta} = 57.3 \left[ \frac{\rho V^2 S \bar{c}}{2} (C_{m.33\bar{c}} + C_{m\delta_s} \Delta\delta_s + \Delta C_{mFP}) + \frac{\rho V S \bar{c}^2}{4} (C_{m\dot{\theta}} \dot{\theta} + C_{m\dot{\alpha}} \dot{\alpha}) - Z_T T - \frac{\rho V^2 S \bar{c}}{2} \left( \frac{\Delta X}{\bar{c}} \right) (C_L + \Delta C_{LFP}) \right]$$

## Supplementary Equations

$$\Delta N_z = \frac{V}{g} \frac{\dot{\gamma}}{57.3} \quad (4)$$

$$V = V_{TRIM} + \int \dot{V} dt \quad (5)$$

$$\Delta H = \int V \sin\gamma dt \quad (6)$$

$$\gamma = \gamma_{TRIM} + \int \dot{\gamma} dt \quad (7)$$

$$\alpha_w = \alpha_{wTRIM} + \Delta\alpha \quad (8)$$

$$\Delta\alpha = \int \dot{\theta} dt - \int \dot{\gamma} dt \quad (9)$$

$$\dot{\theta} = \int \ddot{\theta} dt \quad (10)$$

$$\dot{\alpha} = \dot{\theta} - \dot{\gamma} \quad (11)$$

$$C_L = f(\alpha), \Delta C_{L_{FP}} = f(\delta_{FP}) \quad (12)$$

$$C_D = f(\alpha), \Delta C_{D_{FP}} = f(\delta_{FP}) \quad (13)$$

$$C_{m.33c} = f(\alpha), \Delta C_{m_{FP}} = f(\delta_{FP}) \quad (14)$$

The above equations, and the Approach Power Compensation System, Stability Augmentation System, DLC System, etc. characteristics, indicated on the block diagram of Figure (B.1), were programmed on two PACE 131 Analog Computers in the McDonnell Flight Simulation Laboratory. A computer wiring diagram is presented in Figures (B.2a) and (B.2b) and a photograph of the installation is shown in Figure (B.3). The data were recorded on one or, when required, two eight channel recorders at a paper speed of ten millimeters per second. Data recorded included flap position and flight path angle and increments of velocity, angle of attack, pitch attitude, normal load factor, altitude, stabilator position and thrust. Representative examples of time histories obtained are presented in Section 2 of the basic report and in Appendix C.

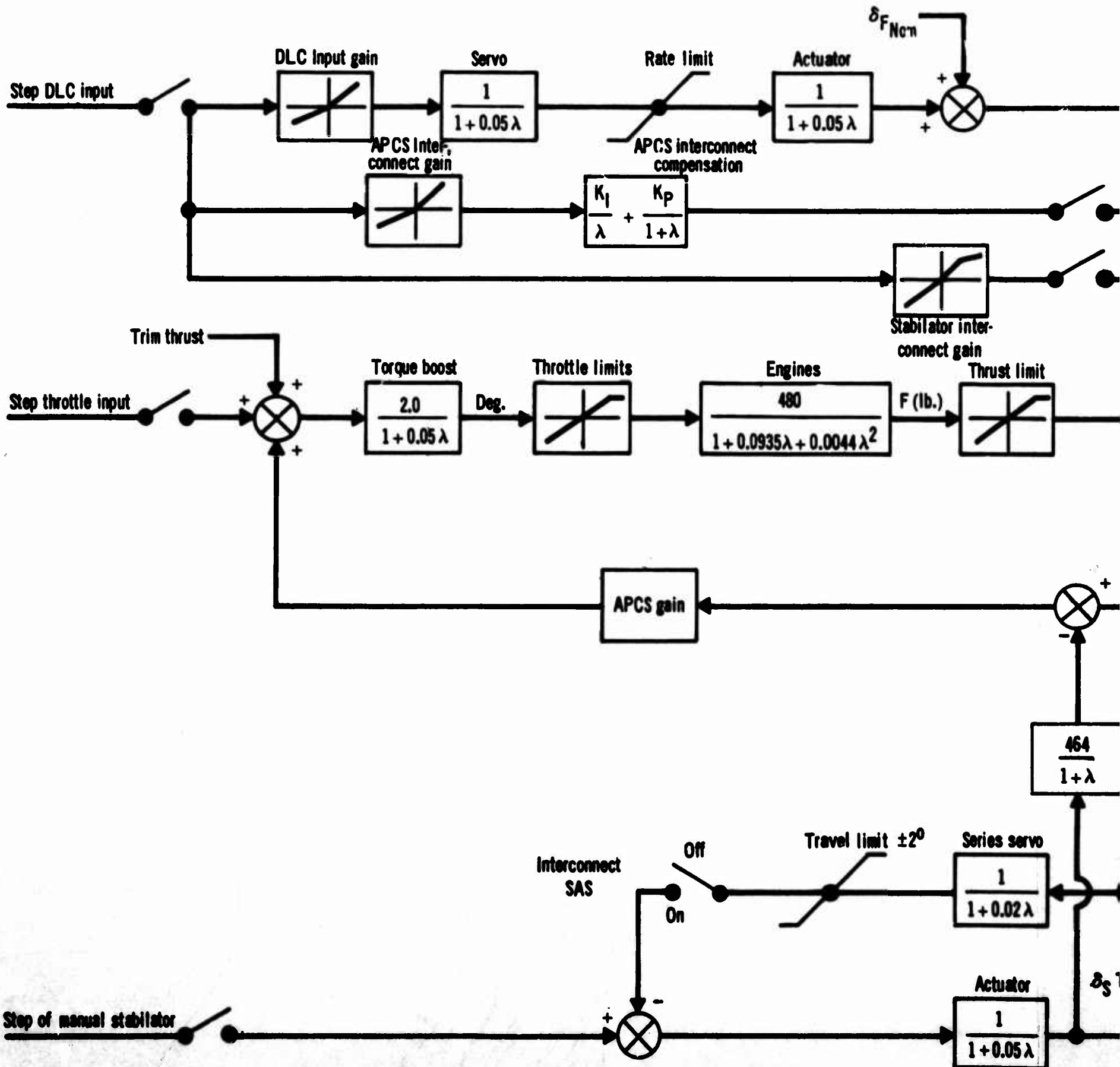
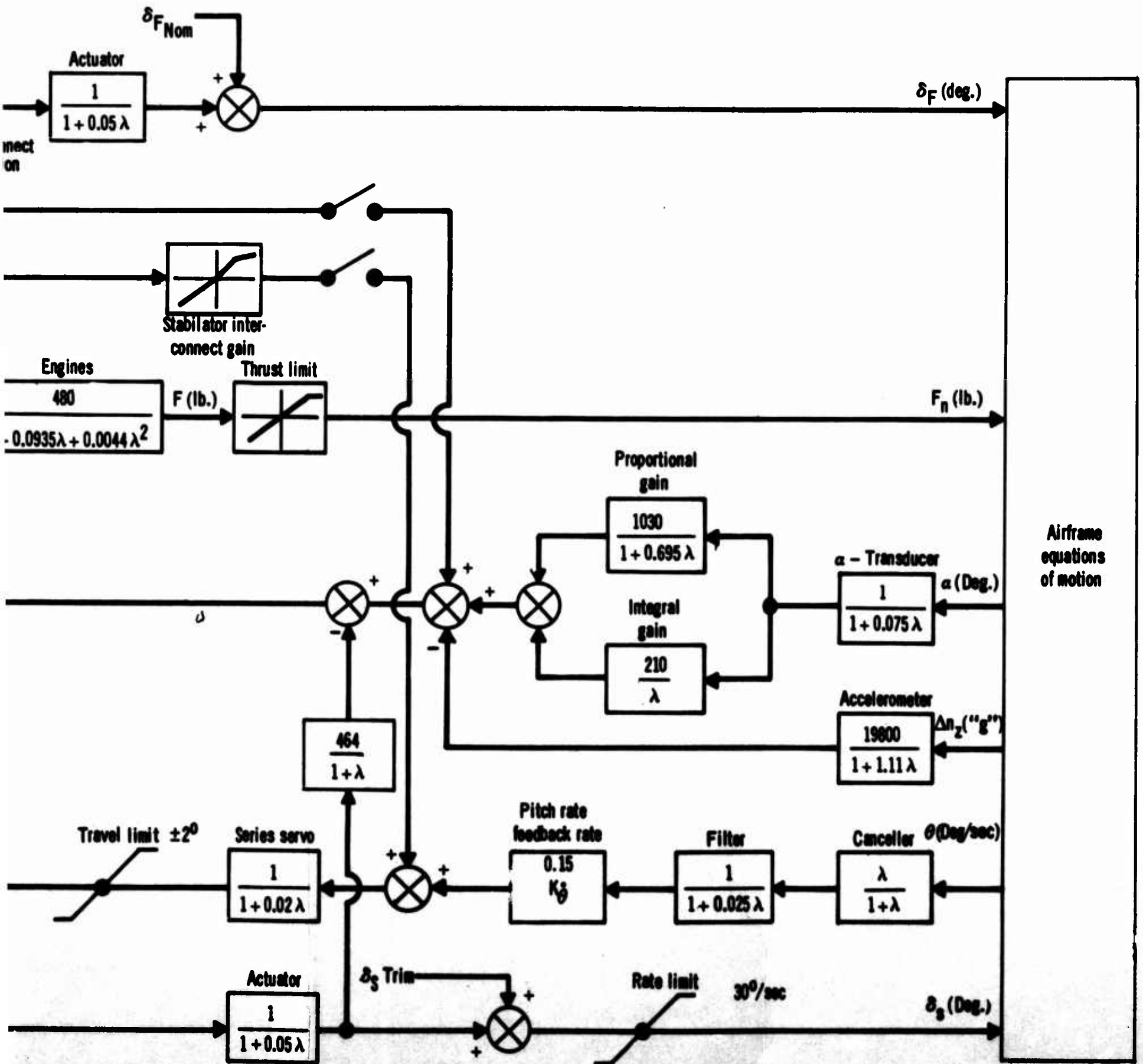


Figure B.1 Block Diagram - DLC Analog Computer Study

1 September 1967



idy

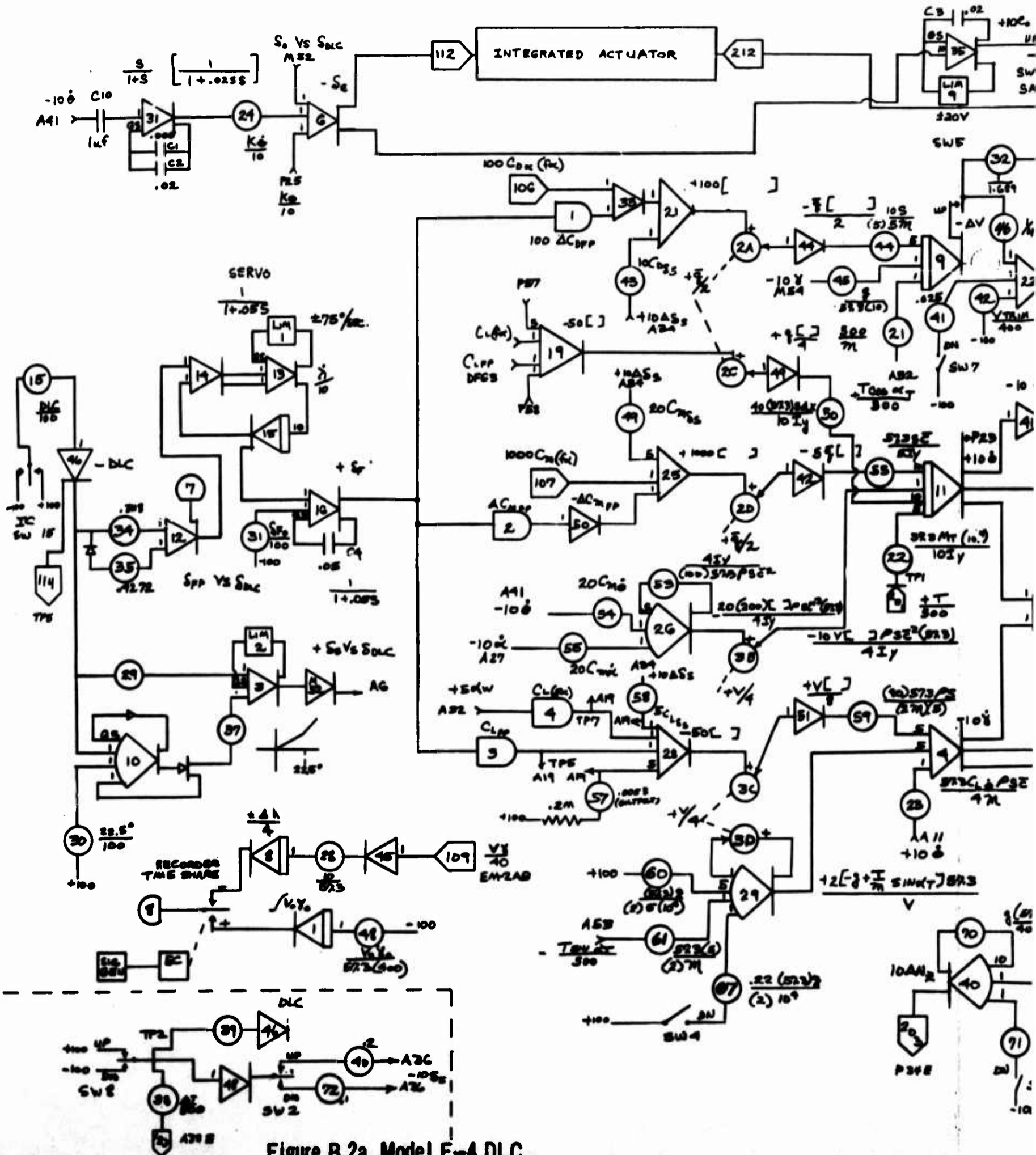
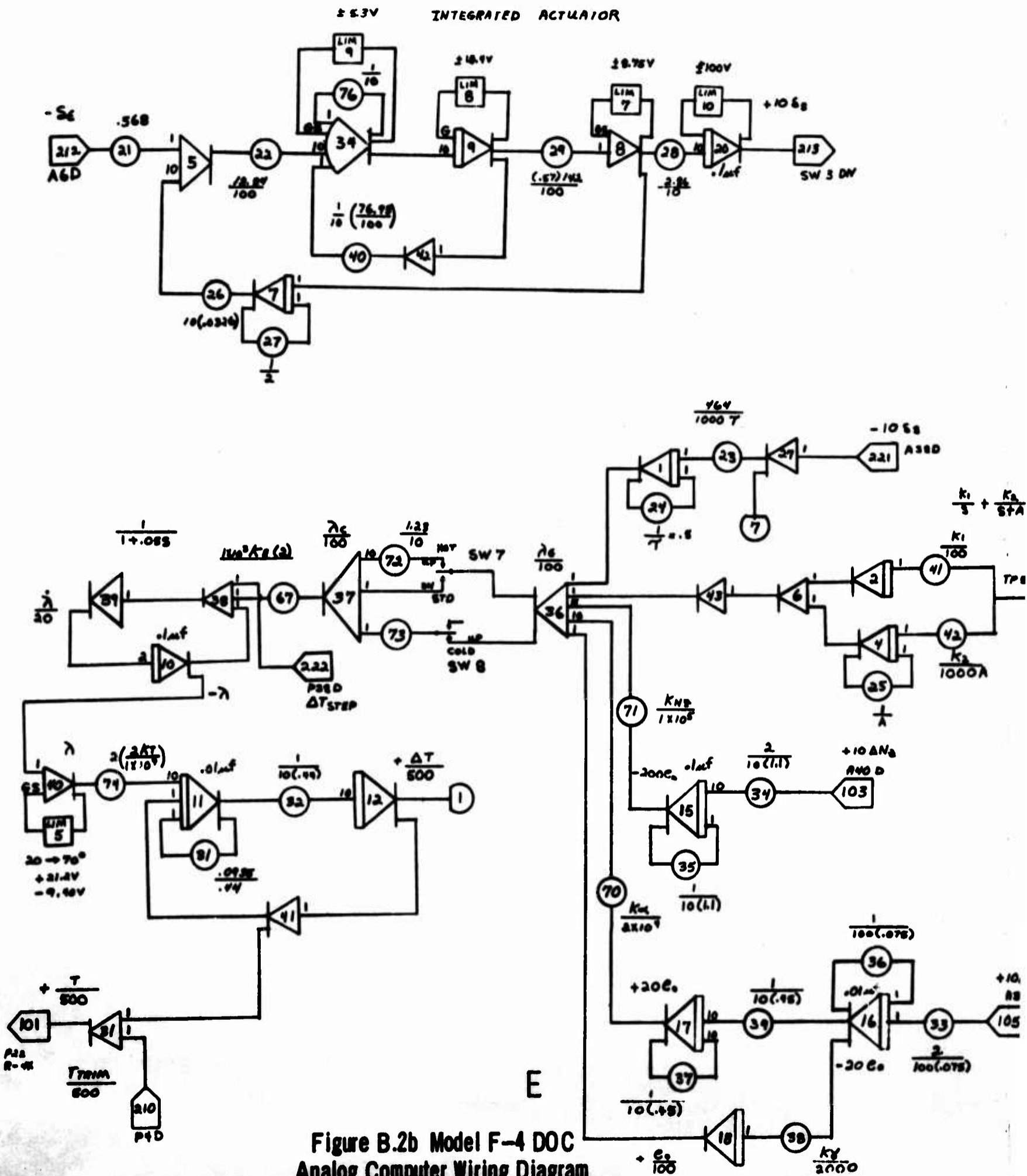


Figure B.2a Model F-4 DLC  
Analog Computer Wiring Diagram  
CR 7500-156







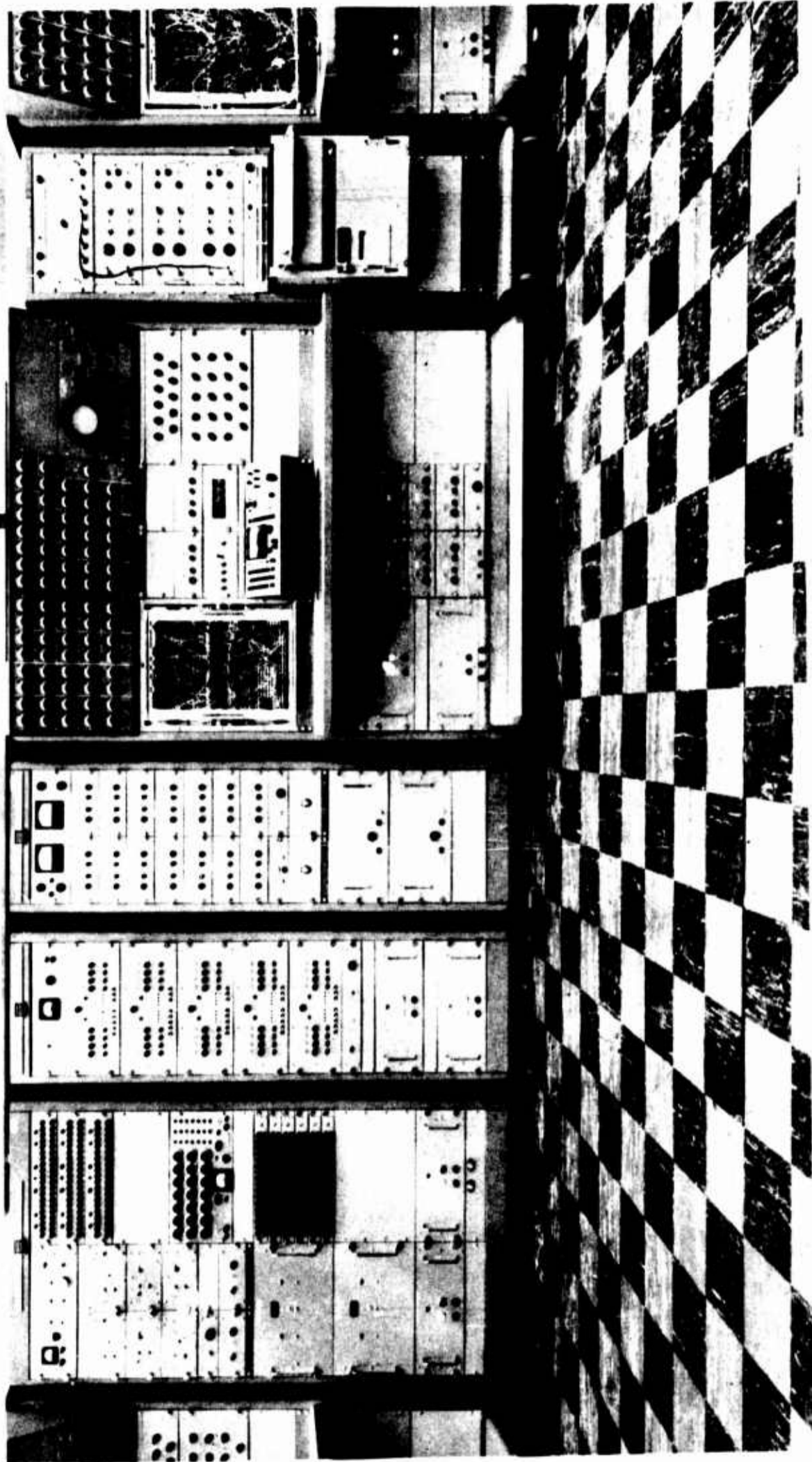


Figure B.3 Analog Computer Installation

## APPENDIX C

## ANALOG PROGRAM RESULTS

The analog computer program described in Appendix B was used to develop and evaluate the Direct Lift Control (DLC) system described in Section 2 of the basic report. Items investigated include flight path control capabilities, wave off characteristics, and, to a limited extent, the effect of DLC system failures. The following paragraphs present a brief description of results obtained.

### C.1 Flight Path Control Capabilities

The flight path control capabilities of the DLC system were investigated to determine the effect of initial flight path angle, gross weight, center of gravity and trim airspeed on the response to DLC commands. In each case the "baseline" data for each nominal flap position were: G.W. = 34,000 lb., C.G. @ 29%  $\bar{c}$ ,  $\gamma_0 = 0^\circ$ ; and  $\alpha_w \text{ TRIM} = 13^\circ$ .

C.1.1. Effect of Initial Flight Path Angle - The majority of the analog data were obtained for an initial flight path angle of zero degrees, i.e., level flight. This not only facilitated data analysis but it also would be the easiest to duplicate in flight. Figures (C.1a) through (C.2b) present typical analog time histories which demonstrate the effect of an initial flight path angle of -3.5 degrees. A "time shared trace" technique which permits simultaneous recording of both original and actual flight paths illustrates the effect of DLC application in Figure (C.1b). Figures (C.3a) through (C.6b) present a comparison of response characteristics obtained at initial flight path angles of 0 degrees and -3.5 degrees. The effect of initial flight angle on incremental load factor, attitude, and altitude is small.

C.1.2 Effect of Gross Weight - As stated above a normal landing gross weight of 34,000 lb. was used throughout most of the analog program. However to determine the effects of gross weight on flight path control capabilities two additional gross weights of 37,000 lb and 31,000 lb were evaluated. Figures (C.7a) through (C.8b) present a comparison of response characteristics obtained at the three gross weights. No change in peak normal load factor is discernible and the differences in pitch angle and altitude that do exist are small.

C.1.3 Effect of Center of Gravity - In addition to the nominal landing center of gravity of 29%  $\bar{c}$ , two additional center of gravity positions of 32 and 26%  $\bar{c}$  were evaluated in a manner similar to the gross weight study. Figures (C.9a) through (C.10b) present comparisons of the responses of the three center of gravity positions. The differences obtained due to this variation are small.

C.1.4 Effect of Trim Velocity - Deviations of  $\pm 10$  KCAS from the normal trim velocities for the two nominal flap positions were evaluated to determine the flight path control capabilities at different landing speeds. As shown in Figures (C.11a) through (C.12b) incremental changes in peak normal load factor, pitch angle and altitude, increase and decrease with corresponding velocity changes but these variations are small.

## C.2 Wave-off Characteristics

A limited evaluation of the wave-off characteristics for the two DLC nominal flap configurations was conducted to permit comparison with similar characteristics for the present Model F-4J full and half flap configurations. Wave-offs from a -3.5 degree glide slope approach were simulated by assuming simultaneous pilot commands of military power, airplane nose up stabilator, and where applicable, full up DLC. A brief summary of the results obtained is given in the following paragraphs.

C.2.1 Two Engine Wave-off - Figure (C.13) compares wave-off characteristics obtained for the 27 degree DLC nominal flap configuration with wave-off characteristics of the Model F-4J full flap configuration. Figure (C.14) presents a similar comparison for the 32 degree DLC nominal flap configuration. Figures (C.15a and C.15b) present typical analog time histories of the above data. In each case, when DLC is not employed the effect of flap configuration is relatively small. When DLC is employed, the stabilator input required by the pilot to obtain the same altitude loss is considerably decreased; however, the use of DLC does not significantly increase the wave-off capabilities, i.e., minimum altitude loss to the point where rate of climb/sink goes to zero. This is further illustrated in Figure (C.16) which presents a summary of wave-off characteristics.

C.2.2 Single Engine - Figure (C.17) compares single engine wave-off characteristics of the two DLC nominal flap configurations with the characteristics of the present Model F-4J half flap, single engine, approach configuration. The use of DLC during single engine approaches was not considered. The effect of flap position is almost negligible and indicates that either DLC-nominal flap position would be suitable as a single engine approach configuration.

## C.3 Failure Analysis

A limited study was conducted to evaluate the consequences of two DLC system failures. The failures considered were:

- (1) a "downstream" failure which results in a full down DLC command to the flaps (i.e. retract flaps) without a corresponding command to the DLC-Stabilator Interconnect, and
- (2) an "upstream" failure which results in a full down DLC command to both the flaps and the DLC-Stabilator Interconnect. It was assumed that insufficient time remained in the approach to disengage DLC and return to the normal half or full flap configuration and that the pilot attempted to counteract the failure with stabilator inputs at various time intervals after failure.

C.3.1 Effect of Stabilator Input - Figures (C.18) and (C.19) present the effect of pilot corrective stabilator input on the maximum deviations of the aircraft from the initial flight path. The "time shared trace" technique discussed in paragraph C.1.1 is used to illustrate the flight path deviation on the analog trace. It is apparent that the "downstream" failure is somewhat self corrective in that the absence of the DLC-Stabilator Interconnect tends to return the aircraft to its original flight path without corrective action by the pilot. An

"upstream" failure, on the other hand, does require considerable pilot corrective action to counteract the effects of the failure.

C.3.2 Effect of Pilot Reaction Time - Figures (C.20) and (C.21) present the effect of time interval between system failure and pilot corrective stabilator input on the deviations of the aircraft from the initial flight path. The self corrective characteristics of the "downstream" failure is again apparent while an "upstream" failure is more sensitive to pilot reaction time. However, there is apparently only a short time interval, in the final approach just prior to touchdown, during which a failure would:

- (1) Result in significant deviations in flight path or sink rate at touchdown.
- (2) Not allow sufficient time to counteract the failure.

$\delta F_{Nom} = 27^\circ$       C.G. at 29%  $\bar{c}$        $V_{Trim} = 142.0$  KCAS  
 G.W. = 34,000 Lb.       $\gamma_0 = 0^\circ$        $\alpha_{wTrim} = 13^\circ$   
 With APCS

Pilot DLC command -  $\delta_{DLC}$  - 100% wheel (positive)

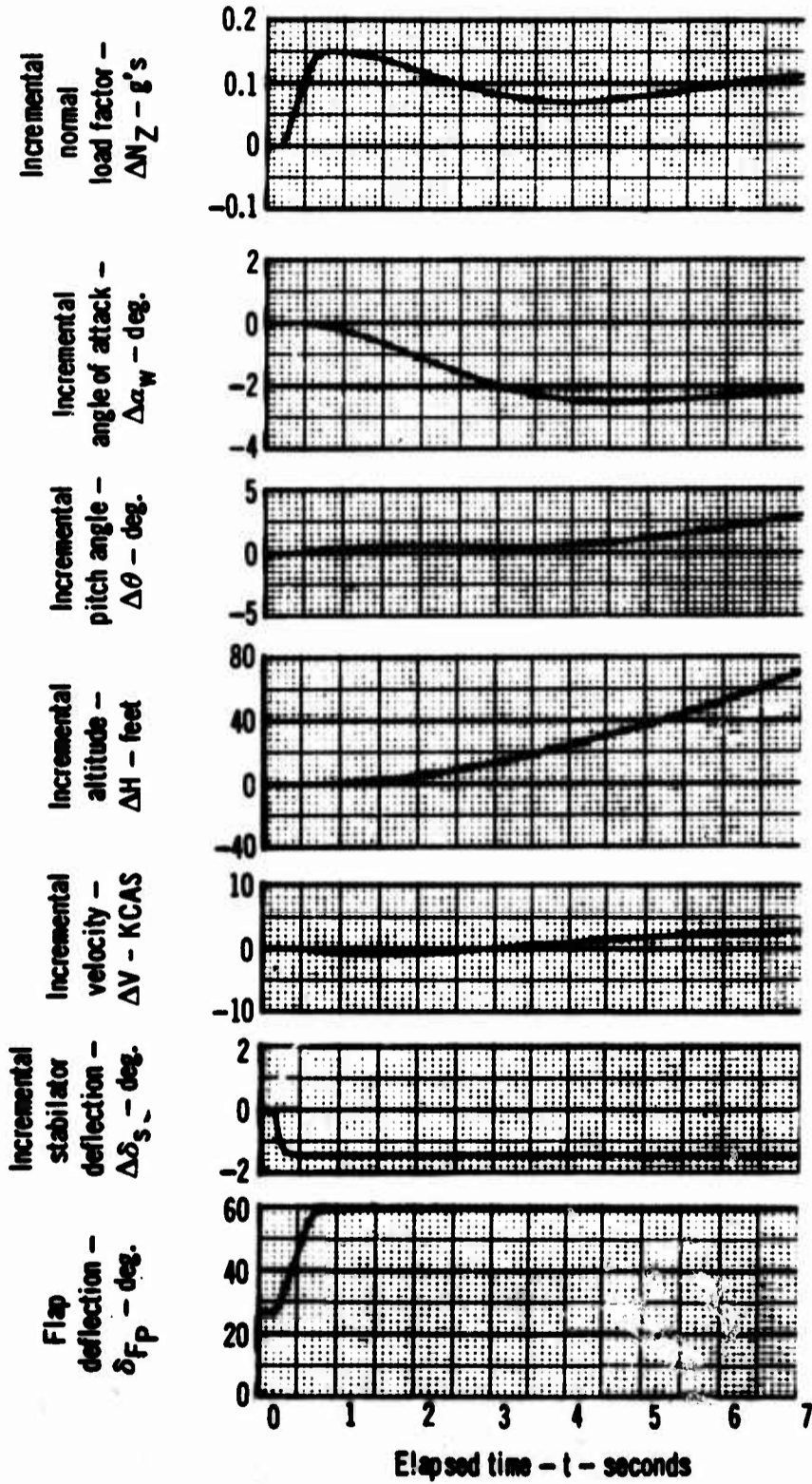


Figure C.1a Model F-4J  
Effect of Initial Flight Path Angle

$\delta_{F_{Nom}} = 27^\circ$       C.G. at 29%  $\bar{c}$        $V_{Trim} = 143.1$  KCAS  
 G.W. = 34,000 Lb.       $\gamma_0 = -3.5^\circ$        $\alpha_{w_{Trim}} = 13^\circ$

With APCS

Pilot DLC command -  $\delta_{DLC}$  - 100% wheel (positive)

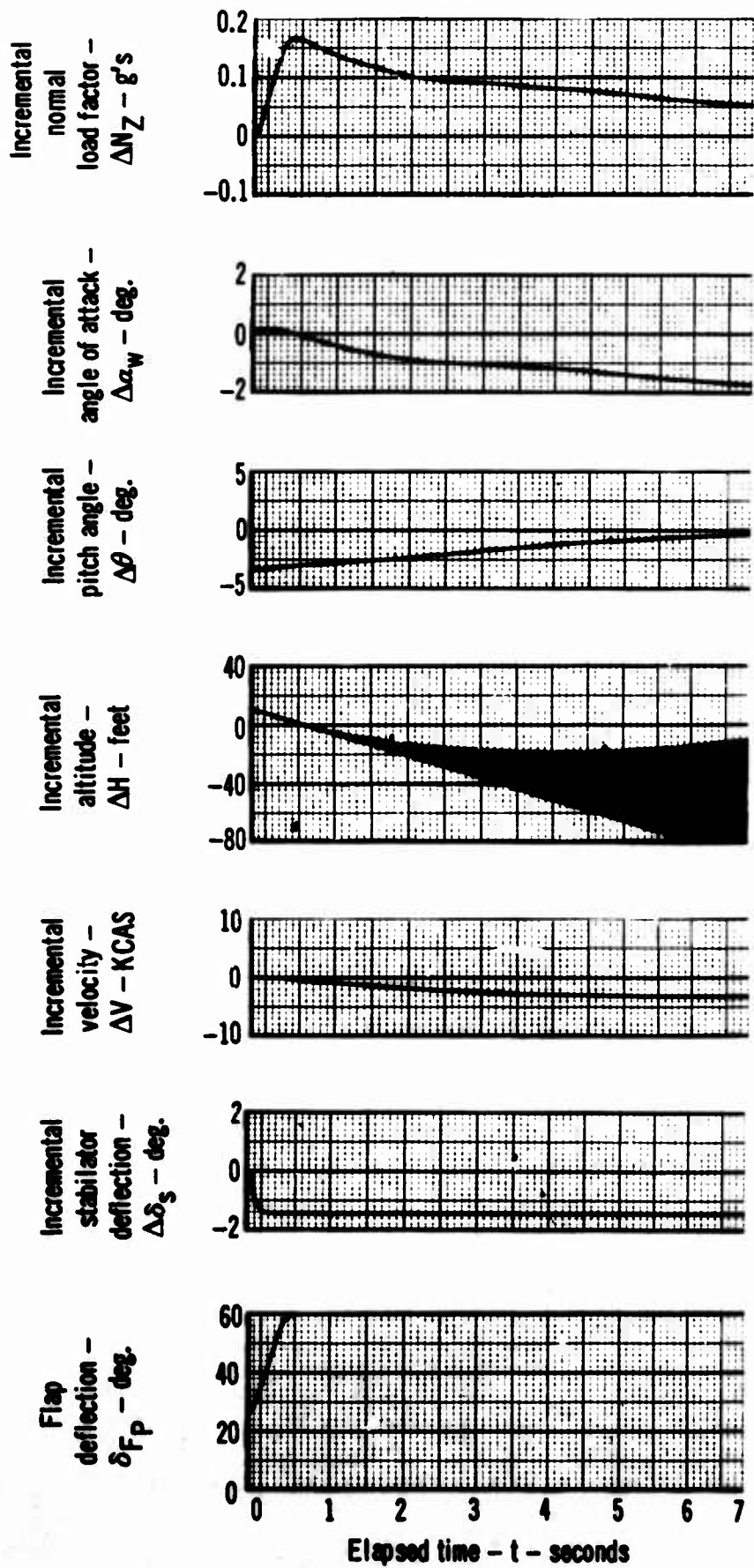


Figure C.1b Model F-4J  
 Effect of Initial Flight Path Angle

$\delta_{F \text{ Nom}} = 32^\circ$       C.G. at 29%  $\bar{c}$        $V_{\text{Trim}} = 140.0$  KCAS  
 G.W. = 34,000 Lb.       $\gamma_0 = 0^\circ$        $\alpha_{w \text{ Trim}} = 13^\circ$   
 With APCS

Pilot DLC command -  $\delta_{\text{DLC}}$  - 100% wheel (positive)

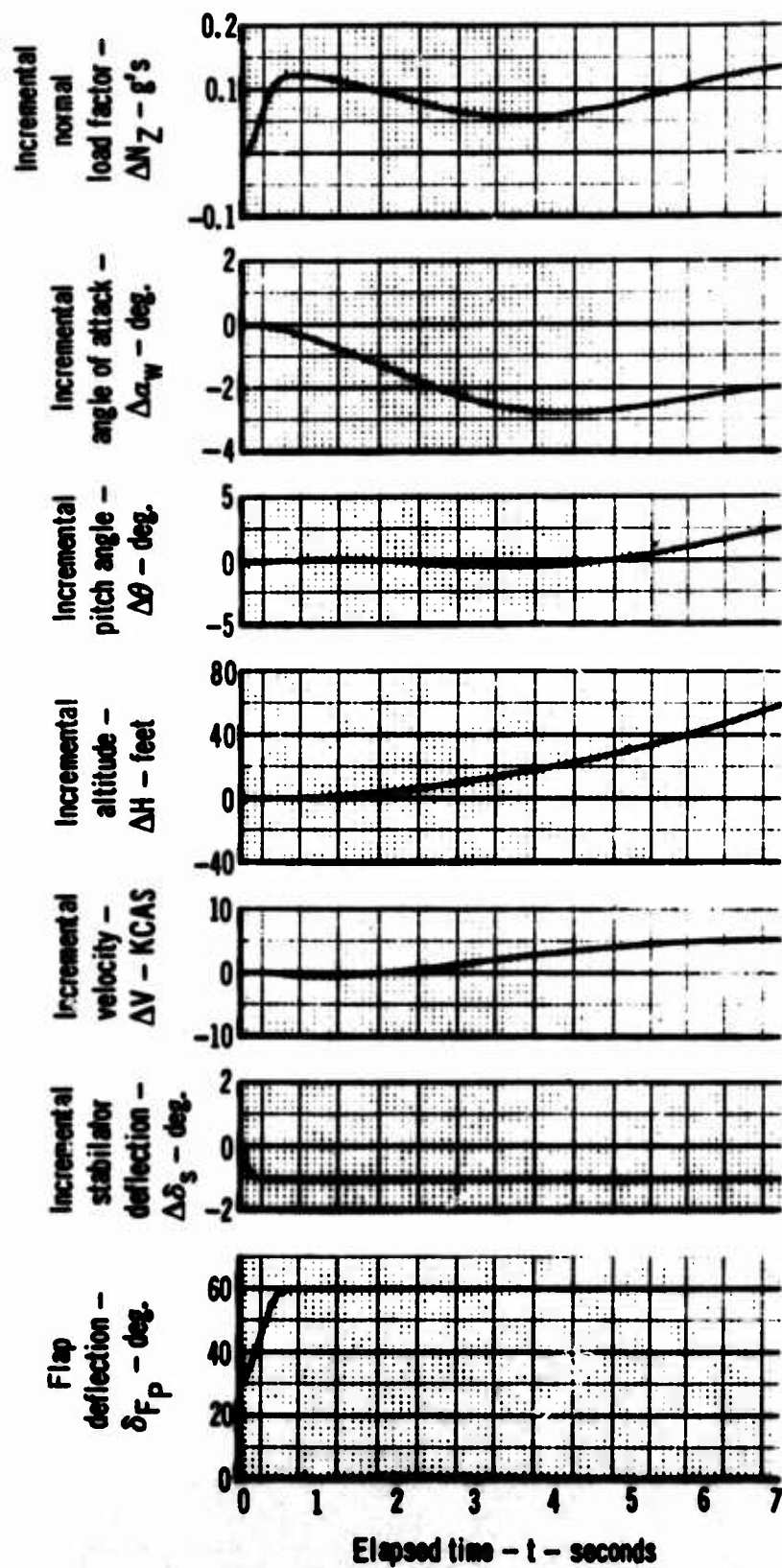


Figure C.2a Model F-4J  
Effect of Initial Flight Path Angle

$\delta_{F \text{ Nom}} = 32^\circ$     C.G. at 29%  $\bar{c}$      $V_{\text{Trim}} = 141.3$  KCAS  
 G.W. = 34,000 Lb.     $\gamma_0 = -3.5^\circ$      $\alpha_{w \text{ Trim}} = 13^\circ$   
 With APCS

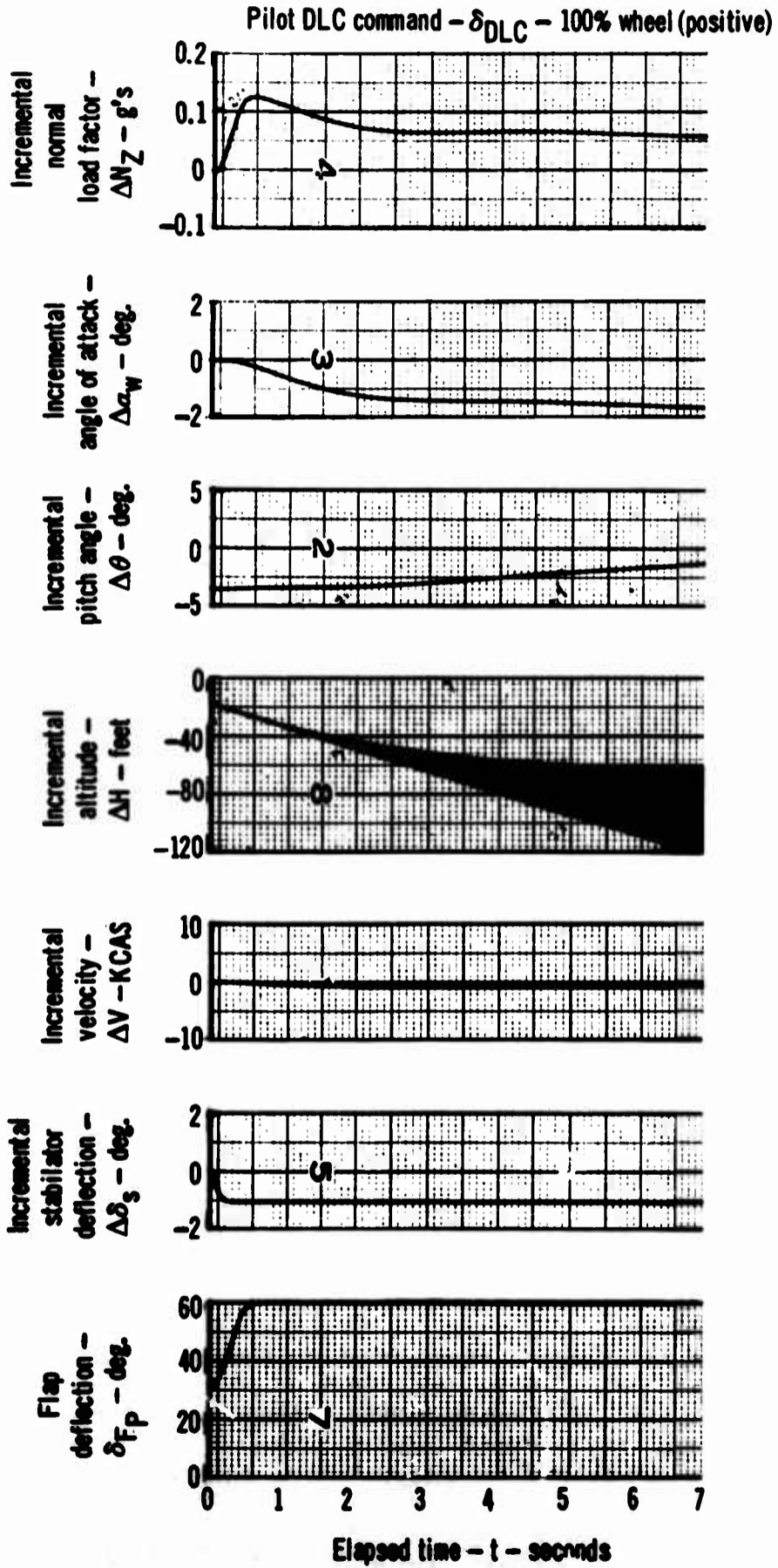


Figure C.2b Model F-4J  
Effect of Initial Flight Path Angle

$$\delta_{F \text{ Nom.}} = 27^\circ; \alpha_{w \text{ Trim}} = 13^\circ$$

Symbol	C.G. (%F)	G.W. (Lb.)	V <sub>Trim</sub> (KCAS)	APCS	Interconnect	$\gamma_0$
————	29	34,000	142.0	Out	In	0°
-----	29	34,000	143.1	Out	In	-3.5°

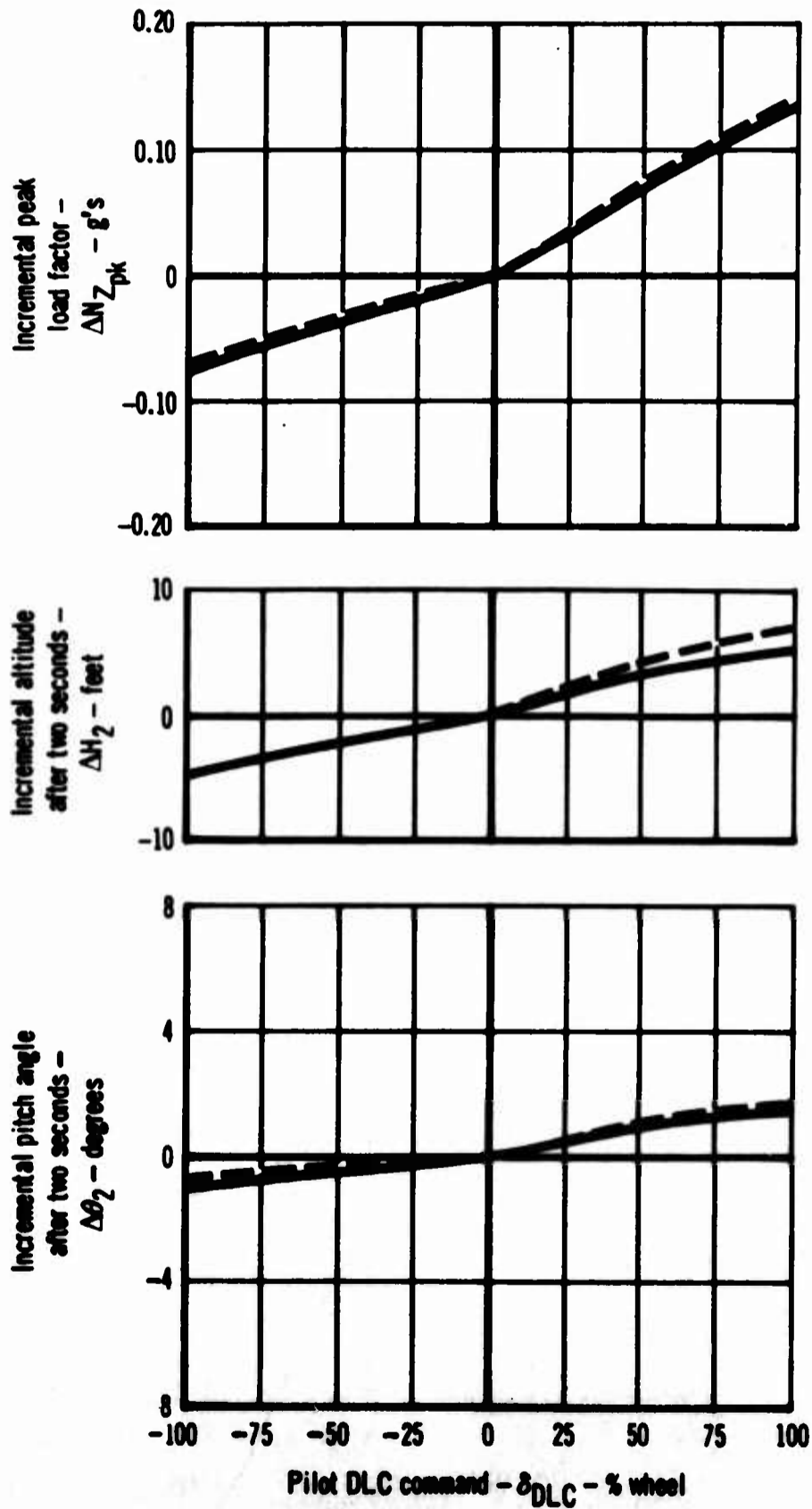


Figure C.3a Model F-4J  
Effect of Initial Flight Path Angle

$\delta_{F\text{Nom.}} = 27^\circ$ ;  $\alpha_{w\text{Trim}} = 13^\circ$

Symbol	C.G. (% $\bar{c}$ )	G.W. (Lb.)	V <sub>Trim</sub> (KCAS)	APCS	Interconnect	$\gamma_0$
—	29	34,000	142.0	Out	In	0°
- - -	29	34,000	143.1	Out	In	-3.5°

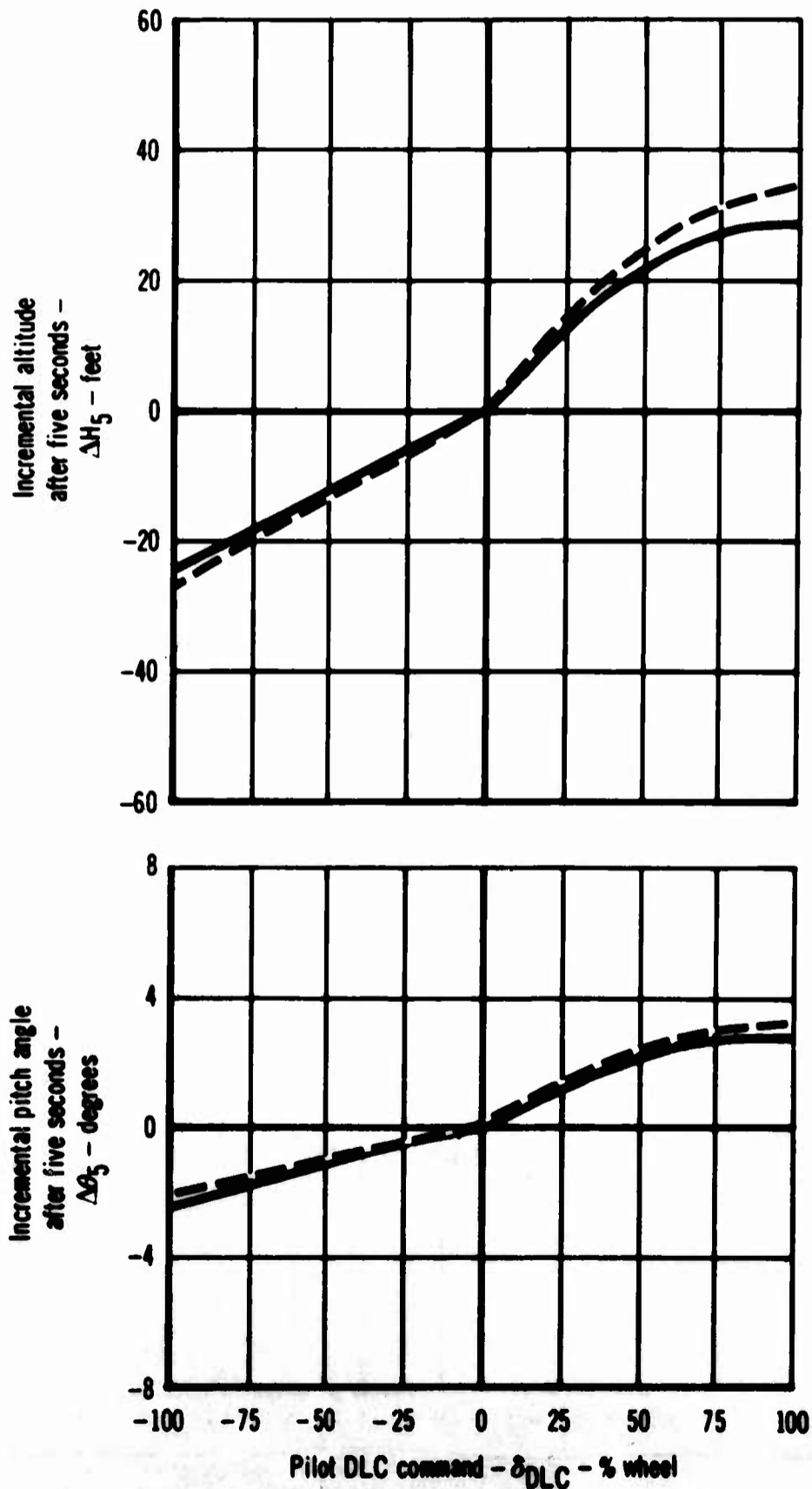


Figure C.3b Model F-4J  
Effect of Initial Flight Path Angle

$\delta_{F\text{Nom.}} = 32^\circ$ ;  $\alpha_{w\text{Trim}} = 13^\circ$

Symbol	C.G. (%C)	G.W. (Lb.)	V <sub>Trim</sub> (KCAS)	APCS	Interconnect	$\gamma_0$
—	29	34,000	140.0	Out	In	0°
- - -	29	34,000	141.3	Out	In	-3.5°

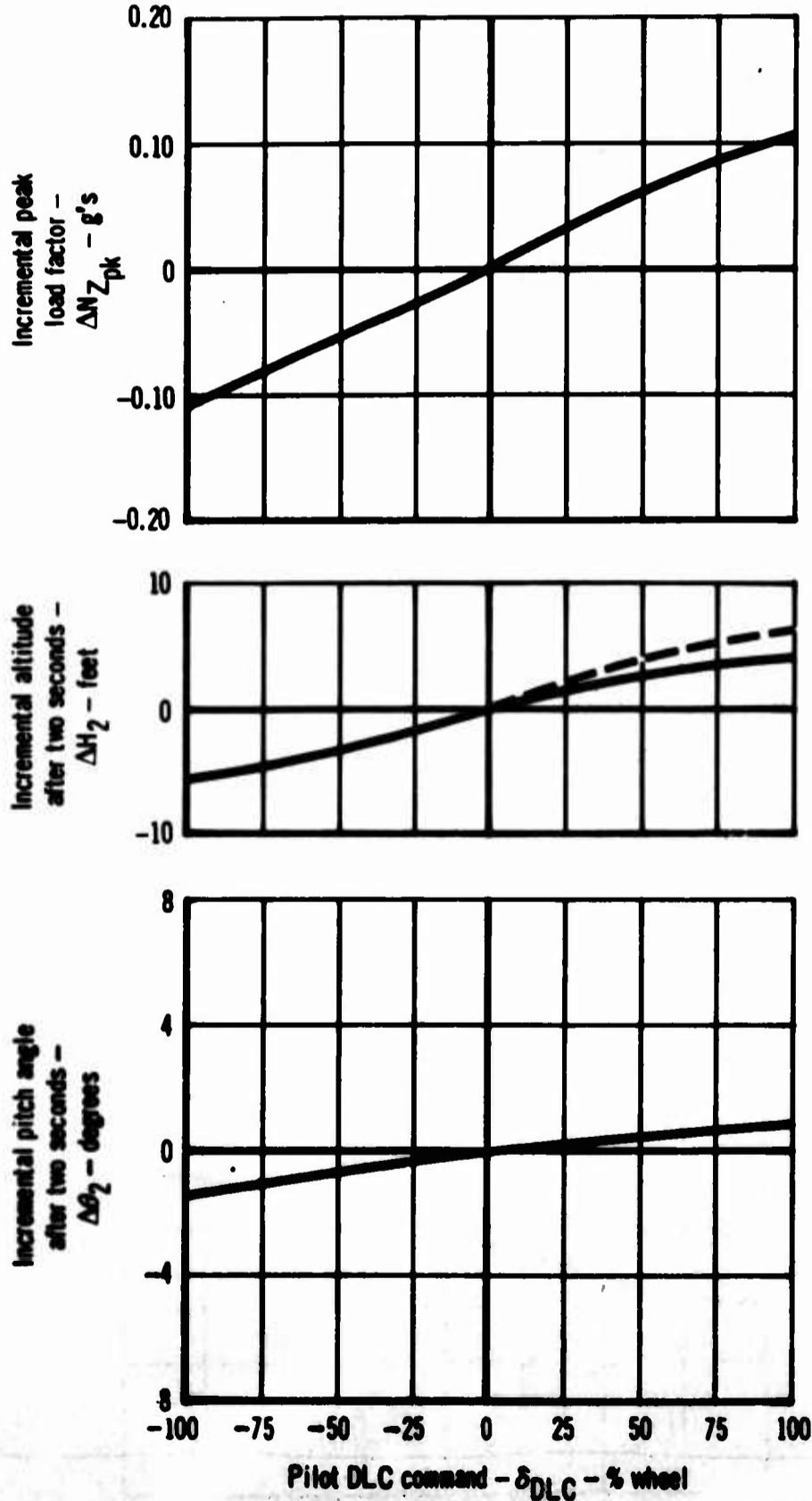


Figure C.4a Model F-4J  
Effect of Initial Flight Path Angle

$\delta_{F \text{ Nom.}} = 32^\circ$ ;  $\alpha_{w \text{ Trim}} = 13^\circ$

Symbol	C.G. (% $\bar{c}$ )	G.W. (Lb.)	$V_{\text{Trim}}$ (KCAS)	APCS	Interconnect	$\gamma_0$
————	29	34,000	140.0	Out	In	$0^\circ$
- - - -	29	34,000	141.3	Out	In	$-3.5^\circ$

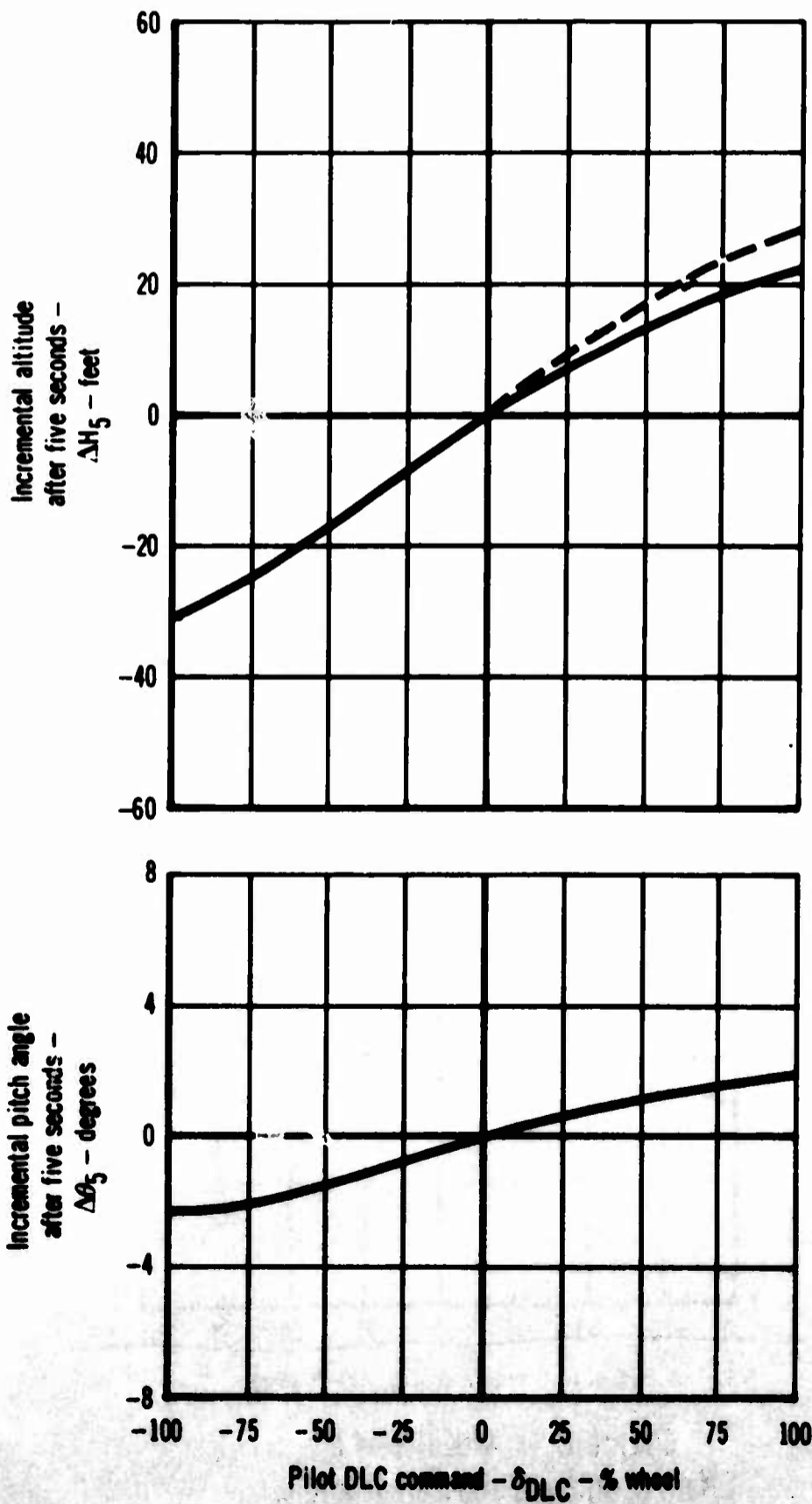


Figure C.4b Model F-4J  
Effect of Initial Flight Path Angle

$\delta_{F \text{ Nom.}} = 27^\circ$ ;  $\alpha_{w \text{ Trim}} = 13^\circ$

Symbol	C.G. (% $\bar{c}$ )	G.W. (Lb.)	$V_{\text{Trim}}$ (KCAS)	APCS	Interconnect	$\gamma_0$
—	29	34,000	142.0	In	In	$0^\circ$
- - -	29	34,000	143.1	In	In	$-3.5^\circ$

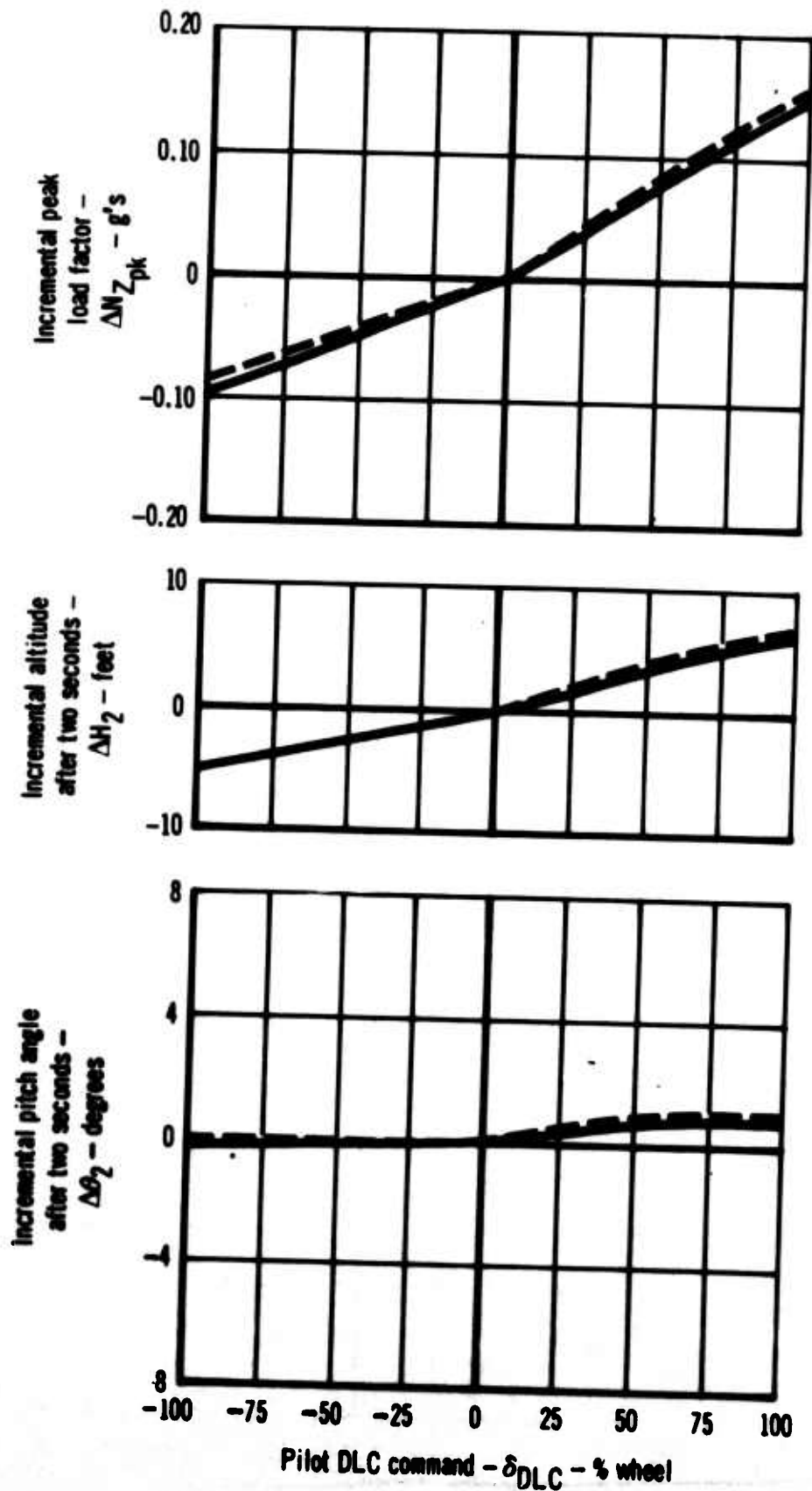


Figure C.5a Model F-4J  
Effect of Initial Flight Path Angle

$$\delta_{F_{Nom.}} = 27^{\circ}; \alpha_{w_{Trim}} = 13^{\circ}$$

Symbol	C.G. (%C)	G.W. (Lb.)	V <sub>Trim</sub> (KCAS)	APCS	Interconnect	$\gamma_0$
————	29	34,000	142.0	In	In	0°
- - - -	29	34,000	143.1	In	In	-3.5°

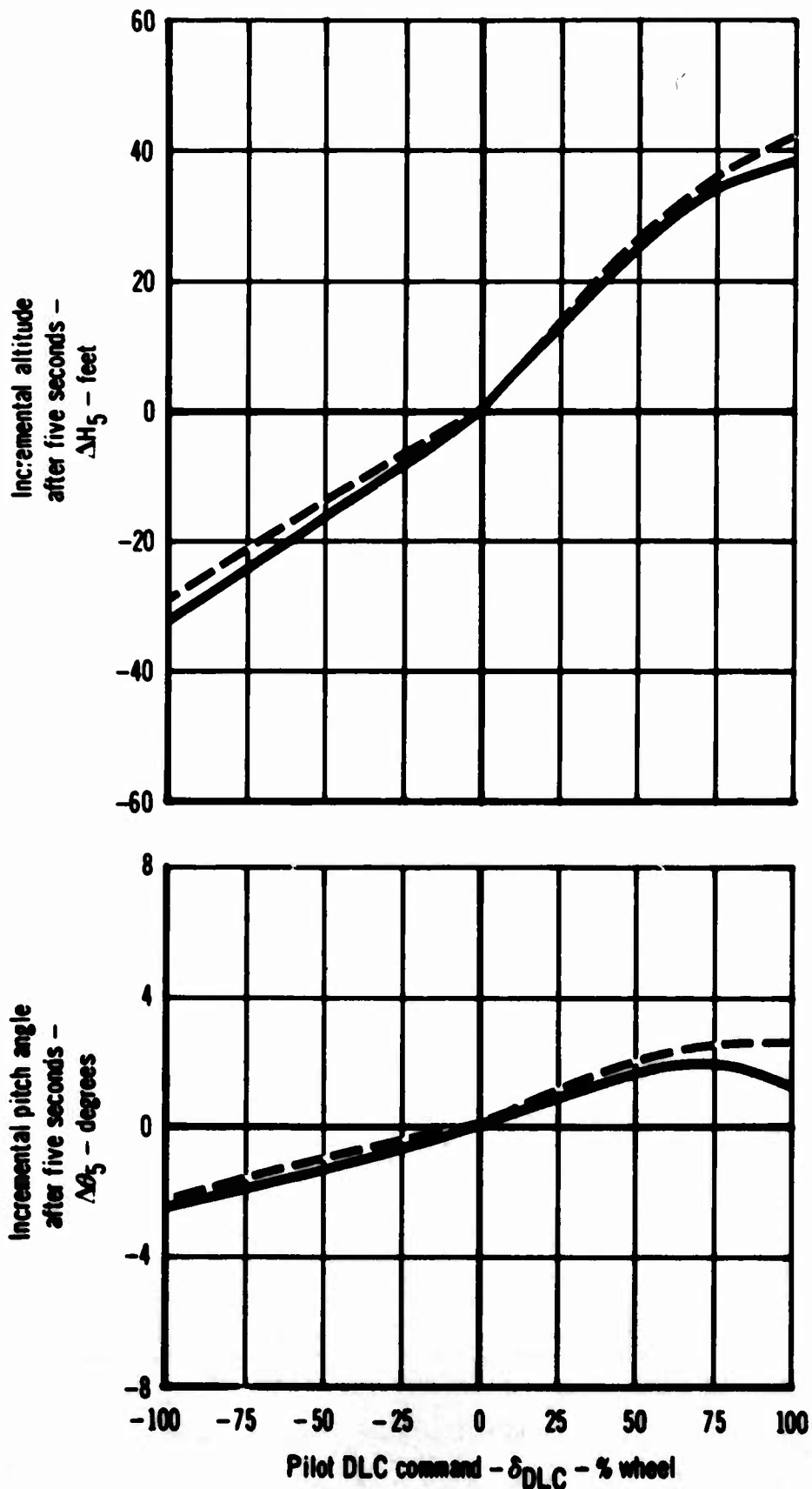


Figure C.5b Model F-4J  
Effect of Initial Flight Path Angle

$$\delta_{F_{Nom.}} = 32^\circ; \alpha_{w_{Trim}} = 13^\circ$$

Symbol	C.G. (% $\bar{c}$ )	G.W. (Lb.)	$V_{Trim}$ (KCAS)	APCS	Interconnect	$\gamma_0$
————	29	34,000	140.0	In	In	$0^\circ$
- - - - -	29	34,000	141.3	In	In	$-3.5^\circ$

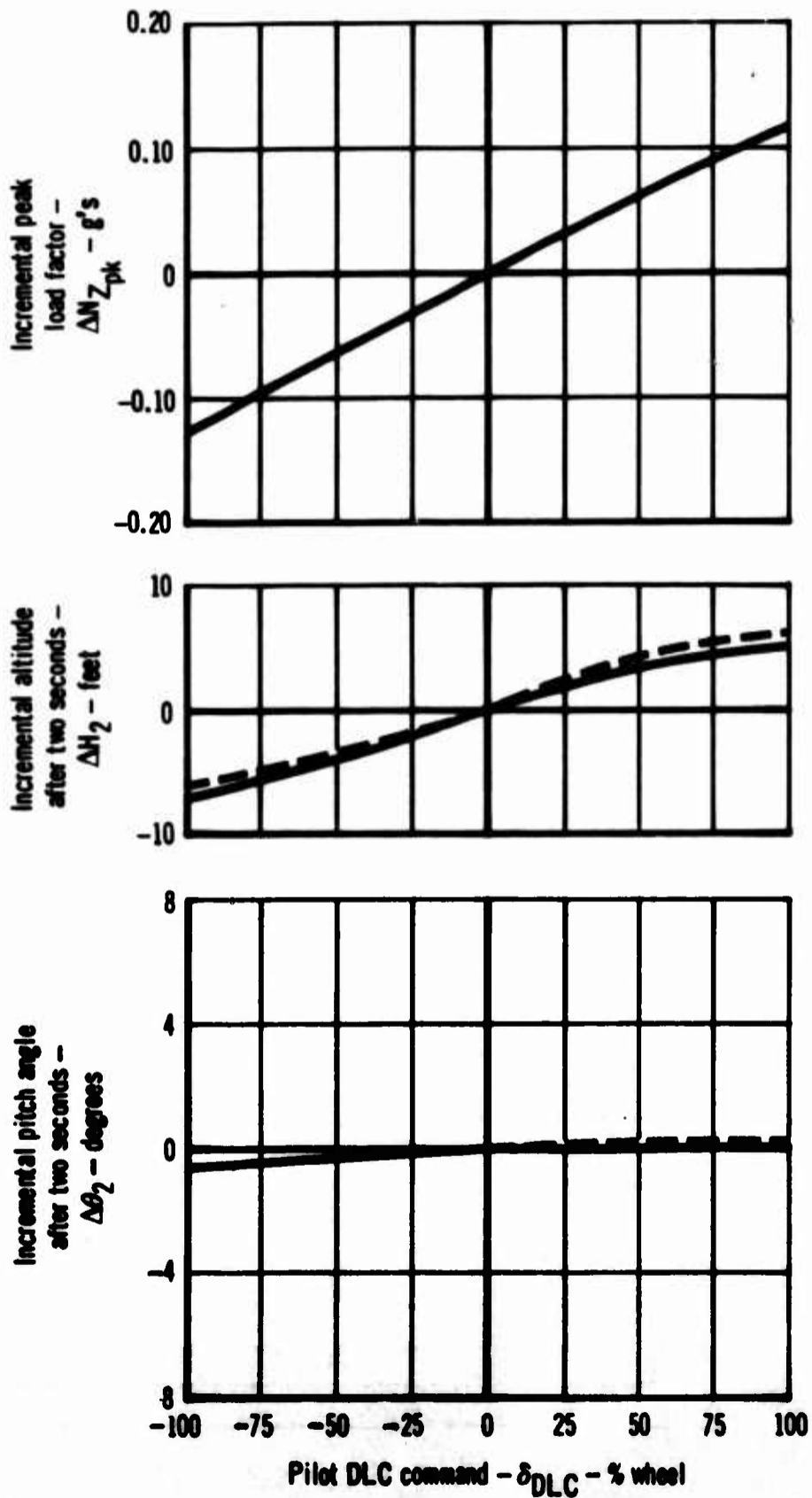


Figure C.6a Model F-4J  
Effect of Initial Flight Path Angle

$$\delta_{F \text{ Nom.}} = 32^\circ; \alpha_{w \text{ Trim}} = 13^\circ$$

Symbol	C.G. (%C)	G.W. (Lb.)	V <sub>Trim</sub> (KCAS)	APCS	Interconnect	$\gamma_0$
————	29	34,000	140.0	In	In	0°
-----	29	34,000	141.3	In	In	-3.5°

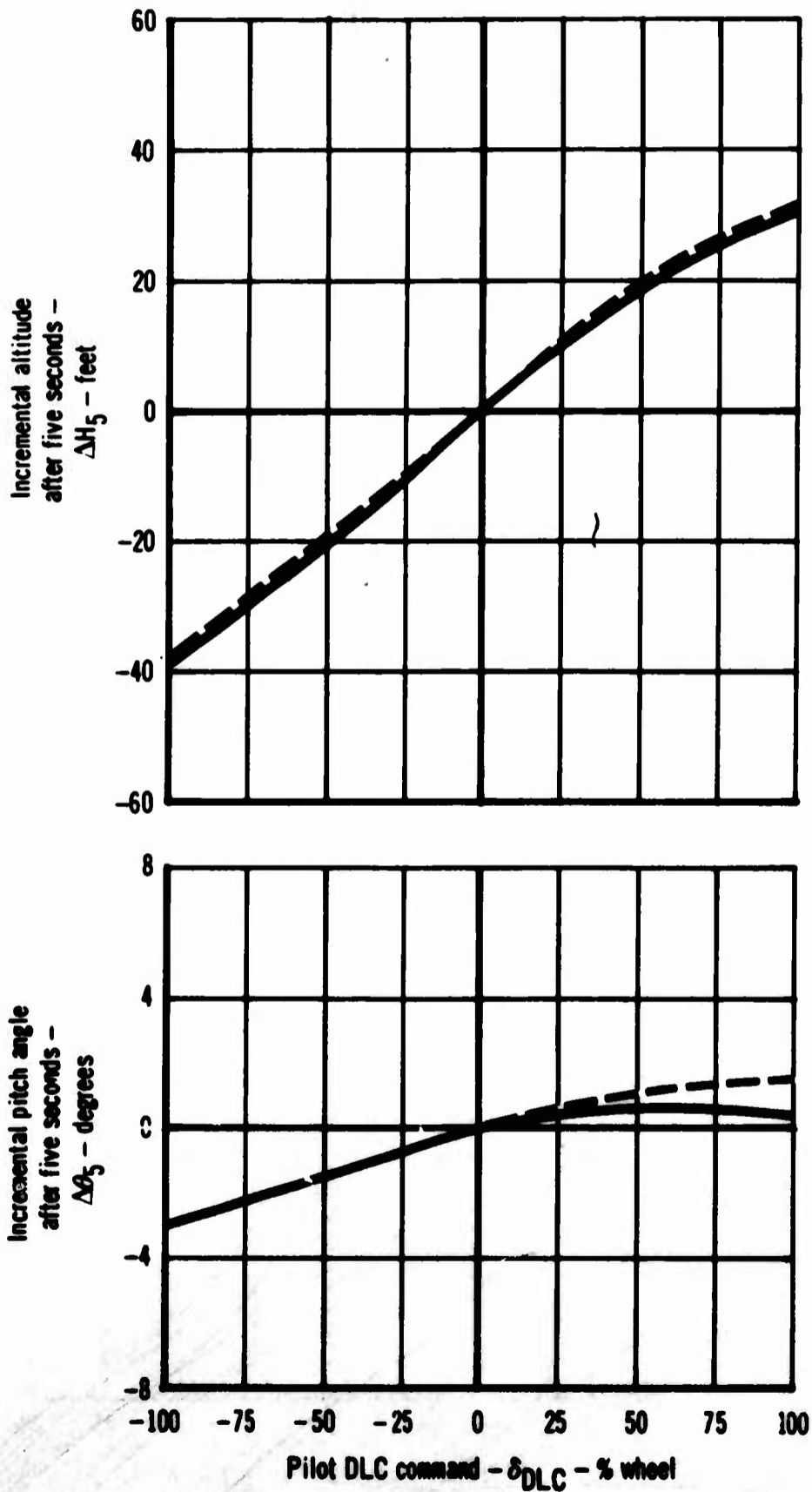


Figure C.6b Model F-4J  
Effect of Initial Flight Path Angle

$$\delta_{F_{Nom.}} = 27^{\circ}; \gamma_0 = 0^{\circ}; a_{w_{Trim}} = 13^{\circ}$$

Symbol	C.G. (% $\bar{c}$ )	G.W. (Lb.)	V <sub>Trim</sub> (KCAS)	APCS	Interconnect
---	29	37,000	148.3	In	In
---	29	34,000	142.0	In	In
.....	29	31,000	135.3	In	In

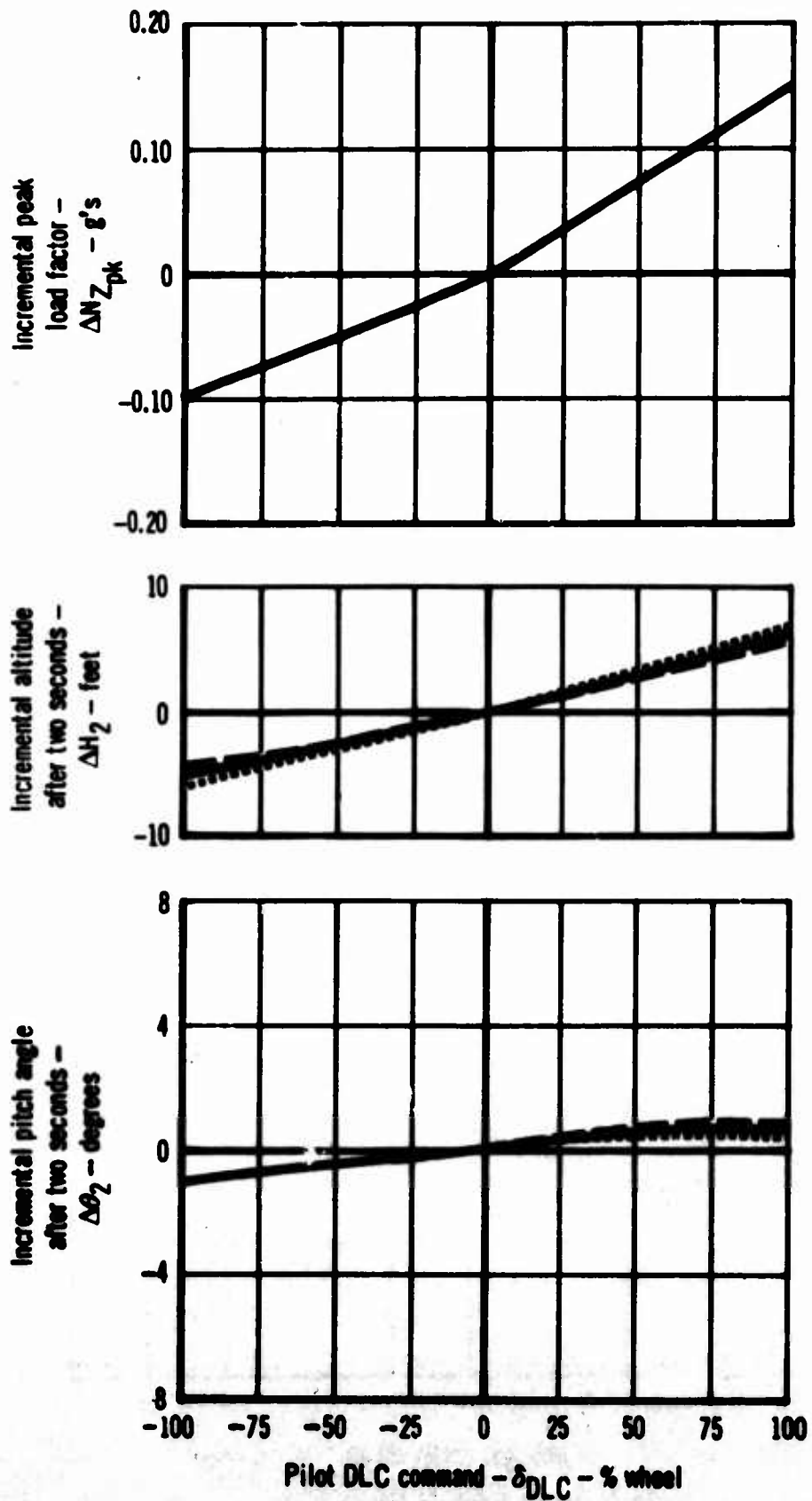


Figure C.7a Model F-4J  
Effect of Gross Weight

$$\delta_{F_{Nom.}} = 27^{\circ}; \gamma_0 = 0^{\circ}; \alpha_{w_{Trim}} = 13^{\circ}$$

Symbol	C.G. (%C)	G.W. (Lb.)	V <sub>Trim</sub> (KCAS)	APCS	Interconnect
---	29	37,000	148.3	In	In
—	29	34,000	142.0	In	In
.....	29	31,000	135.3	In	In

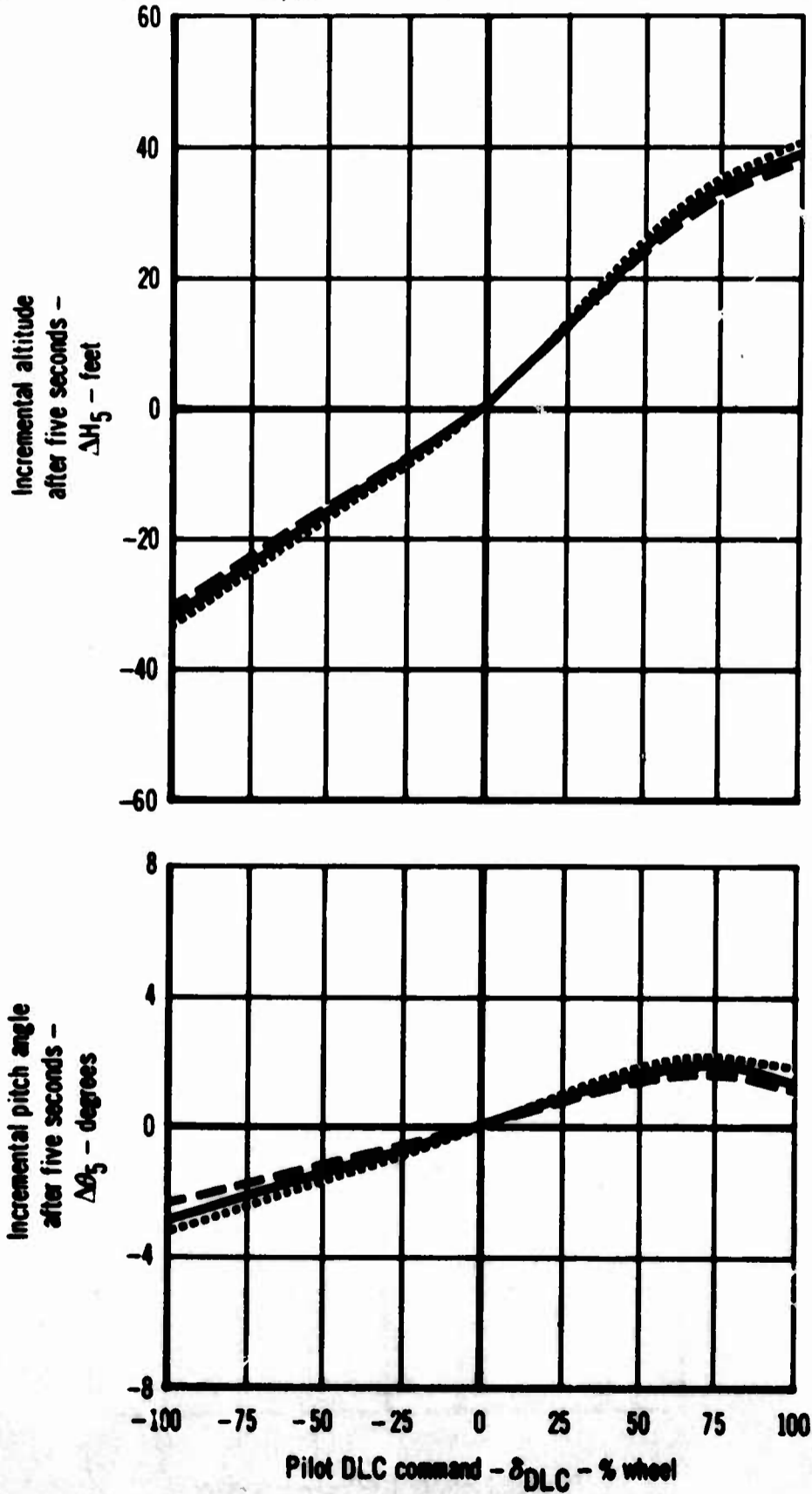


Figure C.7b Model F-4J  
Effect of Gross Weight

$$\delta_{F_{Nom.}} = 32^{\circ}; \gamma_0 = 0^{\circ}; \alpha_{wTrim} = 13^{\circ}$$

Symbol	C.G. (% $\bar{c}$ )	G.W. (Lb.)	$V_{Trim}$ (KCAS)	APCS	Interconnect
— — —	29	37,000	146.3	In	In
— — —	29	34,000	140.0	In	In
.....	29	31,000	133.7	In	In

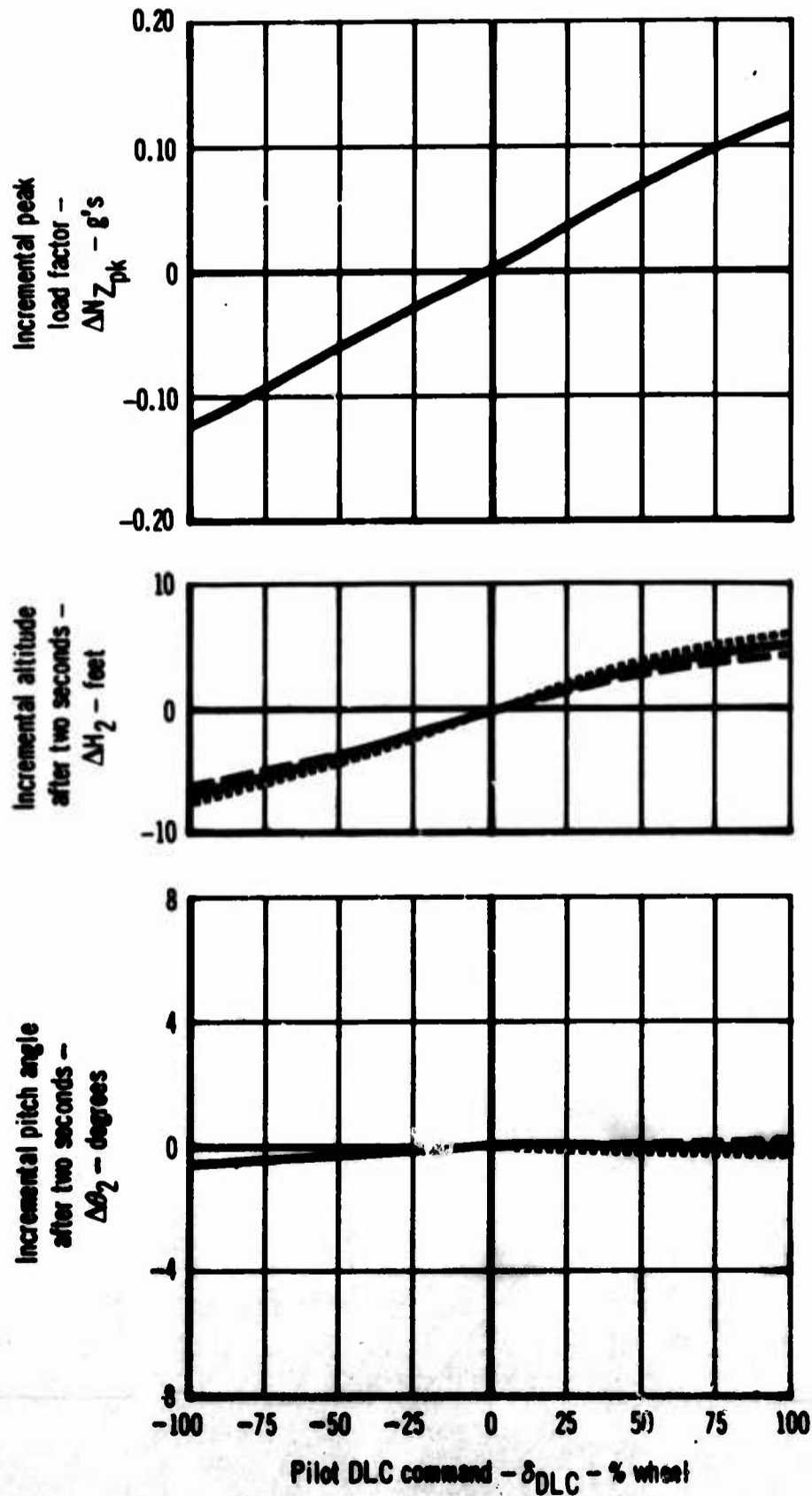


Figure C.8a Model F-4J  
Effect of Gross Weight

$$\delta_{F \text{ Nom.}} = 32^\circ; \gamma_0 = 0^\circ; a_{w \text{ Trim}} = 13^\circ$$

Symbol	C.G. (%C)	G.W. (Lb.)	V <sub>Trim</sub> (KCAS)	APCS	Interconnect
---	29	37,000	146.3	In	In
—	29	34,000	140.0	In	In
.....	29	31,000	133.7	In	In

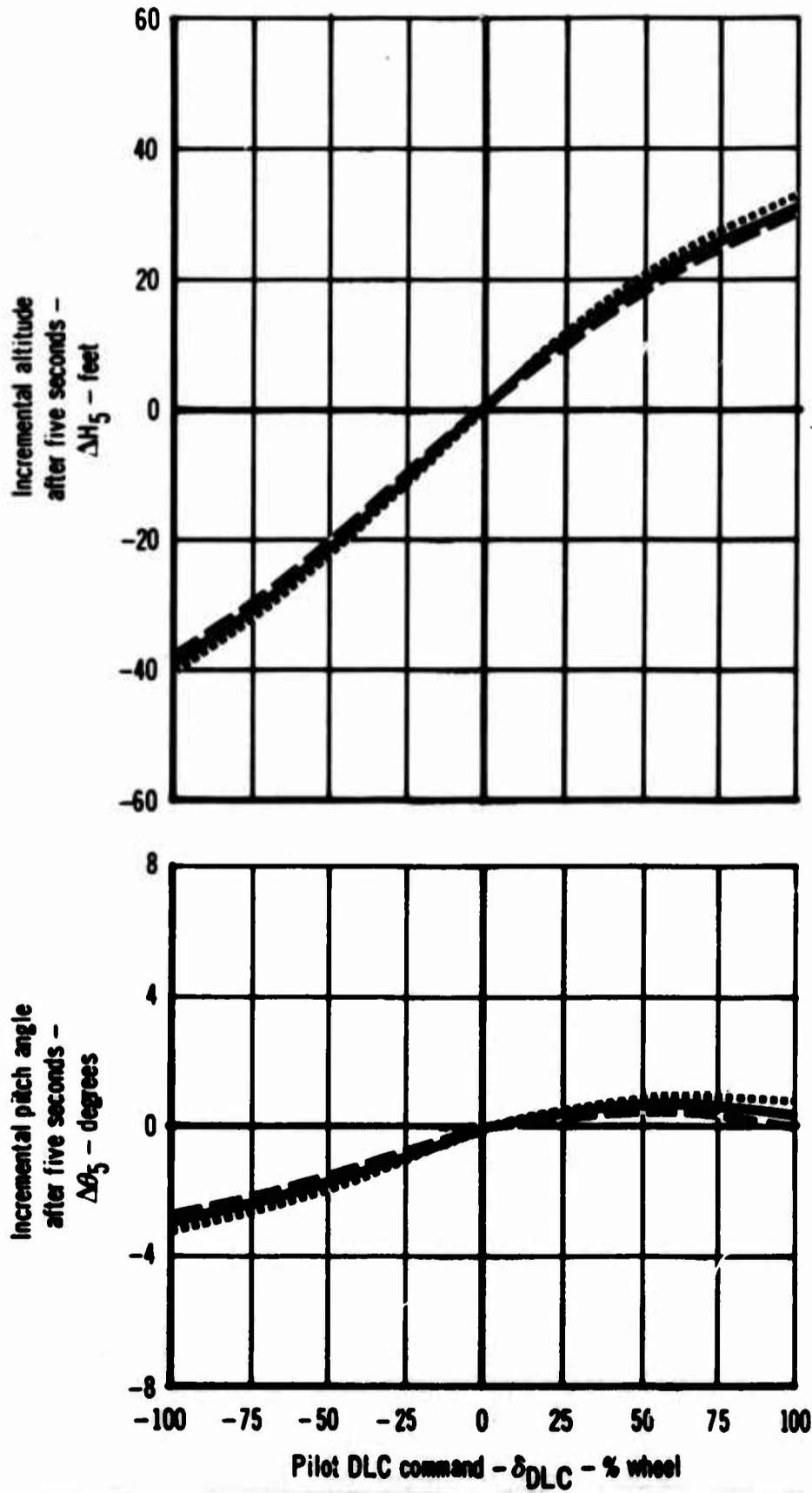


Figure C.8b Model F-4J  
Effect of Gross Weight

$$\delta_{F_{Nom.}} = 27^{\circ}; \gamma_0 = 0^{\circ}; \alpha_{w_{Trim}} = 13^{\circ}$$

Symbol	C.G. (% $\bar{x}$ )	G.W. (Lb.)	V <sub>Trim</sub> (KCAS)	APCS	Interconnect
.....	26	34,000	143.4	In	In
————	29	34,000	142.0	In	In
-----	32	34,000	140.9	In	In

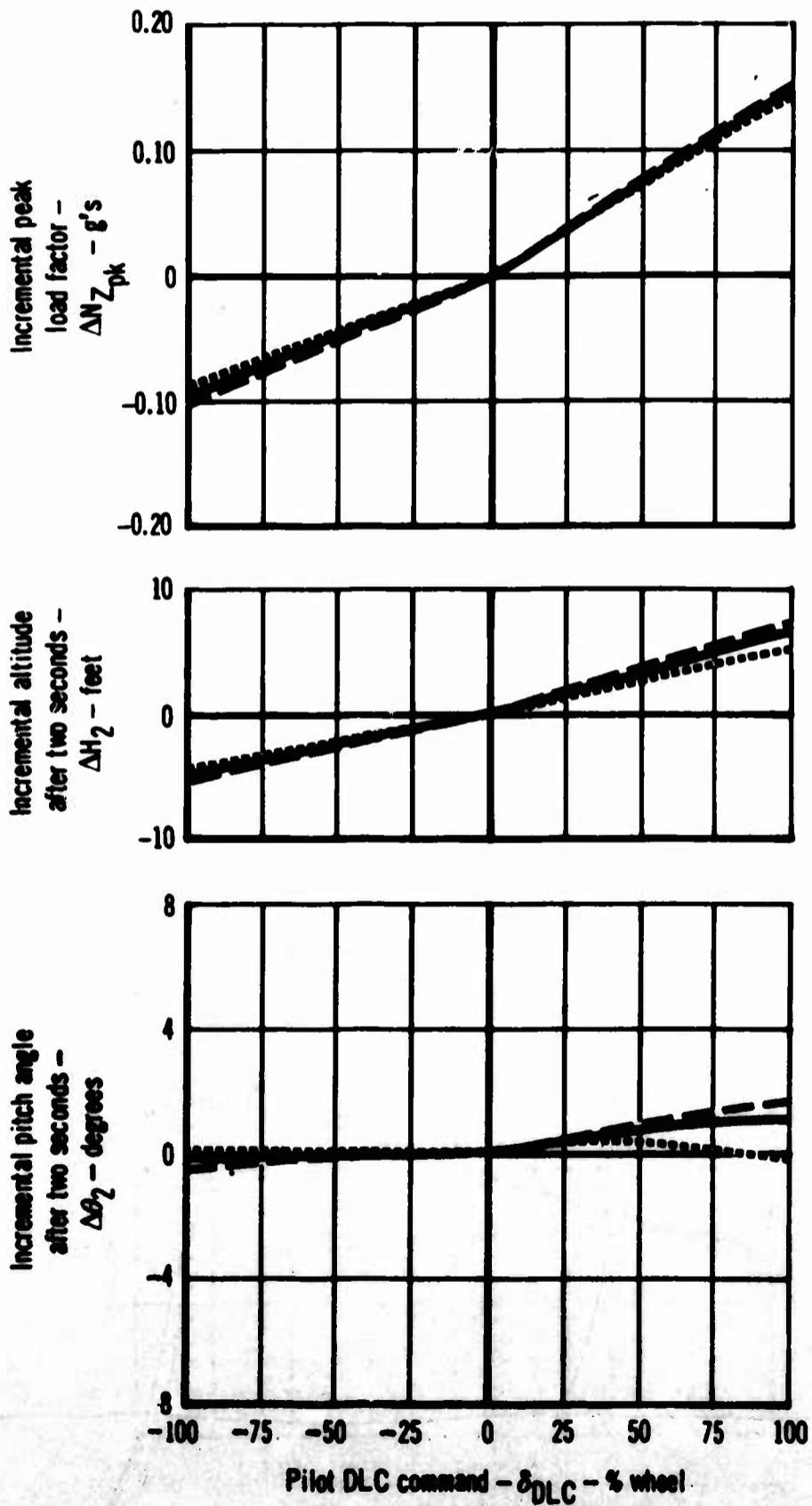


Figure C.9a Model F-4J  
Effect of Center of Gravity

$$\delta_{F \text{ Nom.}} = 27^\circ; \gamma_0 = 0^\circ; \alpha_{w \text{ Trim}} = 13^\circ$$

Symbol	C.G. (% $\bar{c}$ )	G.W. (Lb.)	V <sub>Trim</sub> (KCAS)	APCS	Interconnect
.....	26	34,000	143.4	In	In
————	29	34,000	142.0	In	In
----	32	34,000	140.9	In	In

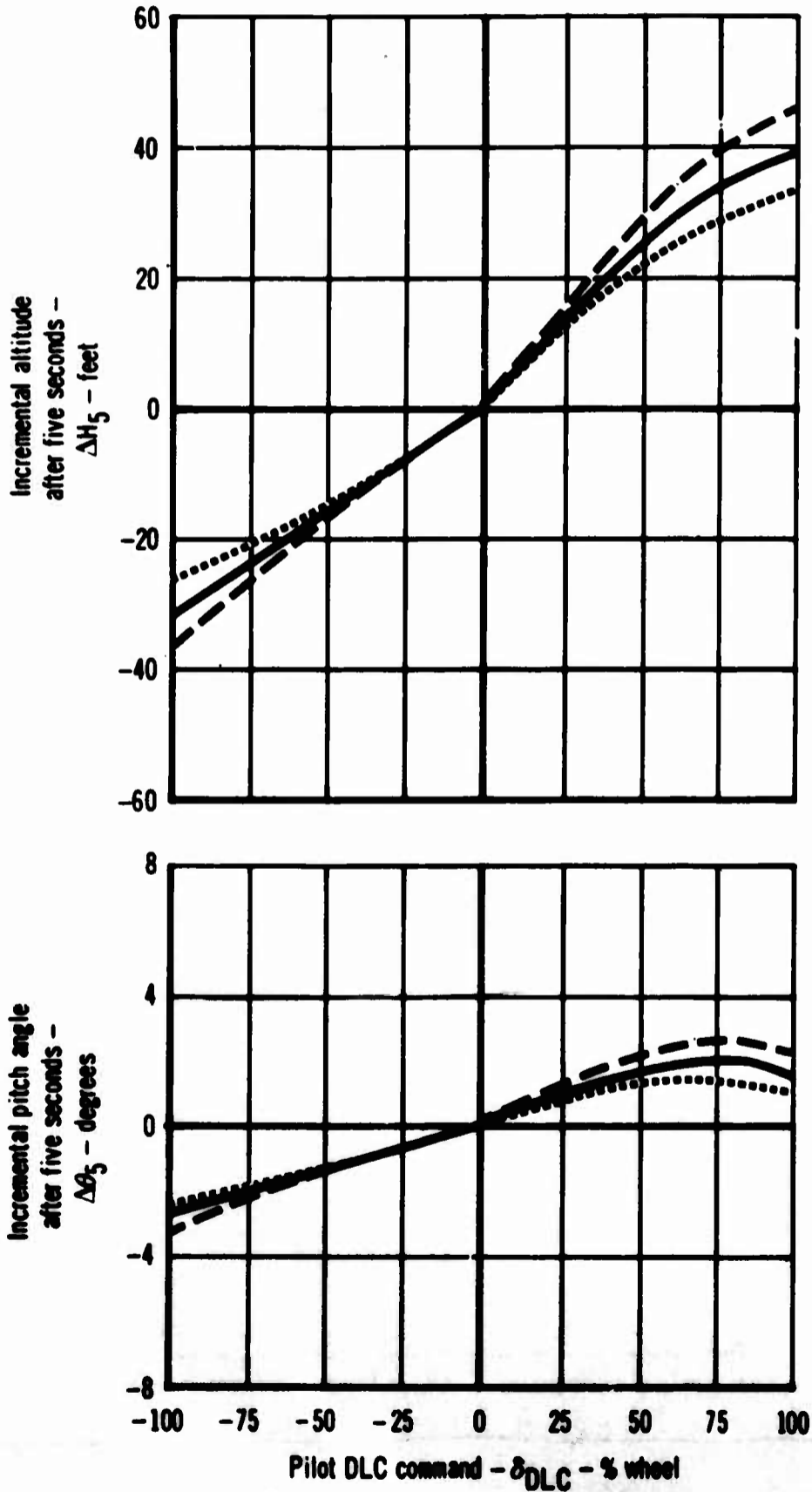


Figure C.9b Model F-4J  
Effect of Center of Gravity

$$\delta_{F_{Nom.}} = 32^\circ; \gamma_0 = 0^\circ; \alpha_{w_{Trim}} = 13^\circ$$

Symbol	C.G. (% C)	G.W. (Lb.)	V <sub>Trim</sub> (KCAS)	APCS	Interconnect
.....	26	34,000	141.2	In	In
—	29	34,000	140.0	In	In
— —	32	34,000	138.9	In	In

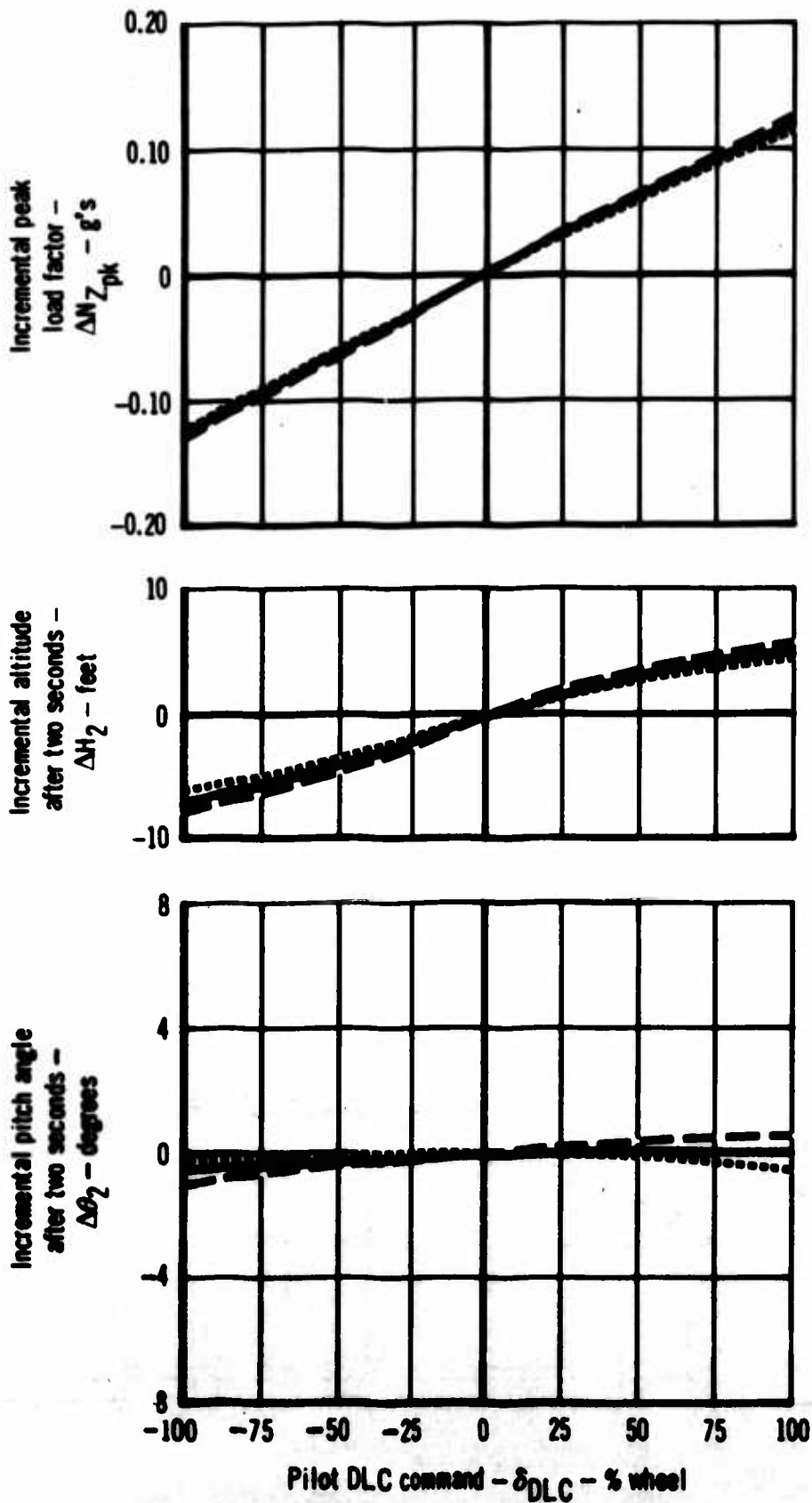


Figure C.10a Model F-4J  
Effect of Center of Gravity

$$\delta_{F \text{ Nom.}} = 32^\circ; \gamma_0 = 0^\circ; \alpha_{w \text{ Trim}} = 13^\circ$$

Symbol	C.G. (% $\bar{c}$ )	G.W. (Lb.)	V <sub>Trim</sub> (KCAS)	APCS	Interconnect
.....	26	34,000	141.2	In	In
————	29	34,000	140.0	In	In
----	32	34,000	138.9	In	In

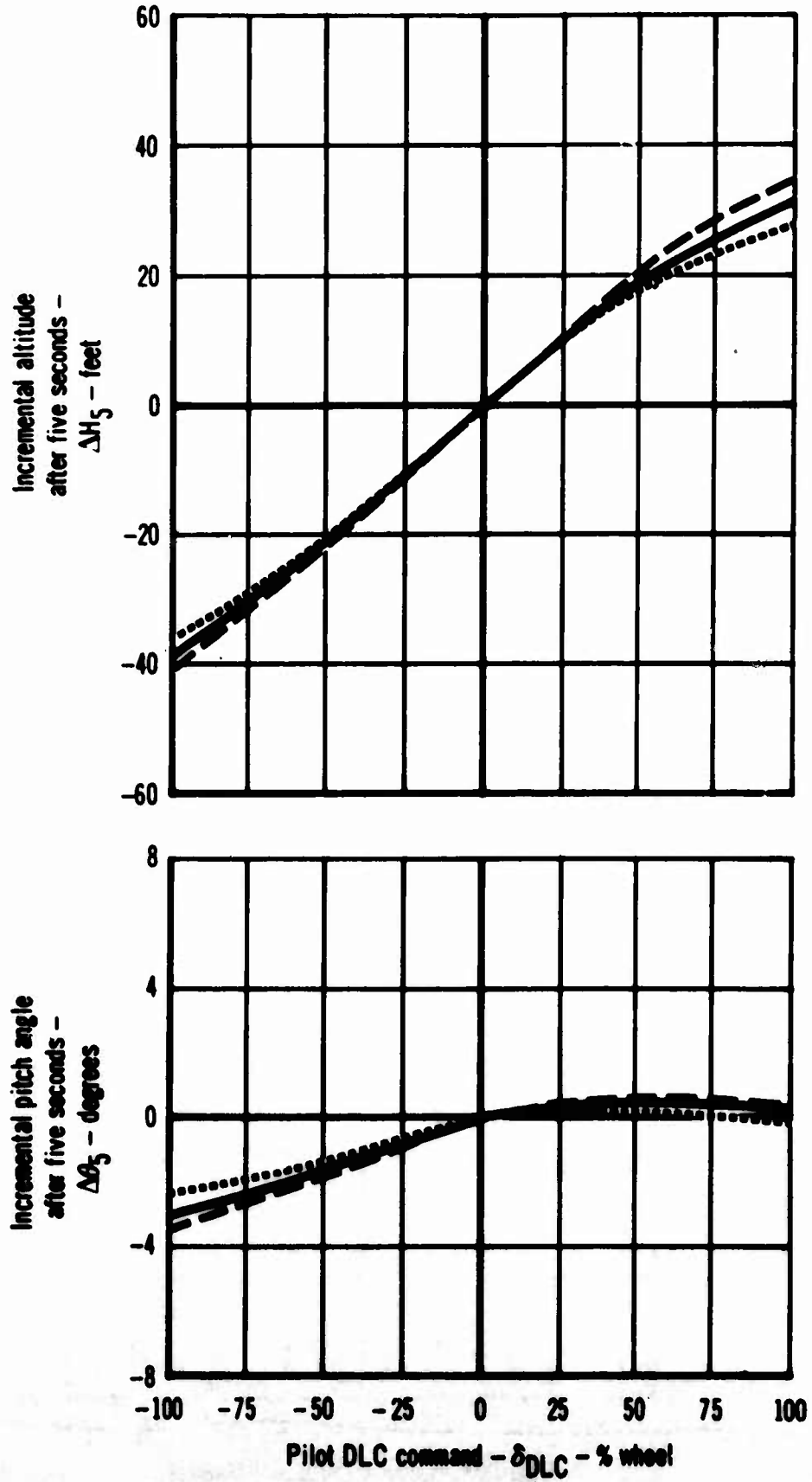


Figure C.10b Model F-4J  
Effect of Center of Gravity

$$\delta_{F_{Nom.}} = 27^{\circ}; \gamma_0 = 0^{\circ}; \alpha_{w_{Trim}} = 13^{\circ}$$

Symbol	C.G. (%C)	G.W. (Lb.)	V <sub>Trim</sub> (KCAS)	APCS	Interconnect
---	29	34,000	152.0	In	In
---	29	34,000	142.0	In	In
.....	29	34,000	132.0	In	In

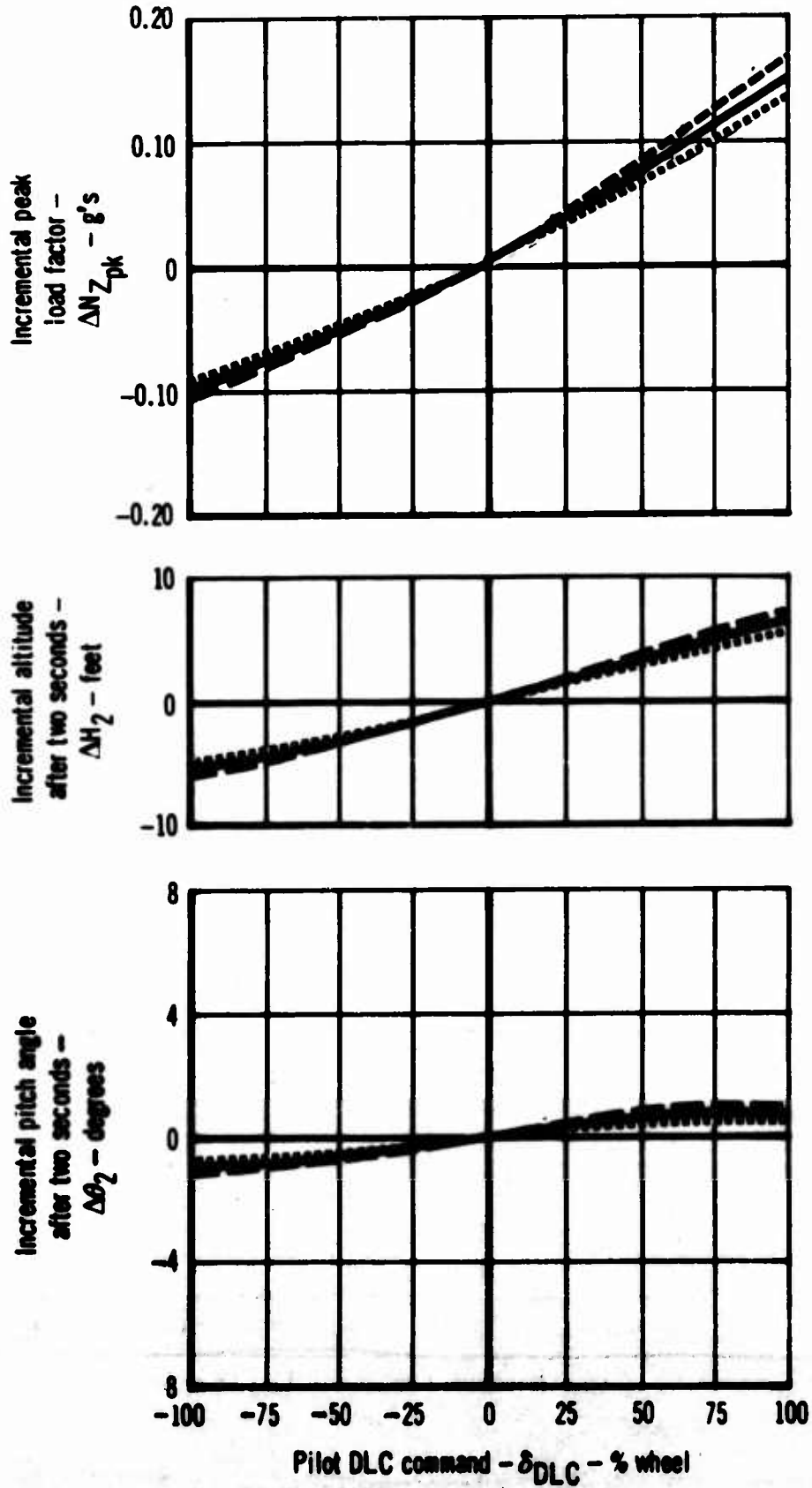


Figure C.11a Model F-4J  
Effect of Trim Velocity

$$\delta_{F_{Nom.}} = 27^{\circ}; \gamma_0 = 0^{\circ}; \alpha_{w_{Trim}} = 13^{\circ}$$

Symbol	C.G. (% $\bar{c}$ )	G.W. (Lb.)	V <sub>Trim</sub> (KCAS)	APCS	Interconnect
.....	29	34,000	152.0	In	In
————	29	34,000	142.0	In	In
----	29	34,000	132.0	In	In

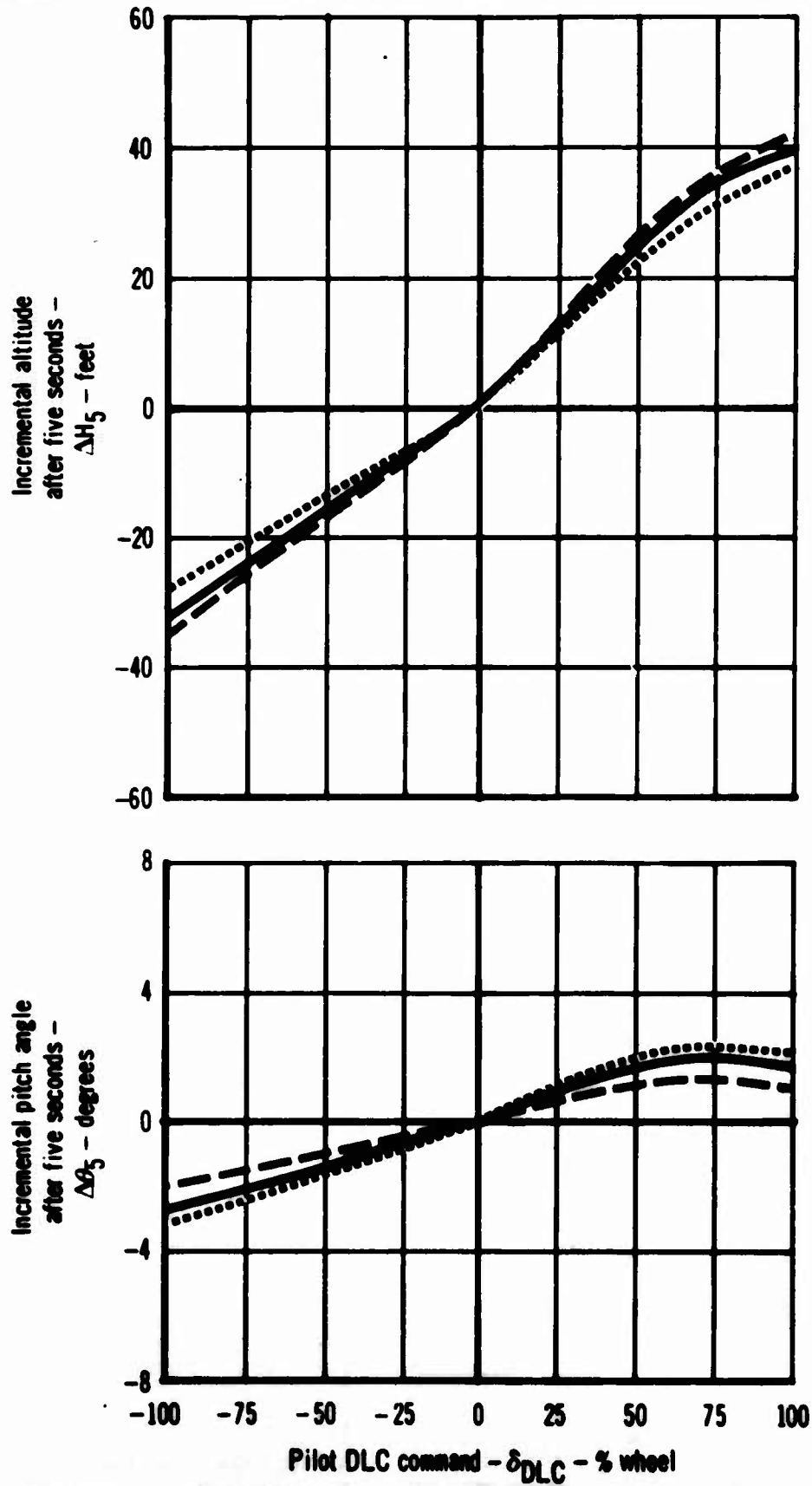


Figure C.11b Model F-4J  
Effect of Trim Velocity

$$\delta_{F_{Nom.}} = 32^{\circ}; \gamma_0 = 0^{\circ}; a_{w_{Trim}} = 13^{\circ}$$

Symbol	C.G. (%E)	G.W. (Lb.)	V <sub>Trim</sub> (KCAS)	APCS	Interconnect
---	29	34,000	150.0	In	In
—	29	34,000	140.0	In	In
.....	29	34,000	130.0	In	In

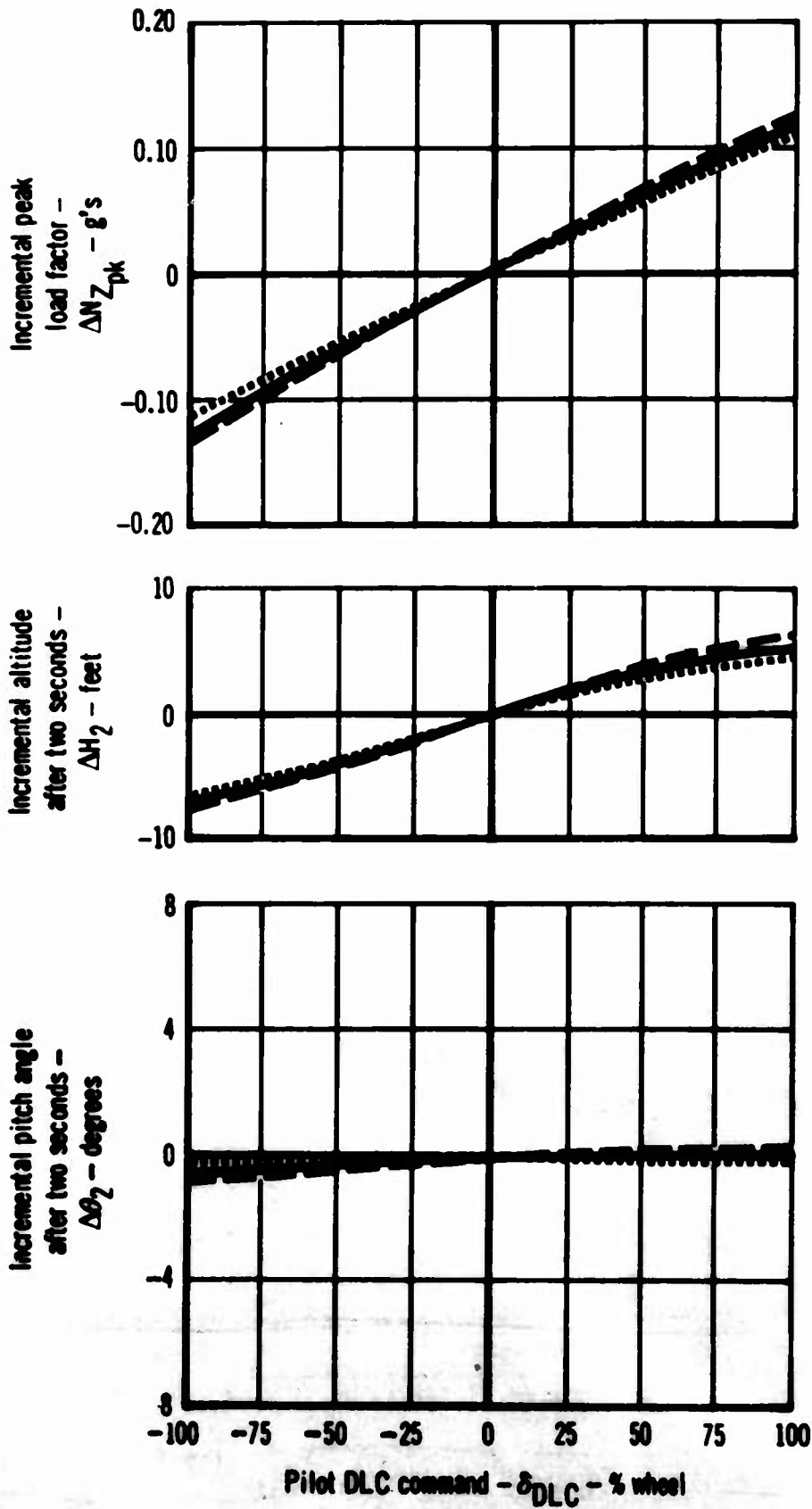


Figure C.12a Model F-4J  
Effect of Trim Velocity

$$\delta_{F \text{ Nom.}} = 32^\circ; \gamma_0 = 0^\circ; \alpha_{w \text{ Trim}} = 13^\circ$$

Symbol	C.G. (%E)	G.W. (Lb.)	V <sub>Trim</sub> (KCAS)	APCS	Interconnect
---	29	34,000	150.0	In	In
—	29	34,000	140.0	In	In
.....	29	34,000	130.0	In	In

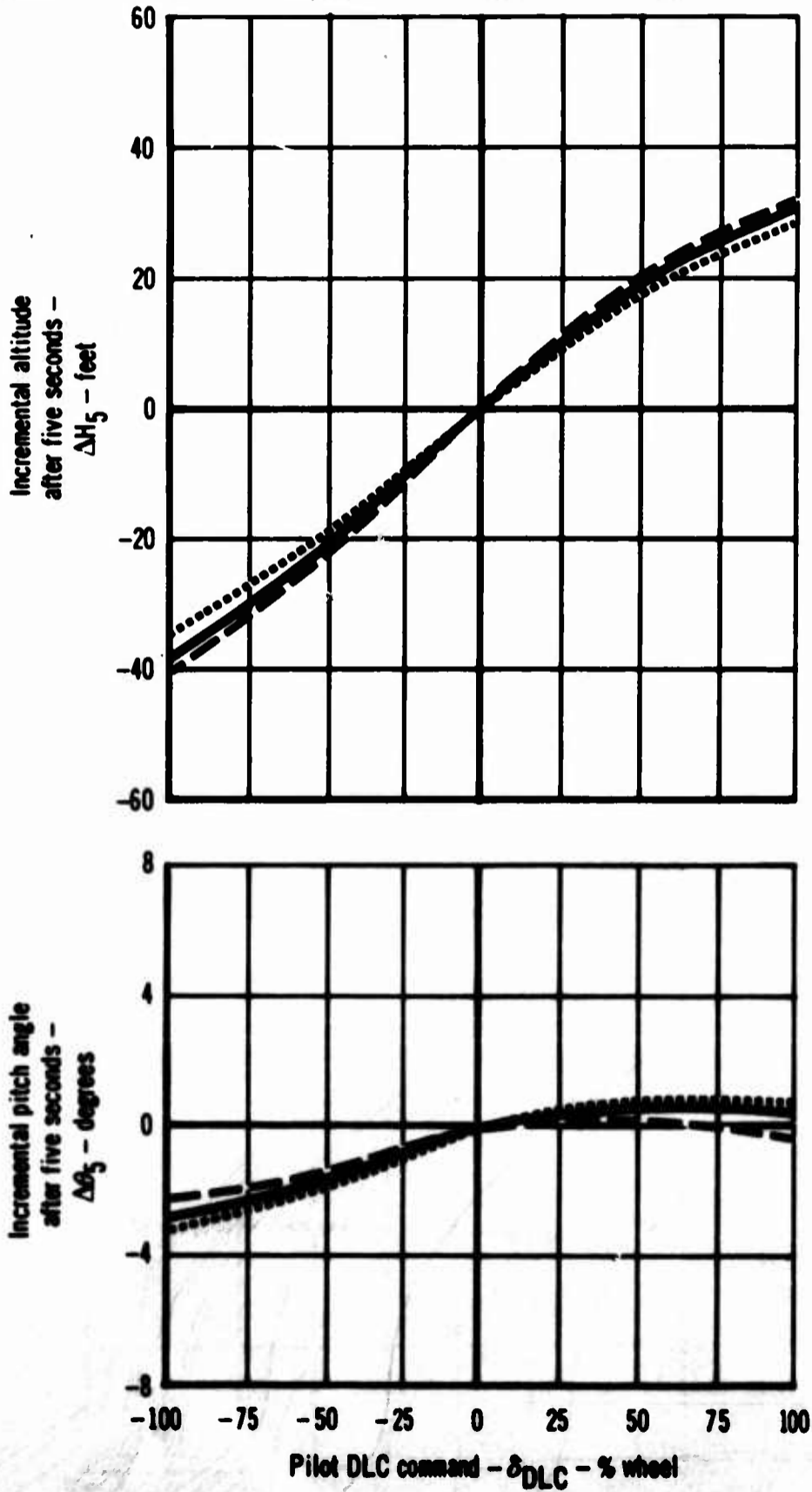


Figure C.12b Model F-4J  
Effect of Trim Velocity

G.W. = 34,000 Lb., C.G. at 29%  $\bar{c}$ ,  $\gamma_0 = -3.5^\circ$ ,  $\alpha_{wTrim} = 13^\circ$

Symbol	$\delta_{F_{Nom}}$ (deg)	$V_{Trim}$ (KCAS)	Power	Interconnect	DLC command
—————	27	143.1	Mil	In	Full up
- - - - -	27	143.1	Mil	In	None
.....	60	132.0	Mil	-	-

Note: Incremental stabilator input, throttle advanced to military power, and where applicable, DLC command applied simultaneously by the pilot.

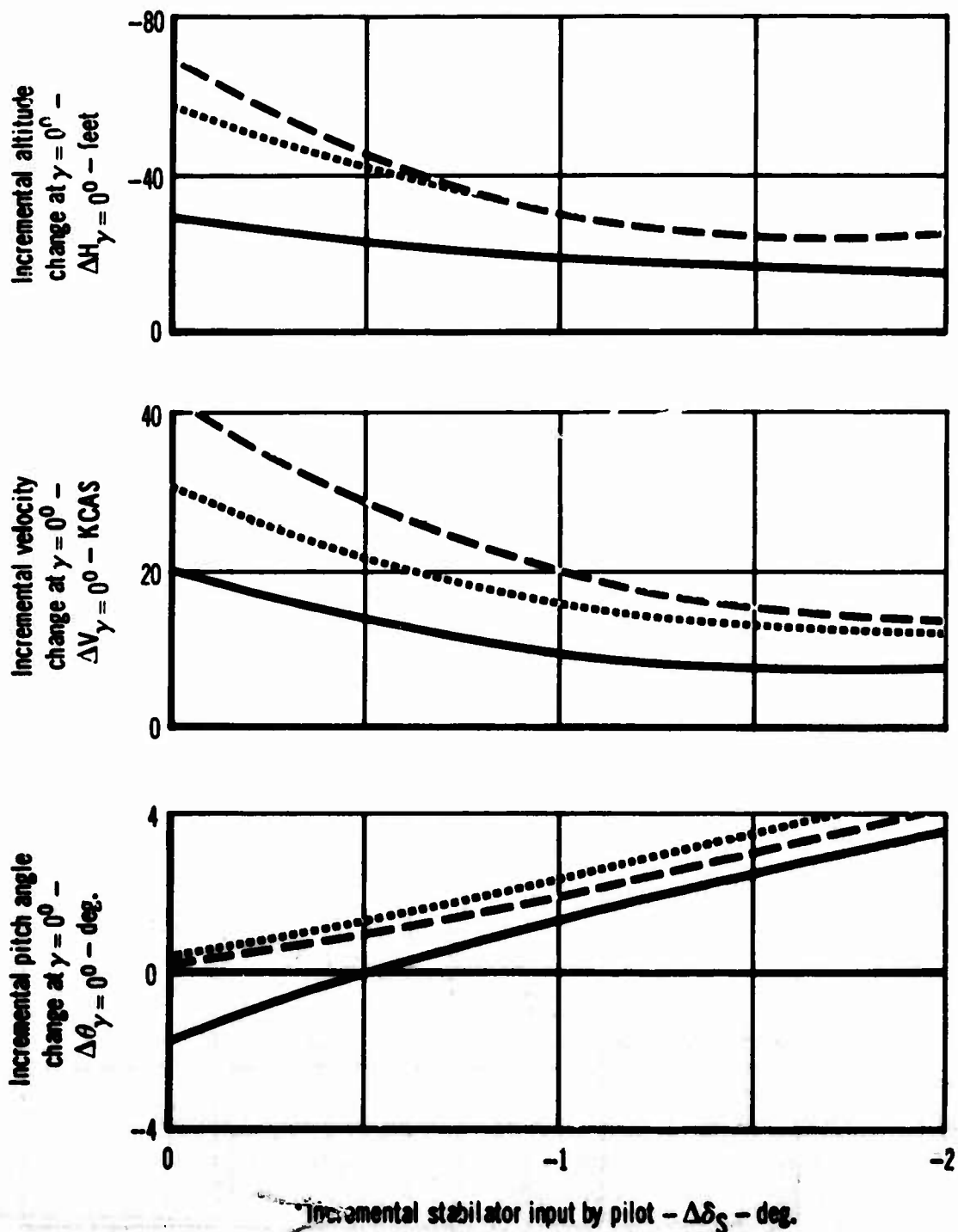


Figure C.13 Model F-4J  
Wave-Off Characteristics

G.W. = 34,000 Lb., C.G. at 29% $\bar{c}$ ,  $\gamma_0 = -3.5^\circ$ ,  $\alpha_{wTrim} = 13^\circ$

Symbol	$\delta_{FNom}$ (deg)	$V_{Trim}$ (KCAS)	Power	Interconnect	DLC command
—	32	141.3	Mil	In	Full up
- - -	32	141.3	Mil	In	None
- - - -	60	132.0	Mil	-	-

Note: Incremental stabilator input, throttle advance to military power, and where applicable, DLC command applied simultaneously by the pilot

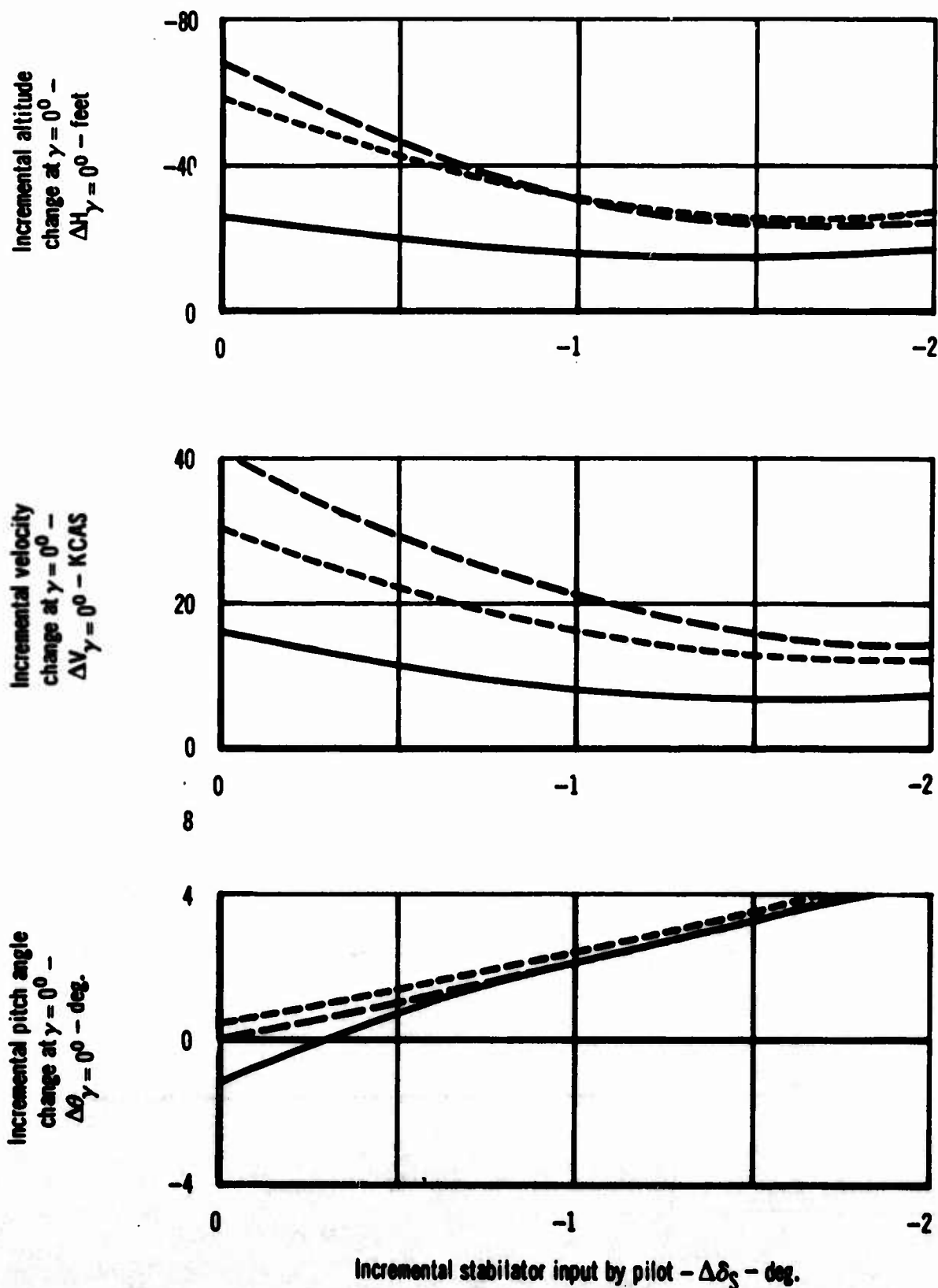


Figure C.14 Model F-4J  
Wave-Off Characteristics

$\delta_{F \text{ Nom}} = 27^\circ$       C.G. at 29%  $\bar{c}$        $V_{\text{Trim}} = 143.1 \text{ KCAS}$   
 G.W. = 34,000 Lb.       $\gamma_0 = -3.5^\circ$        $\alpha_{w \text{ Trim}} = 13^\circ$   
 Military power       $\Delta\delta_s = -1^\circ$

Pilot DLC command -  $\delta_{\text{DLC}}$  - 100% wheel (positive)

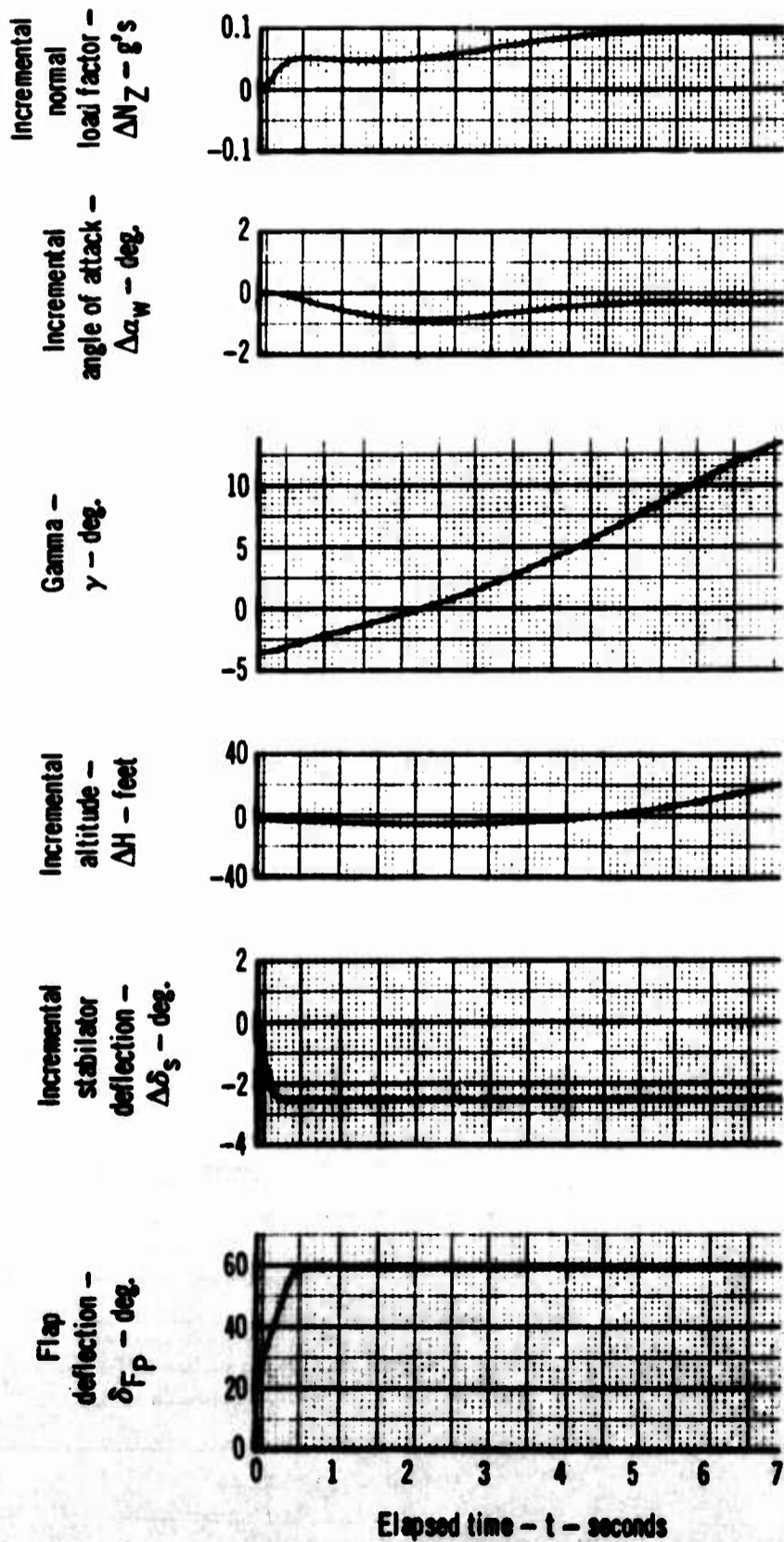


Figure C.15a Model F-4J  
Wave-Off Characteristics

$\delta_{F\text{Nom}} = 27^\circ$	C.G. at 29% $\bar{c}$	$V_{\text{Trim}} = 143.1$ KCAS
G.W. = 34,000 Lb.	$\gamma_0 = -3.5^\circ$	$\alpha_{w\text{Trim}} = 13^\circ$
Military Power	$\Delta\delta_s = -1^\circ$	

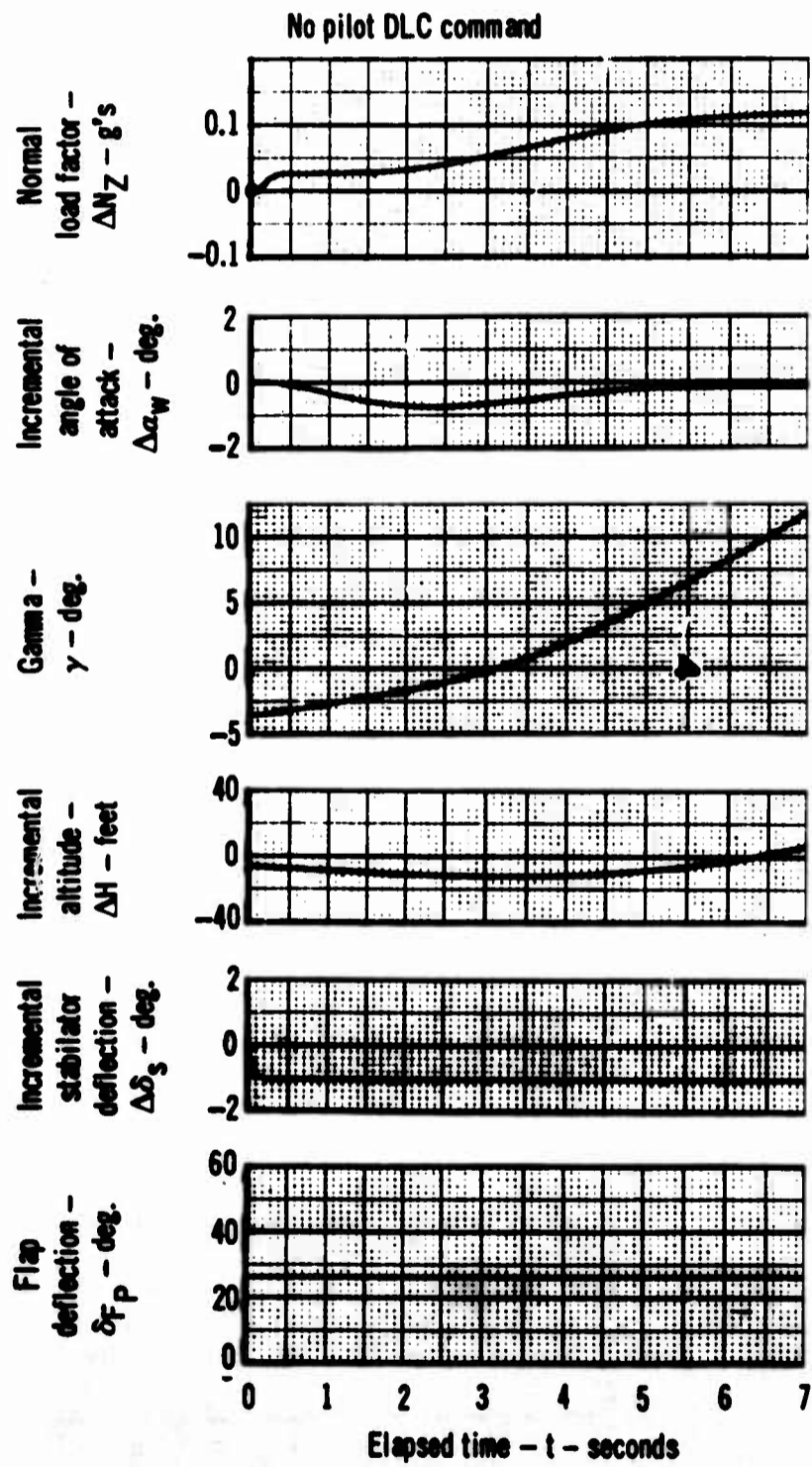


Figure C.15b Model F-4J  
Wave-Off Characteristics

G.W. = 34,000 Lb. C.G. at 29%  $\bar{c}$   
 Initial Flight Path Angle =  $-3.5^\circ$

Symbol	$\delta_{F_{Nom}}$ (deg)	$V_{Trim}$ (KCAS)	Power	Interconnect	DLC command
—————	60	132.0	Mil.	-	-
———	27	143.1	Mil.	In	Full up
- - - - -	27	143.1	Mil.	-	None
— · — · —	32	141.3	Mil.	In	Full up
- · - · - · -	32	141.3	Mil.	-	None

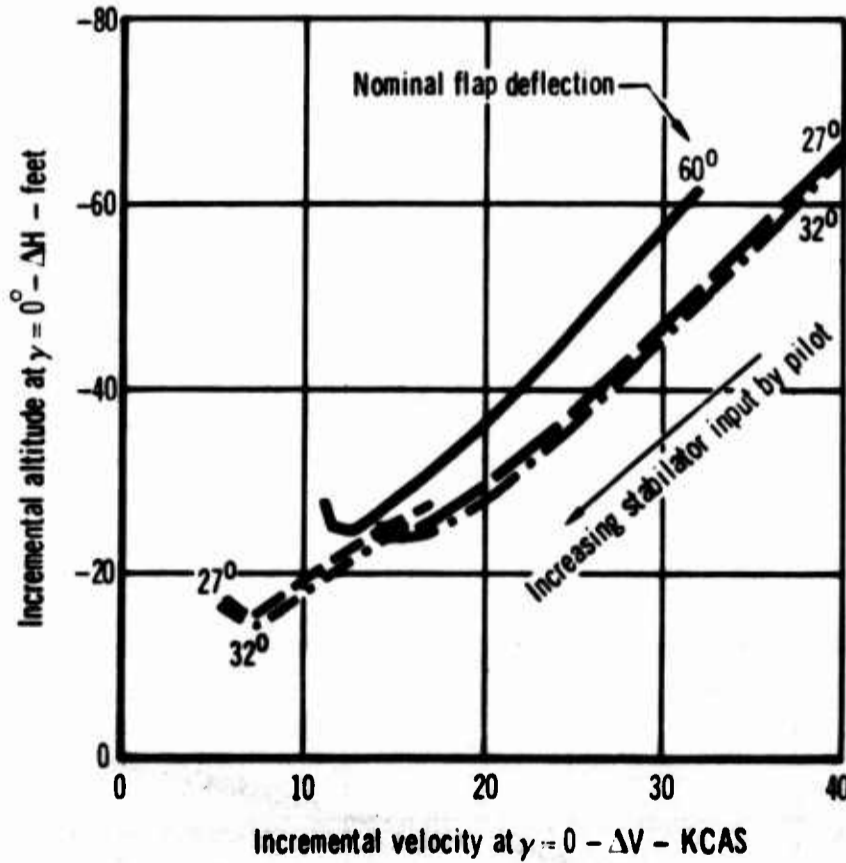


Figure C.16 Model F-4J  
 Wave-Off Characteristics Summary

G.W. = 34,000 Lb., C.G. at 29% $\bar{c}$ ,  $\gamma_0 = -3.5^\circ$ ,  $a_{wTrim} = 13^\circ$

Symbol	$\delta_{FNom}$ (deg)	$V_{Trim}$ (KCAS)	Power	DLC command
—	27	143.1	Mil	None
- - -	30	142.5	Mil	None
- - - -	32	141.3	Mil	None

Note: Incremental stabilator input and throttle advanced to military power simultaneously by the pilot

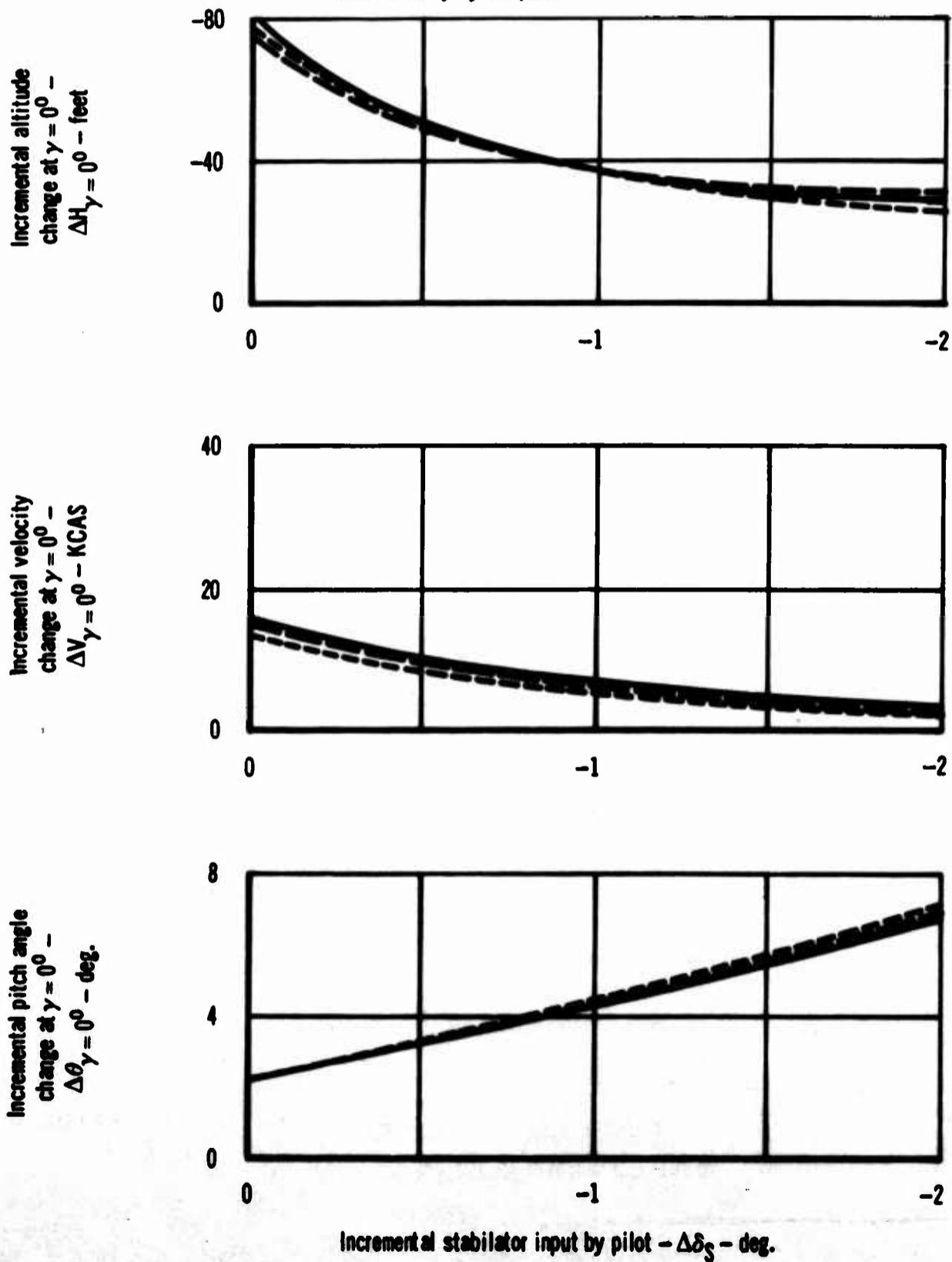


Figure C.17 Model F-4J  
Single Engine Wave-Off Characteristics

$\delta_{FNom} = 27^\circ$   
G.W. = 34,000 Lb.

C.G. at 29%  $\bar{c}$   
 $\gamma_0 = -3.5^\circ$   
 $\Delta t = 1.0$  second

$V_{Trim} = 143.1$  KCAS  
 $\alpha_{wTrim} = 13^\circ$

With APCS  
With Interconnect

Failure occurs at  $t = 0$ ;  $\Delta\delta_s$  input command at  $\Delta t$  seconds

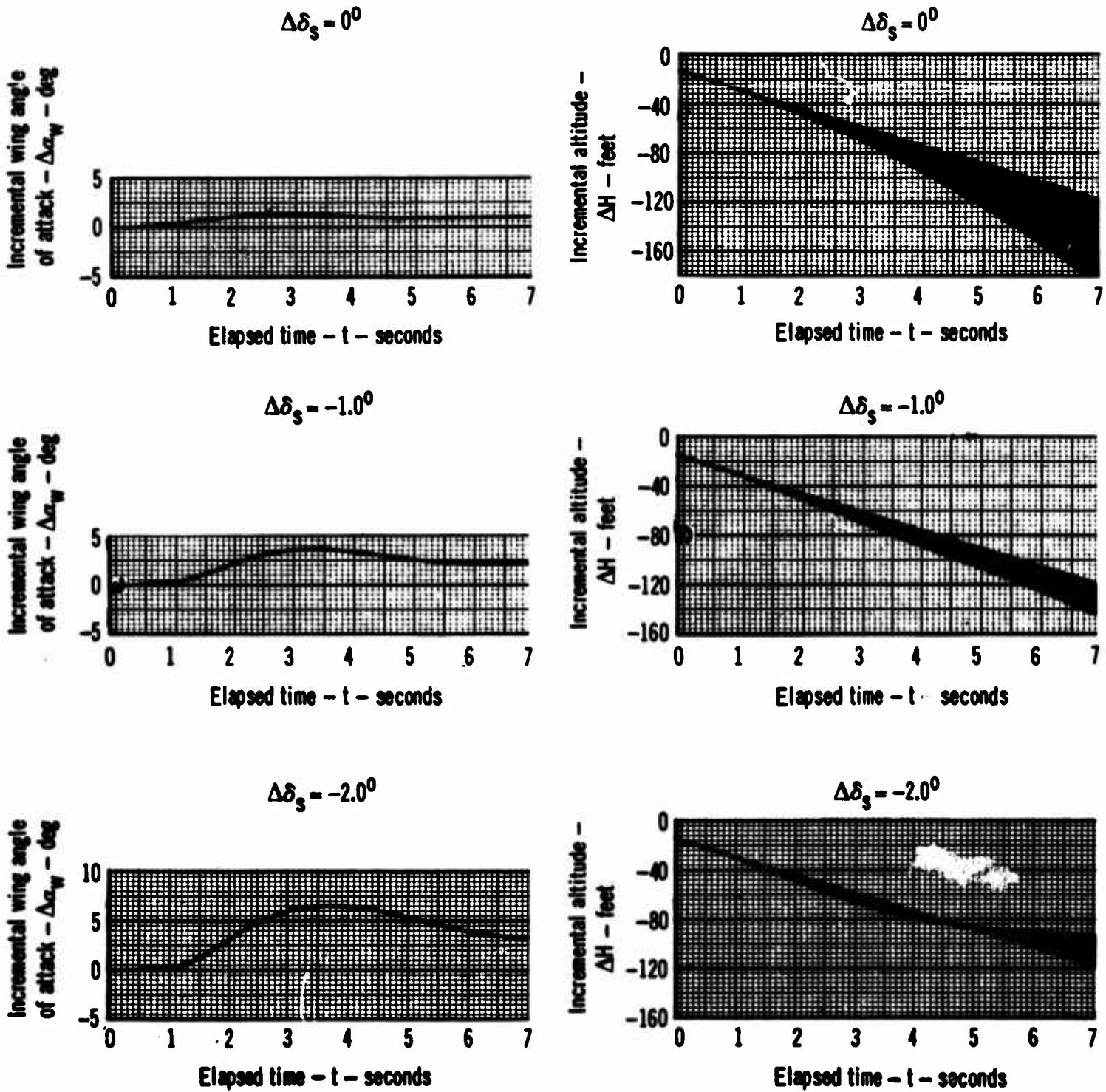
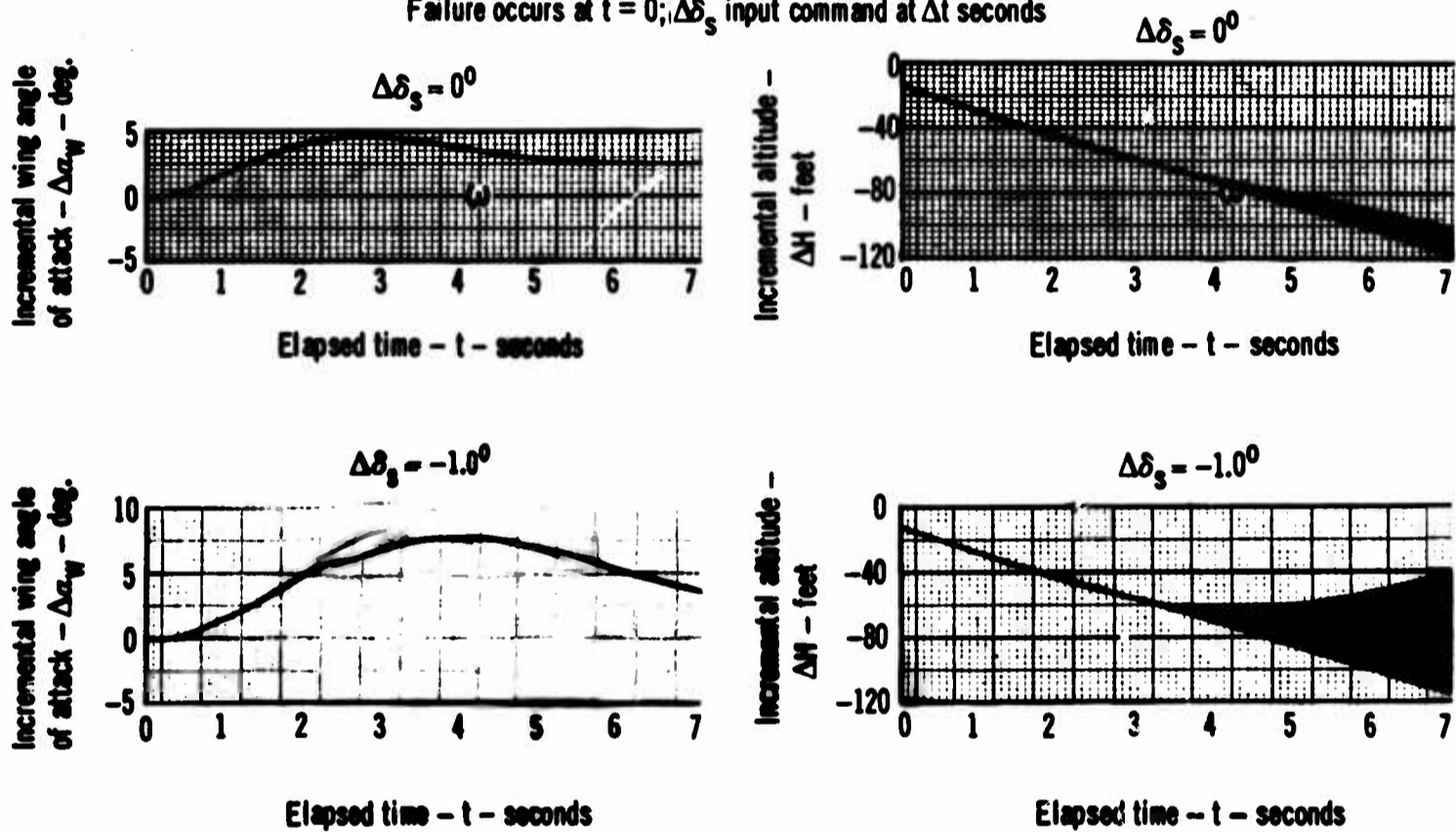


Figure C.18 Model F-4J  
Failure Analysis - Effect of Pilot Control Correction  
DLC Hardover - Upstream of Stabilator - Interconnect

$\delta_{F\text{Nom}} = 27^\circ$       C.G. at 29%  $\bar{c}$        $V_{\text{Trim}} = 143.1$  KCAS  
 G.W. = 34,000 Lb.       $\gamma_0 = -3.5^\circ$        $\alpha_{\text{Trim}} = 13^\circ$   
 $\Delta t = 1.0$  Second

Failure occurs at  $t = 0$ ;  $\Delta\delta_s$  input command at  $\Delta t$  seconds



**Figure C.19 Model F-4J**  
**Failure Analysis - Effect of Pilot Control Correction**  
**DLC Hardover - Downstream of Stabilator - Interconnect**

$\delta_{F \text{ Nom}} = 27^\circ$   
G.W. = 34,000 Lb.

C.G. at 29% $\bar{c}$   
 $\gamma_0 = -3.5^\circ$   
 $\Delta\delta_s = -2.0^\circ$

$V_{\text{Trim}} = 143.1 \text{ KCAS}$   
 $\alpha_{W \text{ Trim}} = 13^\circ$

With APCS  
With Interconnect

Failure occurs at  $t = 0$ ;  $\Delta\delta_s$  input command at  $\Delta t$  seconds

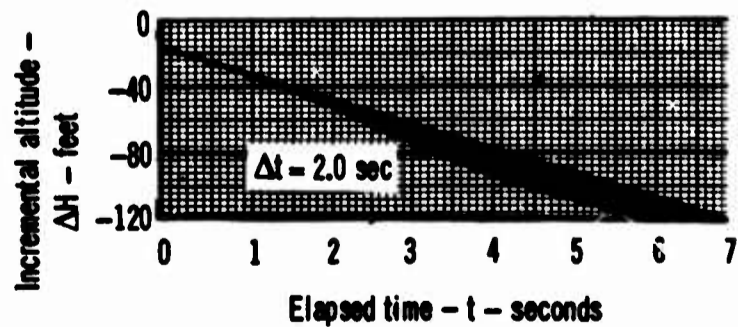
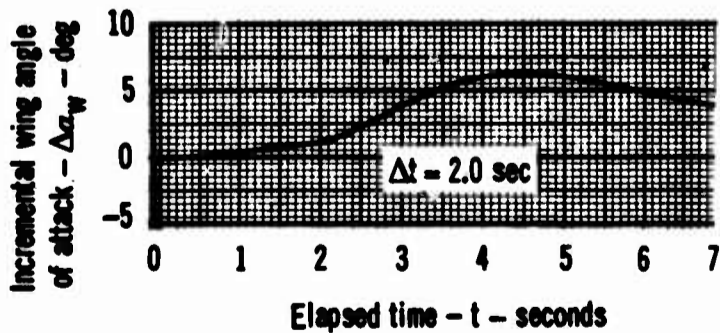
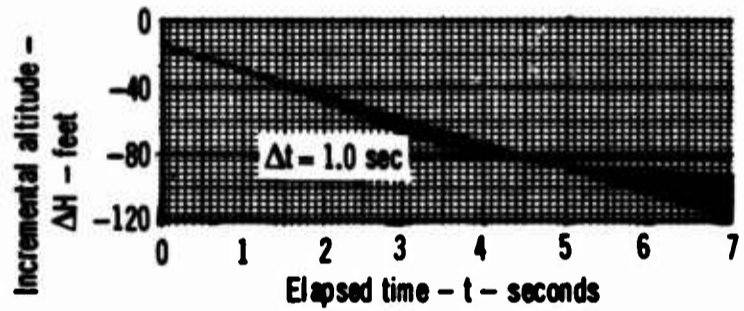
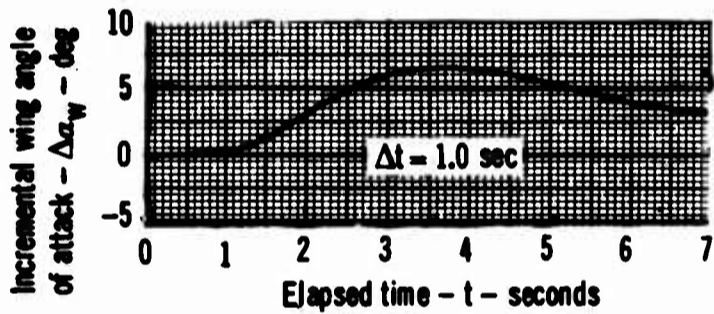
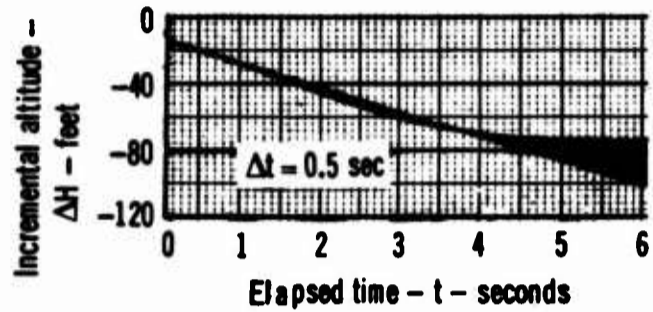
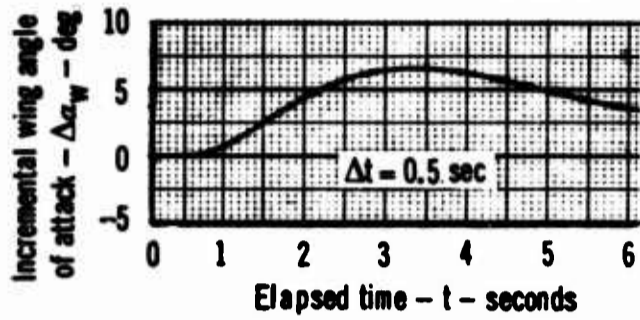


Figure C.20 Model F-4J  
Failure Analysis - Effect of Pilot Reaction Time  
DLC Hardover - Upstream of Stabilator - Interconnect

$\delta_{F\text{Nom}} = 27^\circ$   
G.W. = 34,000 Lb.

C.G. at 29%  $\bar{c}$   
 $\gamma_0 = -3.5^\circ$   
 $\Delta\delta_s = -1.0^\circ$

$V_{\text{Trim}} = 143.1 \text{ KCAS}$   
 $\alpha_{w\text{Trim}} = 13^\circ$

With APCS  
With Interconnect

Failure occurs at  $t = 0$ ;  $\Delta\delta_s$  input command at  $\Delta t$  seconds

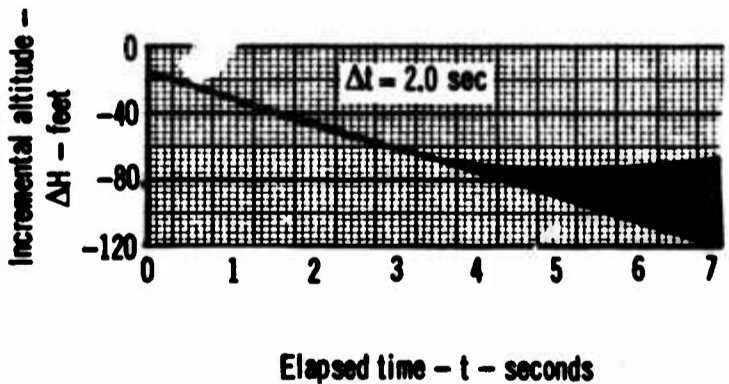
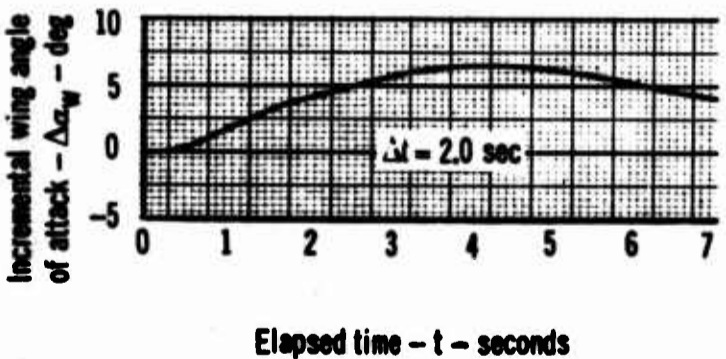
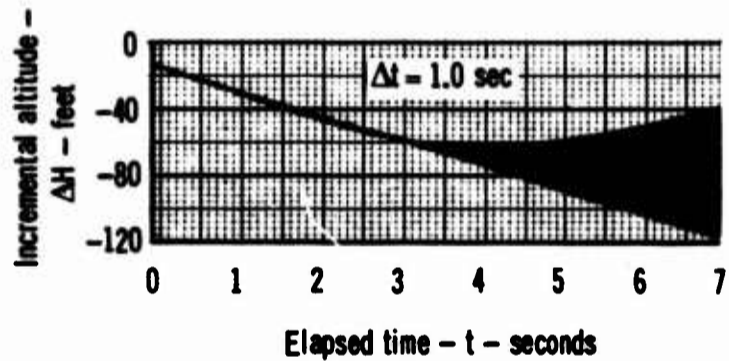
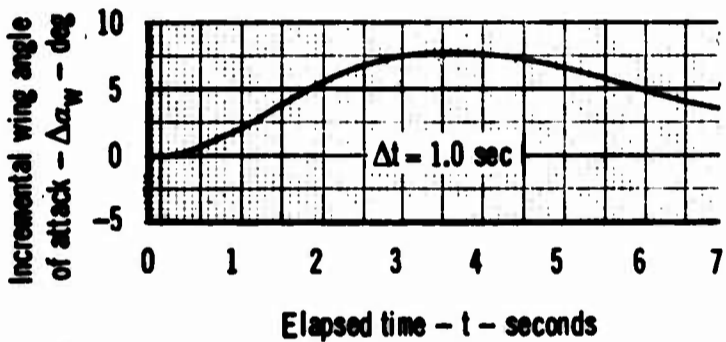
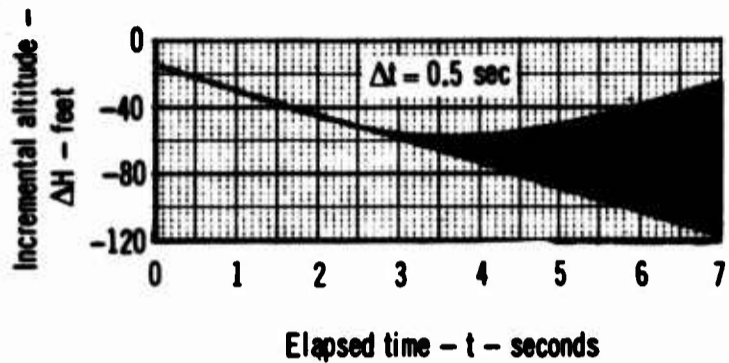
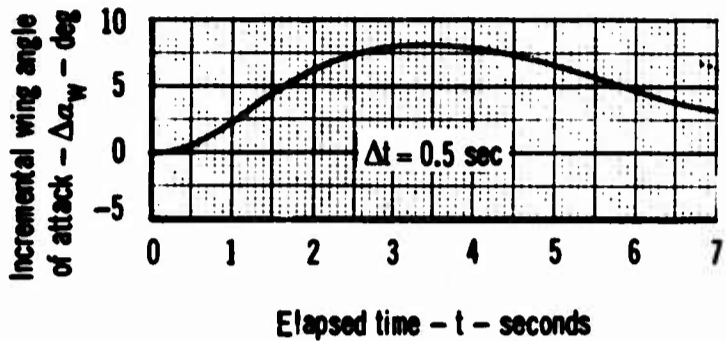


Figure C.21 Model F-4J  
Failure Analysis - Effect of Pilot Reaction Time  
DLC Hardover - Downstream of Stabilator - Interconnect